SANDIA REPORT

SAND2004-1390
Unlimited Release
Printed July 2004

Simulations of the Pipe Overpack to Compute Constitutive Model Parameters for Use in WIPP Room Closure Calculations

Byoung Yoon Park and Francis D. Hansen

Prepared by
Sandia National Laboratories
Albuquerque, New Mexico 87185 and Livermore, California 94550

Sandia is a multiprogram laboratory operated by Sandia Corporation,
a Lockheed Martin Company, for the United States Department of Energy's
National Nuclear Security Administration under Contract DE-AC04-94AL85000.

Approved for public release; further dissemination unlimited.

Sandia National Laboratories

Issued by Sandia National Laboratories, operated for the United States Department of Energy by Sandia Corporation.

NOTICE: This report was prepared as an account of work sponsored by an agency of the United States Government. Neither the United States Government, nor any agency thereof, nor any of their employees, nor any of their contractors, subcontractors, or their employees, make any warranty, express or implied, or assume any legal liability or responsibility for the accuracy, completeness, or usefulness of any information, apparatus, product, or process disclosed, or represent that its use would not infringe privately owned rights. Reference herein to any specific commercial product, process, or service by trade name, trademark, manufacturer, or otherwise, does not necessarily constitute or imply its endorsement, recommendation, or favoring by the United States Government, any agency thereof, or any of their contractors or subcontractors. The views and opinions expressed herein do not necessarily state or reflect those of the United States Government, any agency thereof, or any of their contractors.

Printed in the United States of America. This report has been reproduced directly from the best available copy.

Available to DOE and DOE contractors from
U.S. Department of Energy
Office of Scientific and Technical Information
P.O. Box 62
Oak Ridge, TN 37831

Telephone: (865)576-8401
Facsimile: (865)576-5728
E-Mail: reports@adonis.osti.gov
Online ordering: http://www.osti.gov/bridge

Available to the public from
U.S. Department of Commerce
National Technical Information Service
5285 Port Royal Rd
Springfield, VA 22161

Telephone: (800)553-6847
Facsimile: (703)605-6900
E-Mail: orders@ntis.fedworld.gov
Online order: http://www.ntis.gov/help/ordermethods.asp?loc=7-4-0#online

SAND2004-1390
Unlimited Release
Printed July 2004

Simulations of the Pipe Overpack to Compute Constitutive Model Parameters for Use in WIPP Room Closure Calculations

Byoung Yoon Park
Performance Assessment and Decision Analysis Department

Francis D. Hansen
Carlsbad Programs Group

Sandia National Laboratories
P.O. Box 5800
Albuquerque, NM 87185-1395

Abstract

The regulatory compliance determination for the Waste Isolation Pilot Plant includes the consideration of room closure. Elements of the geomechanical processes include salt creep, gas generation and mechanical deformation of the waste residing in the rooms. The WIPP was certified as complying with regulatory requirements based in part on the implementation of room closure and material models for the waste. Since the WIPP began receiving waste in 1999, waste packages have been identified that are appreciably more robust than the 55-gallon drums characterized for the initial calculations. The pipe overpack comprises one such waste package. This report develops material model parameters for the pipe overpack containers by using axisymmetrical finite element models. Known material properties and structural dimensions allow well constrained models to be completed for uniaxial, triaxial, and hydrostatic compression of the pipe overpack waste package. These analyses show that the pipe overpack waste package is far more rigid than the originally certified drum. The model parameters developed in this report are used subsequently to evaluate the implications to performance assessment calculations.

Intentionally blank

Acknowledgements

Sandia is a multiprogram laboratory operated by Sandia Corporation, a Lockheed Martin Company, for the United States Department of Energy's National Nuclear Security Administration under Contract DE-AC04-94AL85000.

This research is funded by WIPP programs administered by the U.S. Department of Energy.

The authors are indebted to Douglas Ammerman (SNL, Dept. 6141) for providing material properties and other information regarding the pipe overpack models. The authors also would like to acknowledge the valuable consultation provided by Moo Y. Lee (SNL, Dept. 6117) regarding the actual experimental experience for the test simulations. Tom W. Pfeifle provided technical review and Mario J. Chavez provided a Quality Assurance review. The paper has been improved by these individuals.

Intentionally Blank

TABLE OF CONTENTS

1 INTRODUCTION 13

1.1 Background 13
1.2 Objective 14
1.3 Analysis Overview 14
1.4 Report Organization 15

2 ANALYSIS MODEL 17

2.1 Configuration 17
2.2 Material Properties 23
2.3 Waste Constitutive Model 24

3 COMPUTER CODES AND FILE NAME CONVENTION 27

3.1 Computer Codes 27
3.2 File Naming Convention 28

4 UNIAXIAL TEST SIMULATION 30

4.1 Theoretical Background 30
4.2 Mesh Generation and Simulation 31
4.3 Simulation Results 34
4.3.1 Deformation pattern 34
4.3.2 Young's Modulus (E) 35
4.3.3 Poisson's ratio (ν) 37
4.3.4 Shear Modulus and Bulk Modulus 38

5 TRIAXIAL TEST SIMULATION 39

5.1 Theoretical Background 39
5.2 Mesh Generation and Simulation 41
5.3 Simulation Results 44
5.3.1 Deformation pattern 44
5.3.2 Yield surface constants 45

6 HYDROSTATIC TEST SIMULATION 49

6.1 Theoretical Background 49
6.2 Mesh Generation and Simulation 50
6.3 Simulation Results 52
6.3.1 Deformation pattern 52
6.3.2 Pressure-volumetric strain function data 53

7 DISCUSSION AND CONCLUDING REMARKS 55

8 REFERENCES 59

APPENDIX A: CALCULATION SHEET 63

A-1 Shear Modulus and Bulk Modulus 63

A-2 D-P, M-C, and SANTOS input constants 64

APPENDIX B: FASTQ INPUT FILE 72

B-1 12-inch POP Waste Mesh for UTS and TTS 72
B-2 6-inch POP Waste Mesh for UTS and TTS 78
B-3 12-inch POP Waste Mesh for HTS 84
B-4 6-inch POP Waste Mesh for HTS 89

APPENDIX C: SAMPLE SANTOS INPUT FILES FOR TEST SIMULATION 94

C-1 For UTS 94
C-2 For TTS 96
C-3 For HTS 98

LIST OF TABLES

Table 1. Material properties for elastic-plastic power law hardening material 23
Table 2. Material properties for elastic plastic material with combined kinematic and isotropic hardening (Ludwigsen et al., 1998) 23
Table 3. File naming convention (* means wild card)..... 29
Table 4. The shear modulus and the bulk modulus of POP waste..... 38
Table 5. Axial pressure as a function of confining pressure to attain incipient buckling. 47
Table 6. Friction angle and cohesion of 12-inch and 6-inch POP drum..... 48
Table 7. Drucker-Prager constants and SANTOS input constants 48
Table 8. SANTOS input constants for waste constitutive model 56
Table 9. Pressure-volumetric strain data used in the waste constitutive model..... 57

LIST OF FIGURES

Figure 1. Activity flow diagram for calculating the porosity surface of the disposal room containing the POP waste. 16
Figure 2. Photograph of a pipe and a schematic of pipe overpack configuration..... 18
Figure 3. Drawing of 12-inch POP components (WTS, 2003)..... 19
Figure 4. Drawing of 6-inch POP components (WTS, 2003)..... 20
Figure 5. Simplified 12-inch POP drawing for mesh generation..... 21
Figure 6. Simplified 6-inch POP drawing for mesh generation..... 22
Figure 7. Pressure-dependent yield surface for the waste material model (Stone, 1997b)26
Figure 8. The finite element mesh and boundary conditions for the 12-inch POP uniaxial test. 32
Figure 9. The finite element mesh and boundary conditions for the 6-inch POP uniaxial test. 33
Figure 10. Deformation pattern of 12-inch POP from the uniaxial test simulation..... 34
Figure 11. Deformation pattern of 6-inch POP from the uniaxial test simulation..... 35
Figure 12. The axial stress-strain curve of 12-inch POP drum..... 36
Figure 13. The axial stress-strain curve of 6-inch POP drum..... 36
Figure 14: The radial-axial strain curve of 12-inch POP drum 37
Figure 15: The radial-axial strain curve of 6-inch POP drum 38
Figure 16. Deviatoric section of Mohr-Coulomb and Drucker-Prager criteria. 40
Figure 17. The finite element mesh and boundary conditions for the 12-inch POP triaxial test. 42
Figure 18. The finite element mesh and boundary conditions for the 6-inch POP triaxial test. 43
Figure 19. Deformation pattern of 12-inch POP triaxial simulation with 1.5 MPa confining pressure. 44
Figure 20. Deformation pattern of 6-inch POP triaxial simulation with 1.5 MPa confining pressure. 45
Figure 21. von Mises stress contour for 12-inch POP drum at 11.2 MPa axial pressure . 46
Figure 22. von Mises stress contour for 12-inch POP drum at 11.3 MPa axial pressure . 47
Figure 23. The finite element mesh and boundary conditions for the 12-inch POP hydrostatic test. 50
Figure 24. The finite element mesh and boundary conditions for the 6-inch POP hydrostatic test. 51
Figure 25. 12-inch POP hydrostatic test: Deformation with hydrostatic pressure 52
Figure 26. 6-inch POP hydrostatic test: Deformation with hydrostatic pressure 53
Figure 27. Pressure-volumetric strain curve for the 12-inch POP waste drum. 54
Figure 28. Pressure-volumetric strain curve for the 6-inch POP waste drum. 54
Figure 29. Simulated volumetric strain for POP compared to the standard 55-gal drum. 57

ACRONYMS

AMWTP	Advanced Mixed Waste Treatment Project
CCA	Compliance Certification Application
CRA	Compliance Recertification Application
CP	Confining Pressure
DOE	U.S. Department of Energy
D-P	Drucker-Prager
EPA	U.S. Environmental Protection Agency
FEM	Finite Element Method
HTS	Hydrostatic Test Simulation
M-C	Mohr-Coulomb
PA	Performance Assessment
POP	Pipe OverPack
PROP	PROPerty
QA	Quality Assurance
SNL	Sandia National Laboratories
TRU	Transuranic Waste
TTS	Triaxial Test Simulation
WIPP	Waste Isolation Pilot Plant
WTS	Westinghouse TRU Solutions
WWIS	WIPP Waste Information System
UTS	Uniaxial Test Simulation

Intentionally Blank

1 INTRODUCTION

The Waste Isolation Pilot Plant (WIPP) is an operating deep geological disposal system (repository) for radioactive waste. Additional information can be obtained from a continually updated Internet web page (http://www.wipp.carlsbad.nm.us). The facility is located in southeastern New Mexico, near Carlsbad, and situated 655 meters below the surface in a bedded salt formation. The WIPP has been certified as meeting regulatory requirements and has been receiving and disposing waste since the spring of 1999. The WIPP is to be "recertified" at least every five years, as part of the regulatory statutes. This report supports the compliance recertification application (CRA) by evaluating the structural mechanics of waste packages called pipe overpacks. These calculations were performed in lieu of laboratory experiments, such as the compression experiments on standard waste drums, which supported the original certification.

1.1 Background

The compliance certification of WIPP was predicated on many assumptions, including mechanical properties of the waste. As of this writing, the repository has received thousands of waste shipments, of which many contained waste packages significantly different from the basic 55-gallon drum configuration used in the original compliance disposal room calculations. This report examines the mechanical characteristics and response of one such waste package known as the pipe overpack or POP.

The structural response of the underground setting has been modeled many times over the years. The conceptual model for room closure describes salt creep into a disposal room, in which the rock salt impinges on the waste and compresses the waste until stress equilibrium is approached. The models for salt and other lithologies proximal to the rooms are well understood and documented (NRC, 1996). An appropriate model for waste deformation in response to the stresses and strains resulting from salt creep must be determined for a variety of waste packages. The waste constitutive model used in the compliance certification application (CCA) was developed from empirical stress-deformation results obtained from compression tests on surrogate waste in 55-gallon drums (Butcher et al., 1991). Similar test data for the POP waste configurations do not exist; however, the material properties of the elements of the composite POP package are known and parameters can be determined by modeling the POP waste package in compression. This report describes the analyses conducted to determine model parameters for the POP.

The motivation for these calculations derives from ongoing dialogue between the U.S. Department of Energy (DOE) and the U.S. Environmental Protection Agency (EPA) concerning the realization that assorted waste packages are being disposed at the WIPP (Gross, 2002). The inventory is recorded in exacting detail, which includes waste packaging. From the WIPP waste information system (WWIS) dated July 29, 2003 there are 39,415 total containers in Panel 1, of which 16,989 are POPs. Another notable example of a possible future waste package includes super-compacted wastes from the Advanced Mixed Waste Treatment Project (AMWTP) (Hansen et al., 2003). Both waste package configurations--POPs and AMWTP--are structurally more rigid than a typical 55-gallon waste drum, and may affect repository processes. The super-compacted AMWTP waste

and the waste in POPs could create stiff columns within the disposal rooms that can influence room closure. It is possible that rigid waste columns would increase overall waste porosity by shielding adjacent standard waste from compaction. This effect would be reflected in the porosity surface look-up table accessed for performance assessment (PA) calculations.

1.2 Objective

This analysis determines model parameters for the POP waste packages. It provides the details of the simulations from which the POP mechanical response can be compared to the constitutive model used in the final disposal room structural response calculations (Stone, 1997a). A subsequent report (Park and Hansen, 2003) will advance this information in concert with structural calculations to develop porosity surfaces for PA. The calculations reported here are required to define the structural response of the underground because the rigidity of the POP has not been determined via mechanical tests in the laboratory. If the POP crushes readily, the resulting porosity surface would replicate the baseline case determined for the 55-gallon drums. If the POP possess sufficient structural integrity that they tend to prop open the room, the resulting porosity surface would depart appreciably from the CCA baseline. Thus, an evaluation of the POP structural response has been approached computationally.

Once the parameters are determined for the volumetric plasticity model used by Stone (1997a), the effects on will be evaluated in a series of scoping calculations. Estimates of room closure will be made for a variety of waste-form columns to ascertain the bounds of closure and porosity surfaces. To implement new or different models for the waste forms, it is necessary to compute parameters for the waste constitutive model such as shear modulus, bulk modulus, deviatoric yield surface constants, and a pressure-volumetric strain function. In this analysis, laboratory tests for uniaxial, triaxial and hydrostatic stress conditions are simulated to compute model parameters for the POP waste configurations.

1.3 Analysis Overview

These analyses are prerequisite to comprehensive assessment of waste homogeneity outlined in Analysis Plan AP-107 (Hansen et al., 2003). Results will be described in three parts. The first quantifies the shear modulus and bulk modulus from the uniaxial test simulation. The second develops the deviatoric yield surface constants from the triaxial test simulation. The third yields the pressure-volumetric strain function from the hydrostatic test simulation. The results from these test simulations are then implemented in creep closure calculation of the disposal room to generate the porosity surface data. Figure 1 illustrates how these calculations feed into the flow diagram for calculating the porosity surface of the disposal room, thus providing input for PA analyses. This report includes the procedure to determine the parameters for the constitutive model of POP waste, as shown in the dotted box in Figure 1. The procedures and results of the creep closure analyses of disposal room using SANTOS will be reported in a subsequent report (Park and Hansen, 2003).

The quasistatic large deformation finite element code SANTOS (Stone, 1997b) version 2.1.7, installed on a Compaq Tru64 UNIX V5.1B, was used for these analyses. SANTOS 2.1.7 was qualified though 21 test cases and documented in accordance with Sandia Quality Assurance requirements in the Verification and Validation Plan/Validation Document for SANTOS 2.1.7 (WIPP PA, 2003).

1.4 Report Organization

Section 2 of this report illustrates the precise detail of the POP containers and reviews the mechanical properties for each of the elemental materials included in the waste package. Section 2 also includes design drawings, material properties, and descriptions of the constitutive models used in the analyses. Section 3 documents the computer codes and file name conventions used for these analyses. The subsequent sections provide the simulations of the uniaxial, triaxial and hydrostatic tests, respectively. Each section includes a figure of the model grid, boundary conditions, loading conditions, deformed shapes, and results. In Section 4, the uniaxial test simulation produces shear, bulk, and Young's moduli and Poisson's Ratio. Section 5 describes the triaxial test simulation, showing that yielding is not pressure sensitive. The hydrostatic test simulation described in Section 6 is used to develop the pressure-volumetric strain function. Section 7 discusses the modeling results, relates how this information is subsequently used in structural calculations of the disposal room, and provides concluding remarks.

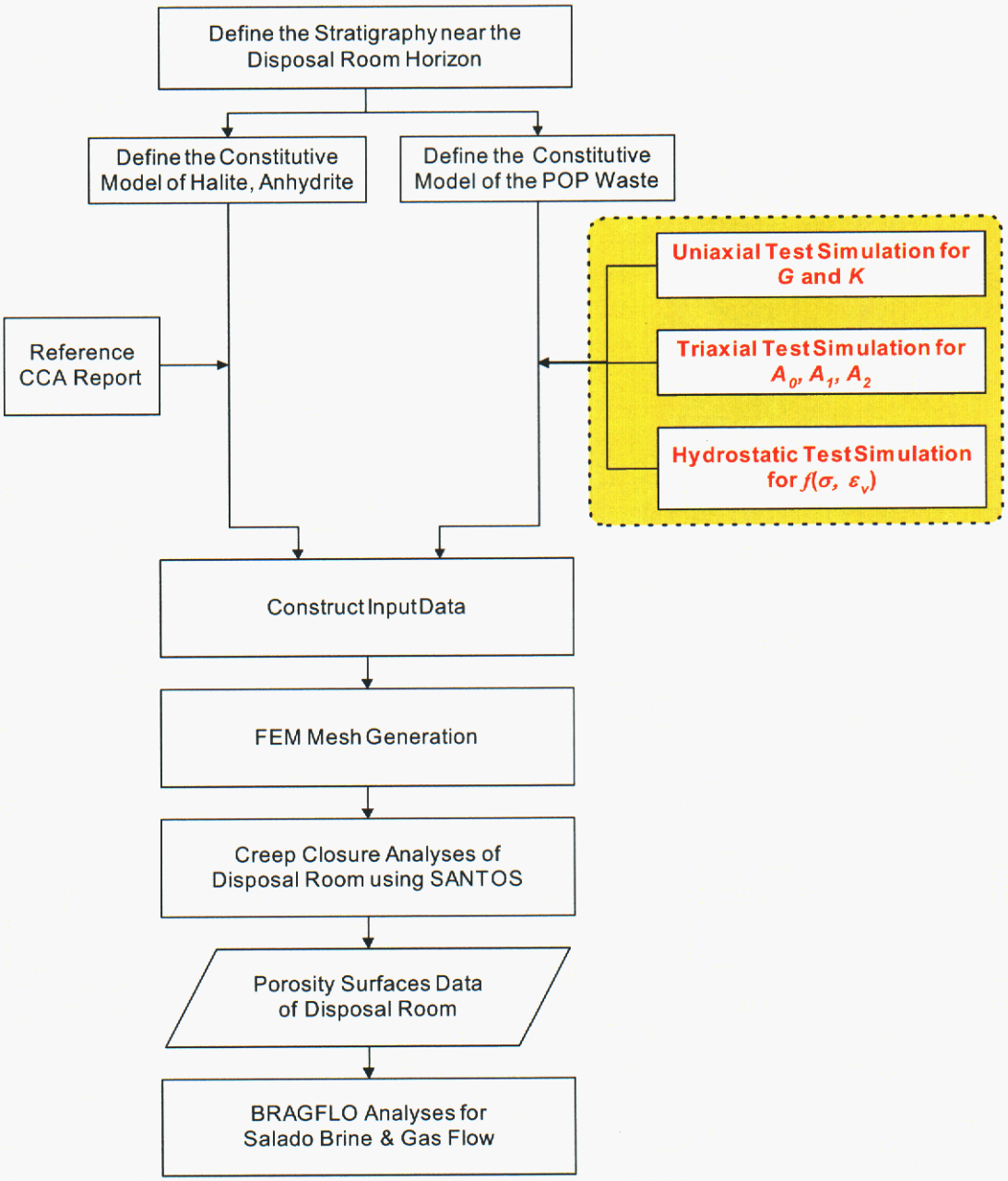

Figure 1. Activity flow diagram for calculating the porosity surface of the disposal room containing the POP waste.

2 ANALYSIS MODEL

2.1 Configuration

The pipe-overpack configuration has been used to ship TRU wastes to WIPP. The filled pipe component is surrounded by an impact limiter and placed inside a 55-gallon standard waste drum. Figure 2 includes a photograph of an actual pipe element and a schematic illustrating the assembly. The protective packing (impact limiter) is typically fabricated from polyethylene or a dense fiberboard. The pipe component and impact limiter have three key functions: (1) maintain separation of fissile material to prevent criticality, (2) provide radiation shielding, and (3) immobilize fine particulate waste materials. The POP has been used extensively for wastes from the Rocky Flats site, which comprise approximately half the disposed drums in Panel 1 of the repository.

Two different inner pipe sections are considered in these analyses. One has a 12-inch diameter pipe and the other uses a 6-inch diameter pipe section. Design drawings are shown in Figures 3 and 4, respectively. The actual design dimensions are used to generate the finite element meshes, as shown in Figures 5 and 6, respectively.

The standard POP consists of a standard 55-gallon drum outer shell, a heavy plastic liner, impact-limiting material (protective packing) and a stainless steel inner cylinder. The standard 55-gallon drum is approximately 23 inches in diameter by 32 inches in height. The drum is made of mild carbon steel with a nominal wall thickness of 0.055 inches. The plastic liner just inside of the steel drum is included in the design to meet shipping requirements. The impact-limiting material consists of layers of Celotex® glued together. The inner package is either a stainless steel pipe section with a welded end plate or a formed cylinder with a welded flange and a bolted blind flange. The inner package rests on a plywood disc. Leak tightness is achieved with O-ring seals between the flanges (Ludwigsen et al., 1998). The wall thicknesses are minimum 0.219 inches for the 12-inch diameter pipe section and minimum 0.245 inches for the 6-inch diameter.

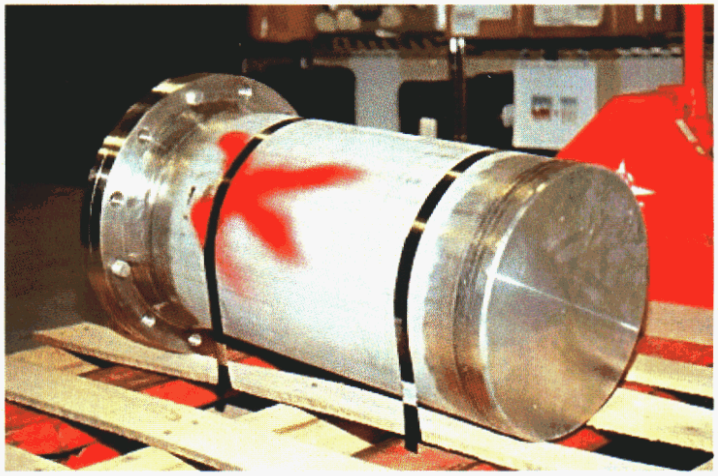

Figure 2. Photograph of a pipe and a schematic of pipe overpack configuration.

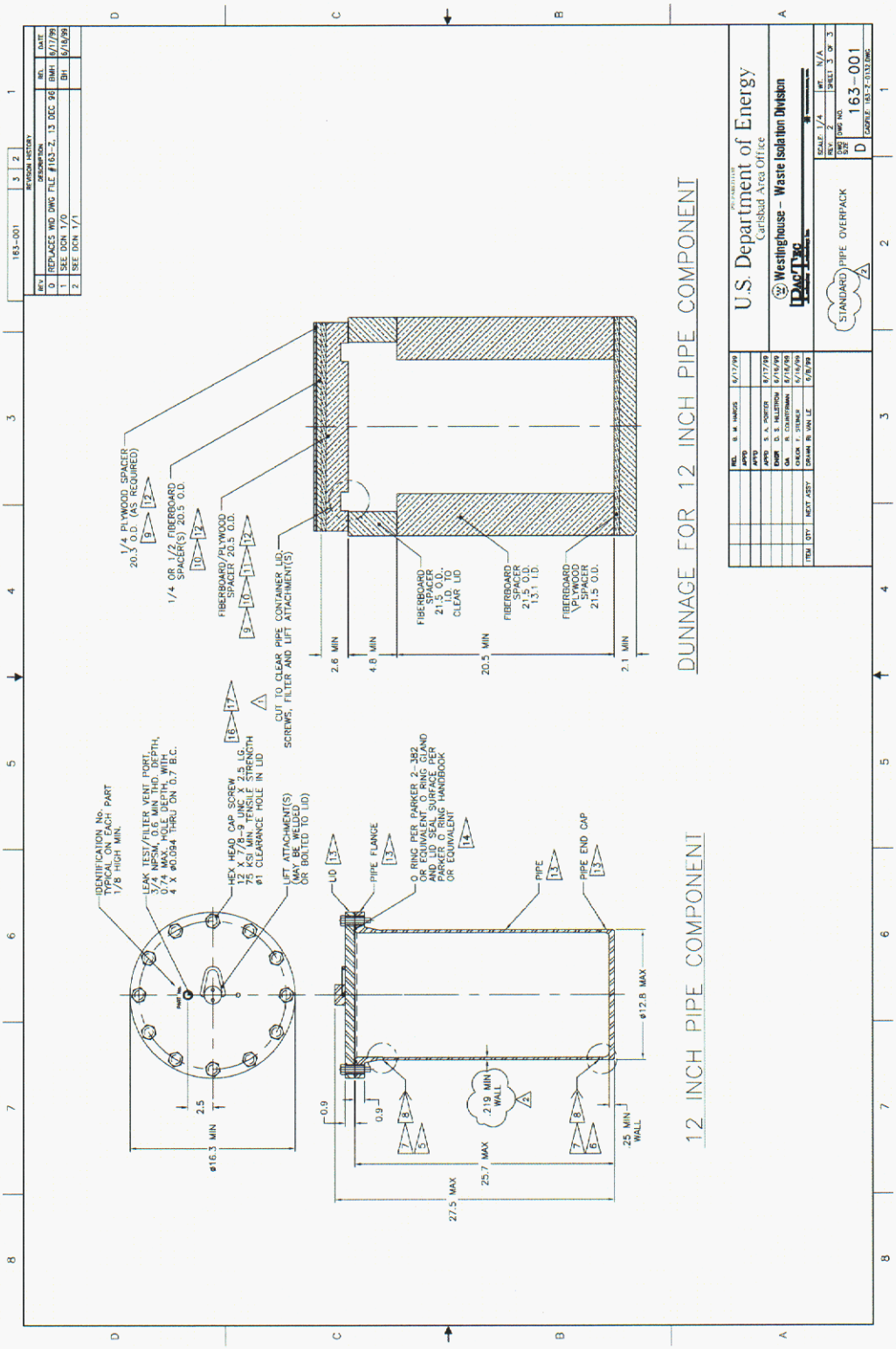

Figure 3. Drawing of 12-inch POP components (WTS, 2003)

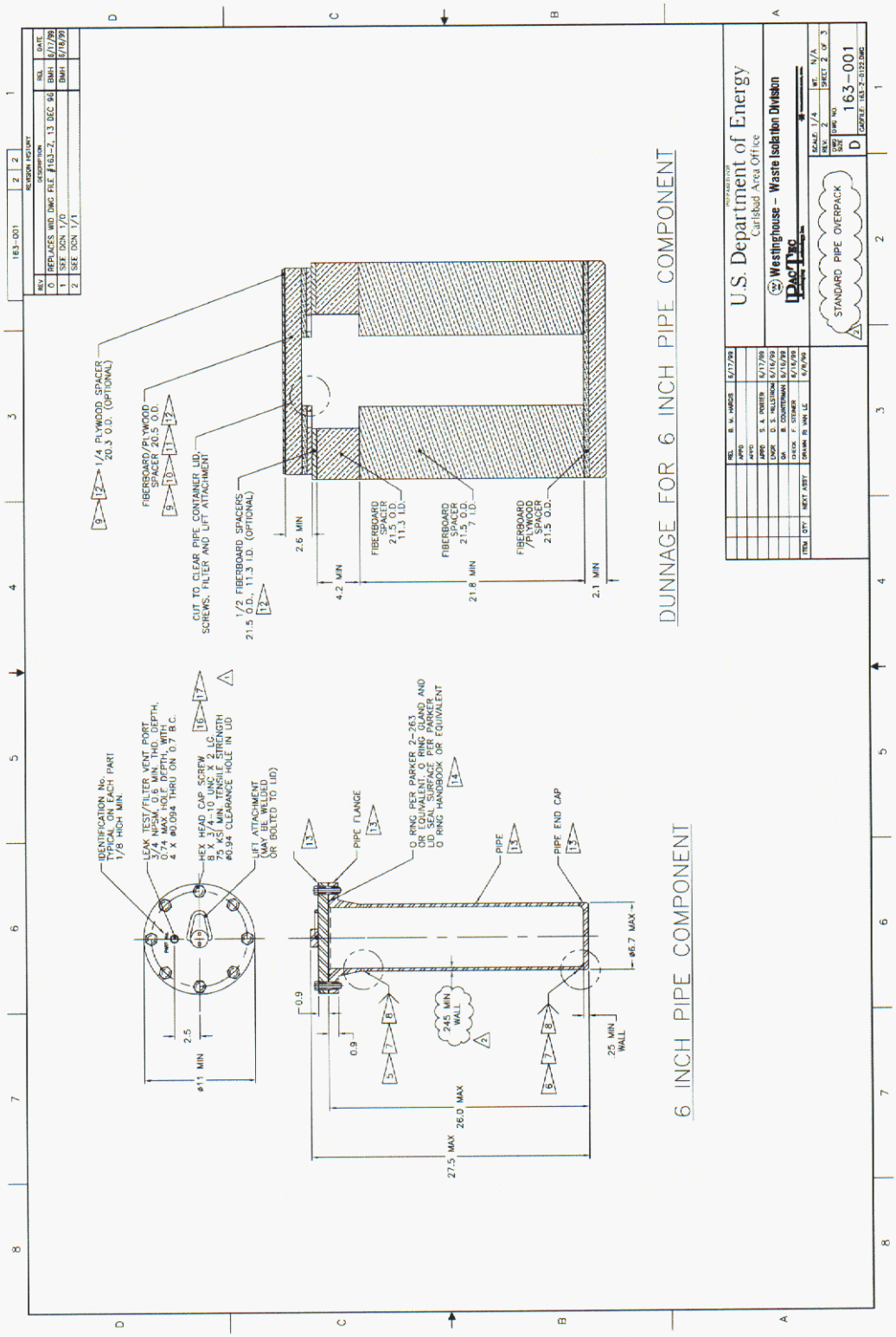

Figure 4. Drawing of 6-inch POP components (WTS, 2003)

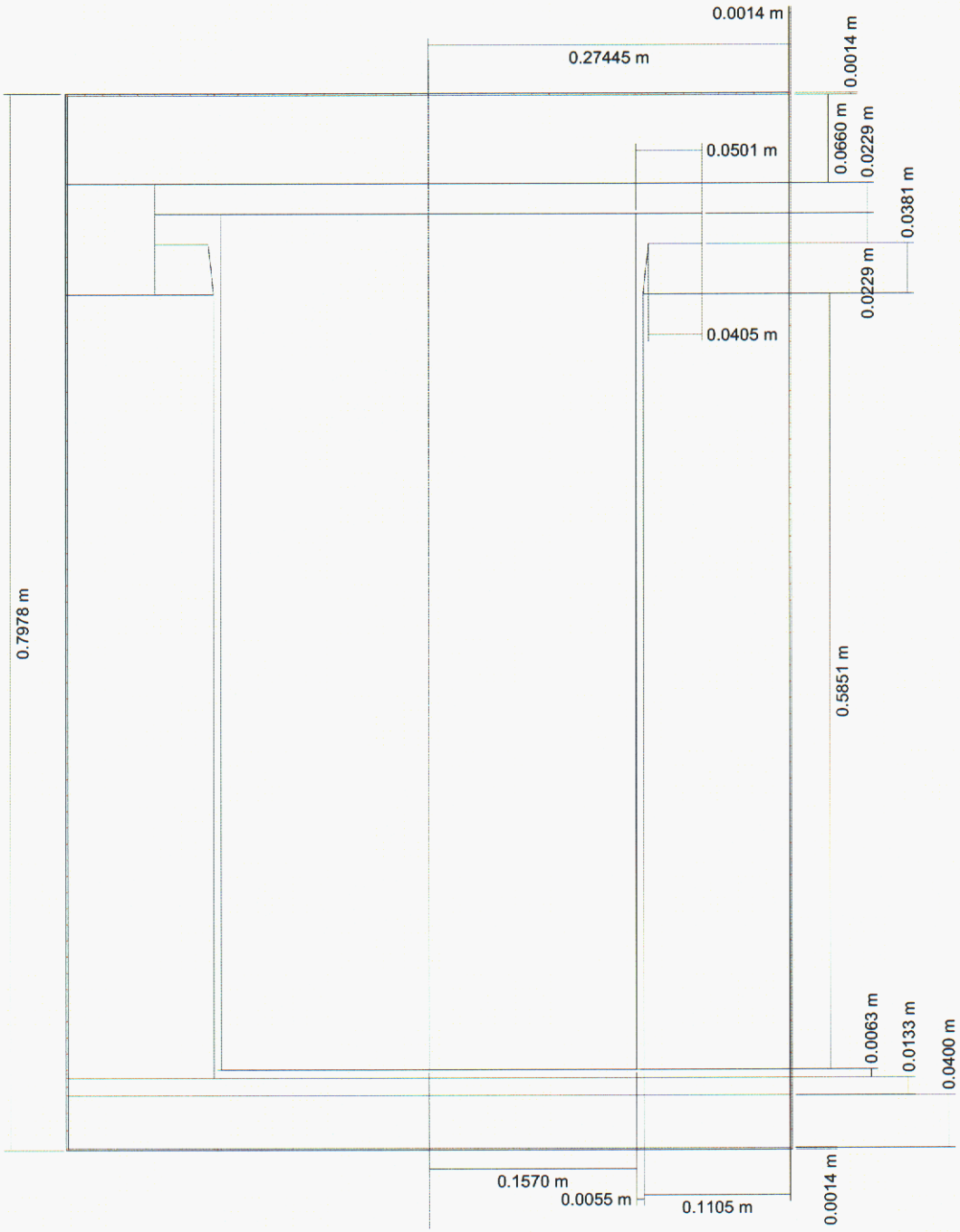

Figure 5. Simplified 12-inch POP drawing for mesh generation

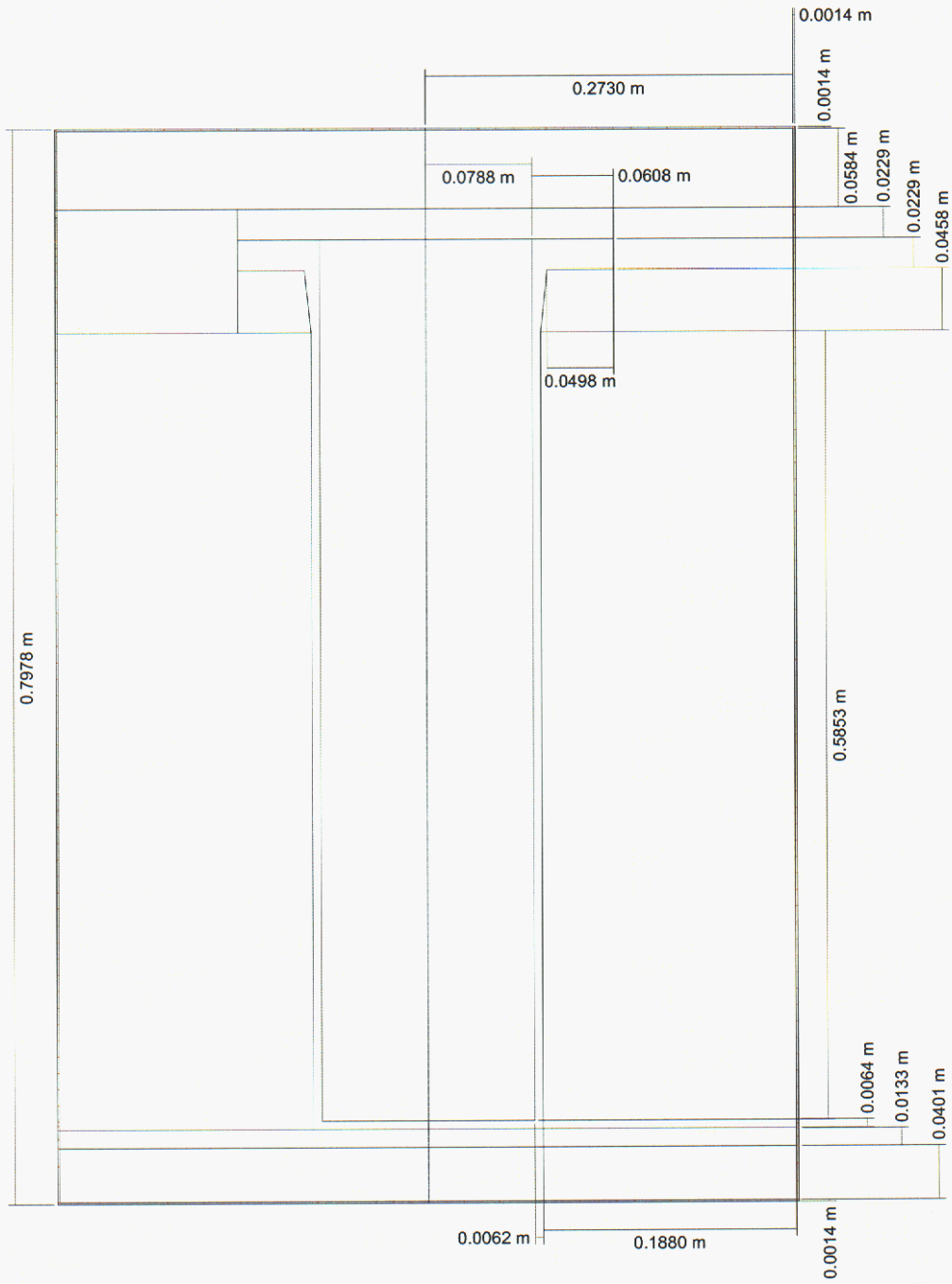

Figure 6. Simplified 6-inch POP drawing for mesh generation

2.2 *Material Properties*

The stainless steel material in the inner pipe was modeled with a realistic analytical material model based on an elastic-plastic power law hardening material (Stone, 1997b) to represent the post-yield plasticity of the material. The upper rigid platen for applying the axial pressure on the drum also was modeled, based on an elastic-plastic power law hardening material. All other materials were modeled with an elastic-plastic material with combined kinematic and isotropic hardening (Stone, 1997b). These materials include the outer steel drum, Celotex® impact limiter, the plywood which contributes little to the behavior of overpack, and the contents. The material properties used in this analysis are shown in Tables 1 and 2. It should be noted that dynamic analyses of the POP have been completed previously by Ludwigsen and co-workers and the material properties used here were excerpted from their report (Ludwigsen et al., 1998).

Table 1. Material properties for elastic-plastic power law hardening material

	Stainless Steel Grade 304 (Ludwigsen et al., 1998)	Rigid Upper Platen (WIPP PA, 2003)
Density (kg/m^3)	7908	1
Young's Modulus (Pa)	1.931×10^{11}	30.0×10^{11}
Poisson's Ratio	0.27	0.3
Yield Stress (Pa)	1.931×10^{8}	1.931×10^{9}
Hardening Constant (Pa)	1.329×10^{9}	1.329×10^{9}
Hardening Exponent	0.74819	0.74819
Luders Strain	0.0	0.0

Table 2. Material properties for elastic plastic material with combined kinematic and isotropic hardening (Ludwigsen et al., 1998)

	Celotex®	Plywood	Contents	Drum Shell
Density (kg/m^3)	256.485	427.476	256.485	7908.0
Young's Modulus (Pa)	6.895×10^{7}	3.103×10^{7}	6.895×10^{7}	1.931×10^{11}
Poisson's Ratio	0.05	0.2	0.2	0.27
Yield Stress (Pa)	3.447×10^{5}	3.477×10^{6}	1.724×10^{5}	2.785×10^{8}
Hardening Modulus (Pa)	2.413×10^{7}	6.895×10^{4}	0.0	6.895×10^{7}
Beta	0.5	0.5	0.0	0.0

The pipe material and the upper platen material described in Table 1 are represented by an elastic-plastic material model with a power law representation of strain hardening. Before yielding stresses are reached, the material is assumed elastic. After the elastic limit of the material is reached, the stress-strain relationship can be represented by the power-law relationship shown in Equation 1 (Stone, 1997b).

$$\bar{\sigma} = \sigma_y + A(\bar{\varepsilon}_p - \varepsilon_L)^n \quad (1)$$

where, $\bar{\sigma}$ = Effective stress state

$\bar{\varepsilon}_p$ = Equivalent plastic strain

σ_y = Initial yield stress

ε_L = Lüders strain or yield plateau strain

A = Hardening constant

n = Hardening exponent

The Lüders strain is the flat region of plasticity just after yield, which is common in mild carbon steels. For the stainless steel grade 304 used in the model, the Lüders strain is negligible and has been set to zero.

The elastic-plastic material model used to model the carbon steel drum, Celotex®, Plywood and the contents has an elastic region up to the yield stress limit and a linear hardening region after yield. Unloading would proceed along a line parallel to the elastic portion of the stress strain curve. The beta constant is a kinematic hardening term that becomes significant when load reversals exist. No load reversal is expected in these analyses, so this term has minimal influence on the results, if any.

The steel drum is modeled with typical values for high strength and mild carbon steels. The Celotex® parameters are based upon uniaxial test data of Celotex® samples. The Celotex® has a small initial yield strength followed by a relatively flat and long plasticity region. The waste contents were modeled as a very compliant material with a density similar to wood. To be conservative, the waste inside the pipe was modeled as contributing little to the stiffness of the inner cylinder.

2.3 Waste Constitutive Model

The stress-strain behavior of the waste was represented by a volumetric plasticity model (Stone, 1997a) with a piecewise linear function defining the relationship between the mean stress and the volumetric strain. Compaction experiments on simulated waste were used to develop this relationship in support of the CCA. The deviatoric response of the waste material was not measured in the experiments. It was anticipated that when a drum filled with loosely compacted waste is compressed axially, the drum will not undergo significant lateral expansion until most of the void space inside the drum has been eliminated.

The volumetric plasticity model is implemented exactly as Stone (1997) developed it for the CCA calculations. The yield surface in the principal stress space is a surface of revolution with its axis centered about the hydrostat and the open end pointing into the compression direction (Figure 7). The open end is capped with a plane that is at right angles to the hydrostat. The deviatoric part is elastic-perfectly plastic so the surface of revolution is stationary in the stress space. The volumetric part has variable strain hardening so the end plane moves outward during volumetric yielding. The volumetric hardening is defined by a set of pressure-volumetric strain relations. A flow rule is used such that devia-

toric strains produce no volume change (associated flow). The model is best broken into volumetric and deviatoric parts with the deviatoric part resembling conventional plasticity. The volumetric yield function is a product of two functions, ϕ_{yd} and ϕ_p.

The yield surface assumed is a surface of revolution about the hydrostat in principal stress space as shown in Figure 7. In addition, a planar end cap on the normally open end is assumed. The yield stress is specified as a polynomial in pressure, p (positive in compression) as

$$\phi_{yd} = a_0 + a_1 p + a_2 p^2 \tag{2}$$

where, a_0, a_1, a_2 are constants defining the deviatoric yield surface, p is the pressure.

The plasticity theories for the volumetric and deviatoric parts of the material response are completely uncoupled. The volumetric response is computed first. The mean pressure, p, is assumed to be positive in compression, and a yield functions is written for the volumetric responses as

$$\phi_p = p - g(\varepsilon_v) \tag{3}$$

where, ε_v is the volumetric strain. The form of g is defined in this problem by a set of piecewise linear segments relating to the pressure-volumetric strain (Stone, 1997b).

This report describes the procedure to compute the SANTOS input data for the POP configuration. The input data consist of the elastic material parameters derived from the uniaxial test simulation, constants defining the yield surface as shown in Figure 7 through the triaxial test simulation, and the pressure-volumetric strain through the hydrostatic test simulation. The POP waste constitutive model corresponds to the soil and crushable foams model which is discussed in more detail in the SANTOS code description document (Stone, 1997b).

The SANTOS input parameters of the soil and crushable foams model contains the following entries:

- PROP (1) - 2μ
- PROP (2) - K : Bulk Modulus
- PROP (3) - A_0
- PROP (4) - A_1
- PROP (5) - A_2
- PROP (6) – Function ID number: Pressure-volumetric strain curve

Note that the material constants A_0, A_1 and A_2 are different from a_0, a_1 and a_2, as discussed in Section 5.1.

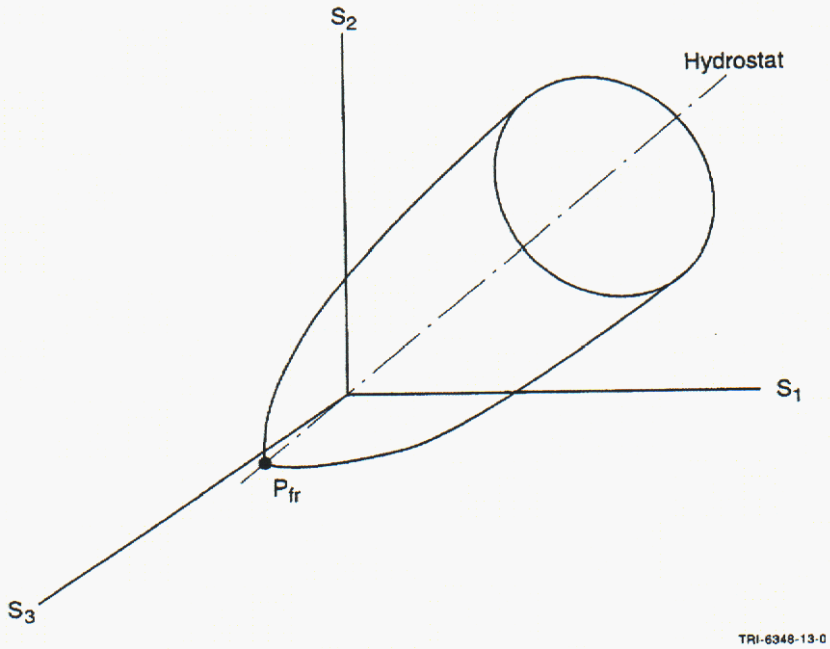

Figure 7. Pressure-dependent yield surface for the waste material model (Stone, 1997b)

3 COMPUTER CODES AND FILE NAME CONVENTION

3.1 Computer Codes

FASTQ version 3.12 is used for generating the FEM mesh for the POP waste drum. The input file for the FASTQ mesh generation is provided in Appendix B. The FASTQ code is an interactive two-dimensional finite element mesh generation program. It is designed to provide a powerful and efficient tool to both reduce the time required of an analyst to generate a mesh, and to improve the capacity to generate good meshes in arbitrary geometries. It has a number of meshing techniques available. FASTQ has been designed to allow user flexibility and control. The user interface is built on a layered command level structure. Multiple utilities are provided for input, manipulation, and display of the geometric information, as well as for direct control, adjustment, and display of the generated mesh. Enhanced boundary flagging has been incorporated and multiple element types and output formats are supported. FASTQ includes adaptive meshing capabilities with error estimation, deformed and undeformed remeshing according to the error, element variable remapping, and some basic post-processing plotting (Blacker, 1988).

SANTOS version 2.1.7 is used for the solver in this analysis. The quasistatic, large-deformation finite element code SANTOS is capable of representing 2D planar or axisymmetric solids (Stone, 1997b). The solution strategy, used to obtain the equilibrium states, is based on a self-adaptive, dynamic-relaxation solution scheme incorporating proportional damping. The explicit nature of the code means that no stiffness matrix is formed or factorized which results in a reduction in computer storage necessary for execution. The element used in SANTOS is a uniform-strain, 4-node, quadrilateral element with an hourglass control scheme to minimize the effects of spurious deformation modes. Finite strain constitutive models for many common engineering materials are available within the code. A robust master-slave contact algorithm for modeling arbitrary sliding contact is implemented. SANTOS version 2.1.7 was installed on the Compaq Tru64 with the UNIX V5.1B. All of the verification and qualification test problems were exercised and documented in accordance with QA requirements (WIPP PA, 2003).

BLOTII2 version 1.39 is used as the final post-processor. The deformation of the drum with uniaxial pressure, triaxial pressure, and hydrostatic pressure are plotted using BLOT. BLOT is a graphics program for post-processing of finite element analyses output in the EXODUS database format. It is command driven with free-format input and can drive any graphics device supported by the Sandia Virtual Device Interface. BLOT produces mesh plots with various representations of the analysis output variables. The major mesh plot capabilities are deformed mesh plots, line contours, filled (painted) contours, vector plots of two/three variables (e.g., velocity vectors), and symbol plots of scalar variables (e.g., discrete cracks). Path lines of analysis variables can also be drawn on the mesh. BLOT's features include element selection by material, element birth and death, multiple views for combining several displays on each plot, symmetry mirroring, and node and element numbering. BLOT can also produce X-Y curve plots of the analysis variables. BLOT generates time-versus-variable plots or variable-versus-variable plots. It also generates distance-versus-variable plots at selected time steps where the distance is the accumulated distance between pairs of nodes or element centers (Gilkey and Glick, 1989).

To calculate the volume change of the POP drum with time, NUMBERS version 1.19 is used. NUMBERS is a shell program that reads and stores data from a finite element model described in the EXODUS database format. Within this program are several utility routines that generate information about the finite element model. The utilities currently implemented in NUMBERS allow the analyst to determine information such as: (1) the volume and coordinate limits of each of the materials in the model; (2) the mass properties of the model; (3) the minimum, maximum, and average element volumes for each material; (4) the volume and change in volume of a cavity; (5) the nodes or elements that are within a specified distance from a user-defined point, line, or plane; (6) an estimate of the explicit central-difference time step for each material; (7) the validity of contact surfaces or slide lines, that is, whether two surfaces overlap at any point; and (8) the distance between two surfaces (Sjaardema, 1989).

These pre- and post-processing utilities are considered systems software and not subject to the requirements of NP 19-1 (Chavez, 2003).

3.2 File Naming Convention

The general path for any of these subdirectories is: /**/waste/. All of the files related to the analyses for the uniaxial test simulation for the 12-inch POP exist in the subdirectory of /**/waste/pop/uni/. Files related to the triaxial test simulation for the 12-inch POP are in the subdirectory of /**/waste/pop/tri/. Files related to the hydrostatic simulation for the 12-inch POP are in the subdirectory of /**/waste/pop/hyd/.

Similarly, all of the files related to the analyses for the uniaxial test simulation for the 6-inch POP exist in the subdirectory of /**/waste/pop6/uni/. Files related to the triaxial test simulation for the 6-inch POP are in the subdirectory of /**/waste/pop6/tri/. Files related to the hydrostatic simulation for the 6-inch POP are in the subdirectory of /**/waste/pop6/hyd/.

All of the files that remain within each subdirectory are listed and described in Table 3.

The prefix of the files, d12_ denotes the 12-inch POP and d06_ denotes the 6-inch POP. In ~/tri/, the suffix of the files, 0.5mpa, 1.0mpa, …, etc. express the confining pressure in the triaxial test simulation, i.e., 0.5mpa means the confining pressure is 0.5 MPa.

Table 3. File naming convention (* means wild card)

File Prefix/Suffix	File Definition
*.fsq	The FASTQ input files for the mesh generation
*.g	The FASTQ output files that will be used for the mesh file of SANTOS
*.i	The SANTOS input files
*.e	The SANTOS output files in the EXODUS database format
*.o	The SANTOS output files in the ASCII format
*.num	The NUMBERS output file in the ASCII format to calculate the volume change of the drum with time from the SANTOS output files, *.e
*.run	The batch files for running SANTOS
Pres-Vol strain_*.xls	The excel file to calculate the pressure-volume strain data
E-Poisson_*.xls	The excel file to calculate the Young's modulus and Poisson's ratio
TwoMu and K_*.mcd	The MathCad file to calculate shear and bulk modulus
_A0 N A1.mcd	The MathCad file to calculate the yield surface constants

4 UNIAXIAL TEST SIMULATION

4.1 Theoretical Background

As discussed in Section 2.3, the input to the soil and crushable foam model in the SANTOS code requires the analyst to provide TWO MU (2μ) and BULK MODULUS (K). The conversion from Young's modulus, E, and Poisson's ratio, ν, to the SANTOS input parameters is given from the following relationships taken from Fung (1965):

$$2\mu = \frac{E}{(1+\nu)} \tag{4}$$

$$K = \frac{E}{3(1-2\nu)} \tag{5}$$

To calculate 2μ and K, Young's modulus, E, and Poisson's ratio, ν, of the POP drum are calculated first. These values can be derived from an experimental uniaxial test of the drum in the laboratory. For this analysis, these values are derived from the numerical simulation of the experimental uniaxial test.

Linear relations between the components of stress and the components of strain are known generally as Hooke's law, where unit deformation of the element up to the proportional limit is given by:

$$\varepsilon_x = \frac{\sigma_x}{E} \tag{6}$$

in which E is the modulus of elasticity (Timoshenko and Goodier, 1970). In this uniaxial simulation, the axial strain is derived from the vertical displacement of the upper platen with the axial pressure.

This compression of the element in the x direction is accompanied by lateral strain components, such that:

$$\varepsilon_{lateral} = -\nu \cdot \varepsilon_{axial} \tag{7}$$

in which the constant of proportionality ν is Poisson's ratio.

In this simulation, the volume and the axial displacement of the drum with the axial pressure will be computed through the uniaxial test simulation. The average cross sectional area of the drum will be calculated from the instantaneous volume divided by the changed height of the drum. The radial strain will be derived from the cross sectional area. The Poisson's ratio is obtained from the lateral strain divided by the axial strain of the drum.

4.2 Mesh Generation and Simulation

Figure 8 shows the mesh discretization and the boundary conditions for the 12-inch POP uniaxial test simulation. Making use of axisymmetry, only half section of the drum is modeled from the drawings illustrated in Figures 5 and 6. The left boundary is the axis of axisymmetry and the right boundary is free. The uniform pressure is applied on the top of the upper platen from 0.0 MPa to 16.0 MPa in 16,000 seconds. The increasing rate of the axial load is 1,000 Pa/s. The model contains 1,767 axisymmetric uniform strain quadrilateral elements and 1,876 nodal points. A zero-displacement boundary condition in the radial direction (U_x=0.0) was applied on the left boundary of the model to represent the axisymmetry condition of the drum. A zero displacement boundary condition (U_y=0.0) was applied on the lower boundary to react to the applied load. Note that the drum shell element looks like a solid line because it is thin (0.0014 m).

Similarly, Figure 9 shows the discretized FEM mesh and boundary conditions for the 6-inch POP uniaxial test simulation. The 6-inch pipe instead of the 12-inch pipe is contained in the drum and the boundary conditions are the same as those used for the 12-inch POP. The model contains 1,763 axisymmetric uniform strain quadrilateral elements and 1,873 nodal points. The FASTQ input files used to generate the mesh for 12-inch POP and 6-inch POP are provided in Appendix B-1 and B-2 respectively. An example of a SANTOS input file used to simulate the uniaxial test for 12-inch POP is provided in Appendix C-1.

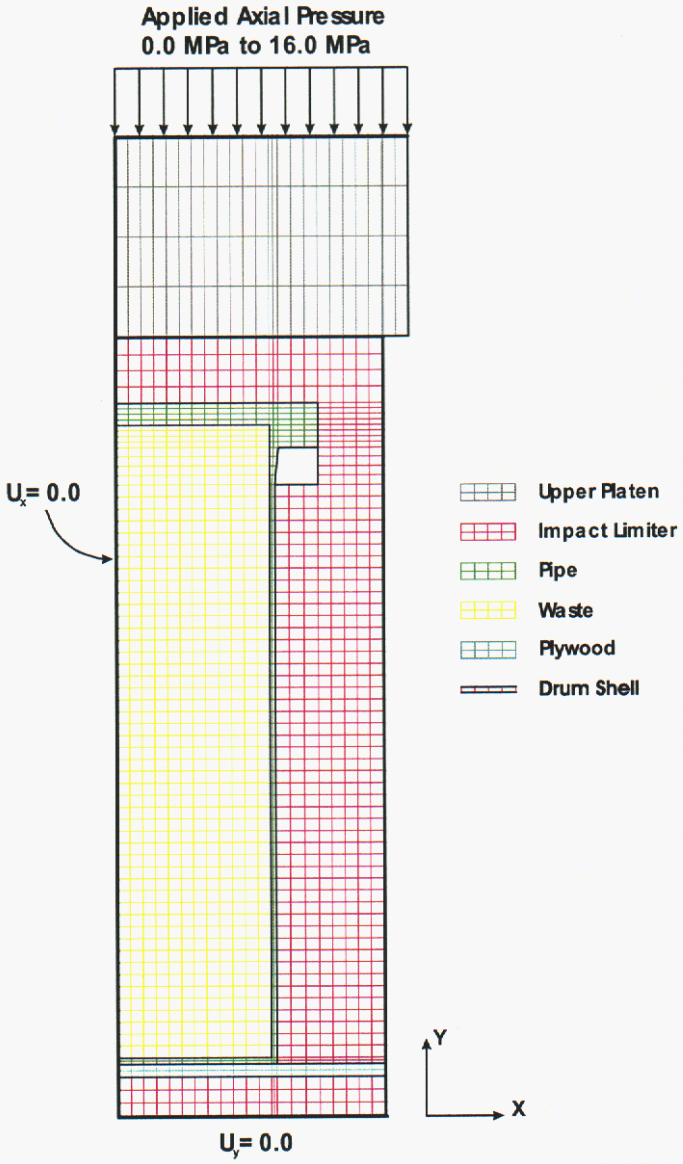

Figure 8. The finite element mesh and boundary conditions for the 12-inch POP uniaxial test.

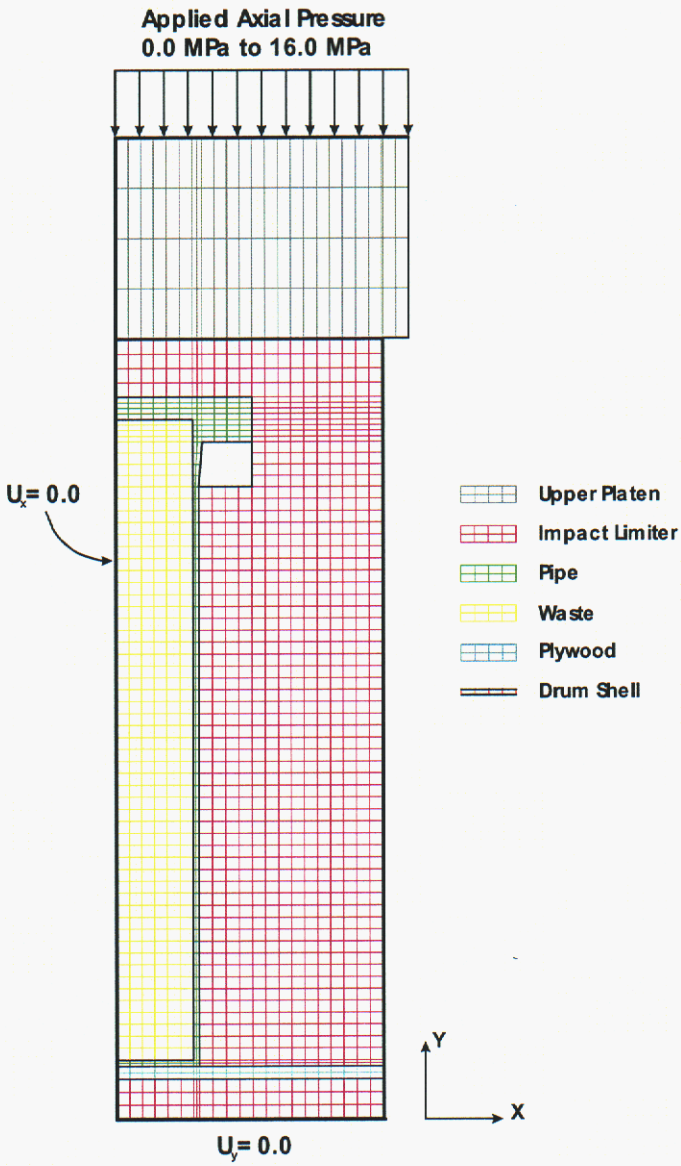

Figure 9. The finite element mesh and boundary conditions for the 6-inch POP uniaxial test.

4.3 Simulation Results

4.3.1 Deformation pattern

Figure 10 shows the deformation pattern of 12-inch POP model on which the axial pressure is applied from 0.0 MPa to 13 MPa at a rate of 1,000 Pa/s. Owing to large strain, the solution fails to converge before 15 MPa, the lithostatic stress, is reached. This occurs in several simulations, but is not of a serious consequence to the conclusions of this effort, as discussed in Section 7. The buckling pattern of the drum shell and the pipe is similar to dynamic experimental test results obtained by Hoffman and Ammerman (1995). They carried out a series of tests investigating the dynamic pulse buckling of a cylindrical shell under axial impact and compared experimental to numerical simulations. They attribute the buckling pattern to load eccentricity relative to the shell wall caused by mid-length expansion of the shell, resulting in a bending moment being applied to shell wall. As the buckles form, a hardening moment develops (due to differential stress states through the wall thickness) which resists further curvature increases. Instability occurs when the applied bending moment is greater than the hardening moment, causing the larger of the two buckles to become unstable. These simulation results are felt to replicate these experimental deformation patterns reasonably well.

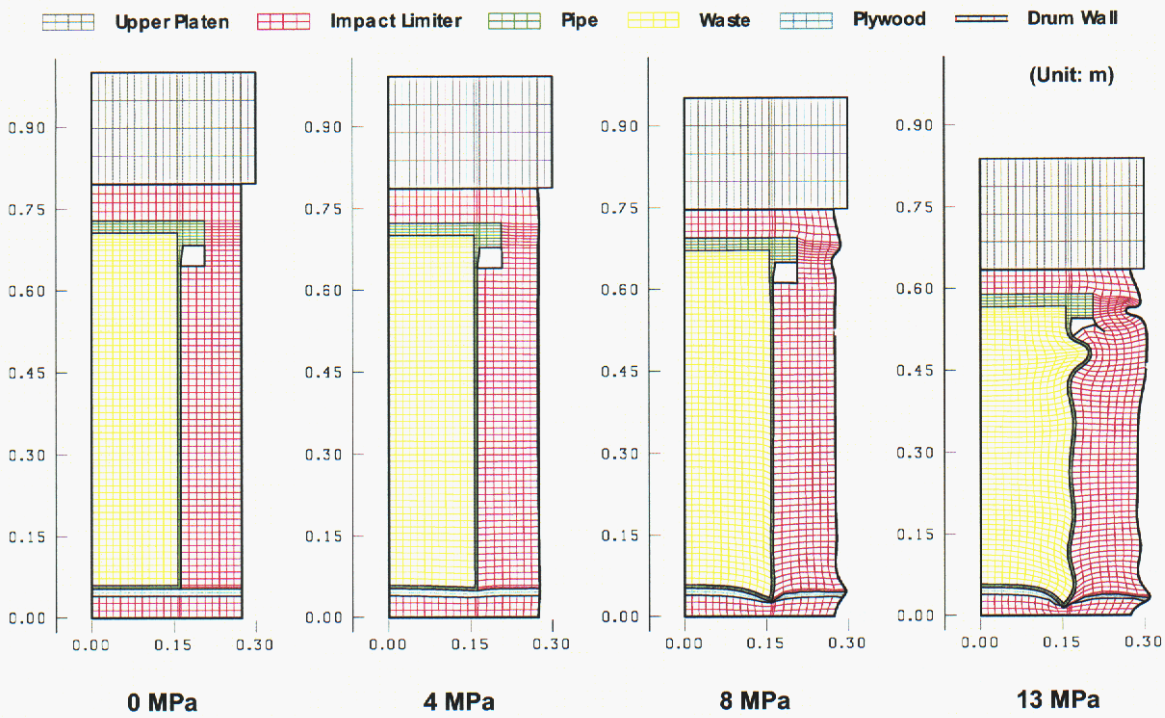

Figure 10. Deformation pattern of 12-inch POP from the uniaxial test simulation

Similarly, Figure 11 shows the deformation pattern of 6-inch POP from the uniaxial test simulation. The pattern is similar to the 12-inch POP's except the vertical displacement

of the 6-inch POP is slightly larger than 12-inch POP's. This result is reasonable because the cross sectional area of 6-inch stainless steel pipe is smaller and less rigid.

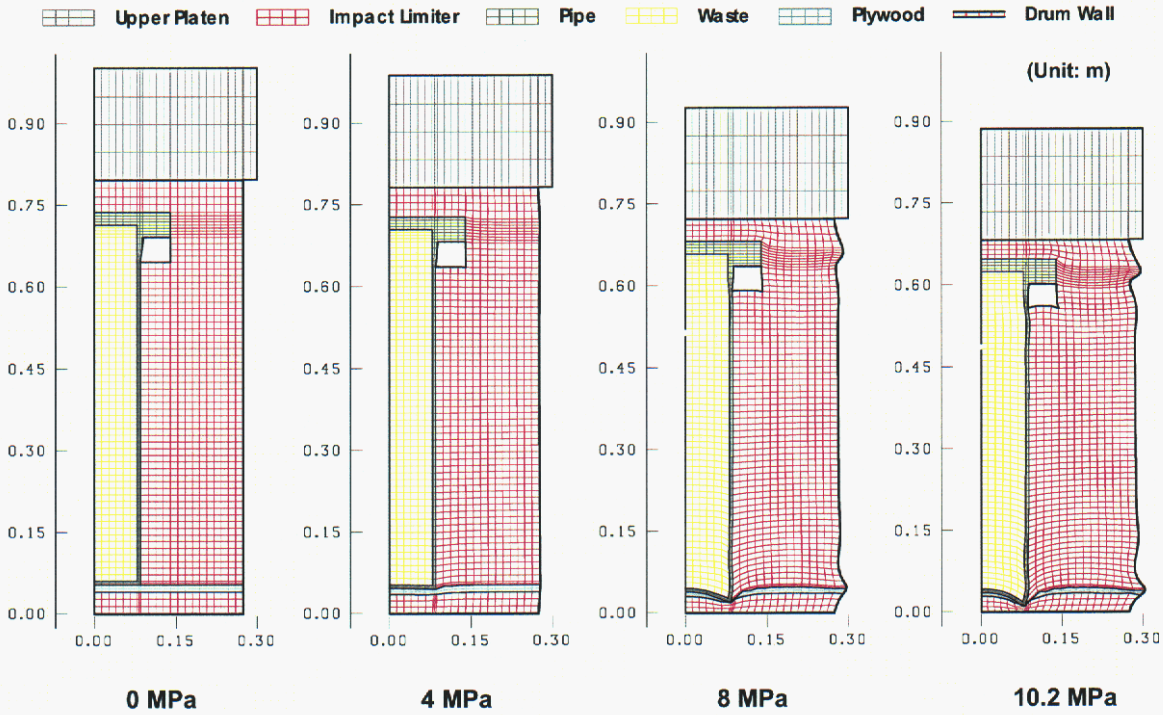

Figure 11. Deformation pattern of 6-inch POP from the uniaxial test simulation

4.3.2 Young's Modulus (E)

The axial stress-strain curve of 12-inch POP drum is plotted in Figure 12 and the axial stress-strain curve of 6-inch POP drum is plotted in Figure 13. The linear portions of the displacement are denoted as point A and point B on the plots, respectively. The slope of the line connected from zero to point A or point B is Young's Modulus. Young's Modulus of 12-inch POP drum is 1.874 GPa and is 1.804 GPa for the 6-inch POP. Obviously, the elastic response is a minor contributor to the overall deformation of these waste configurations.

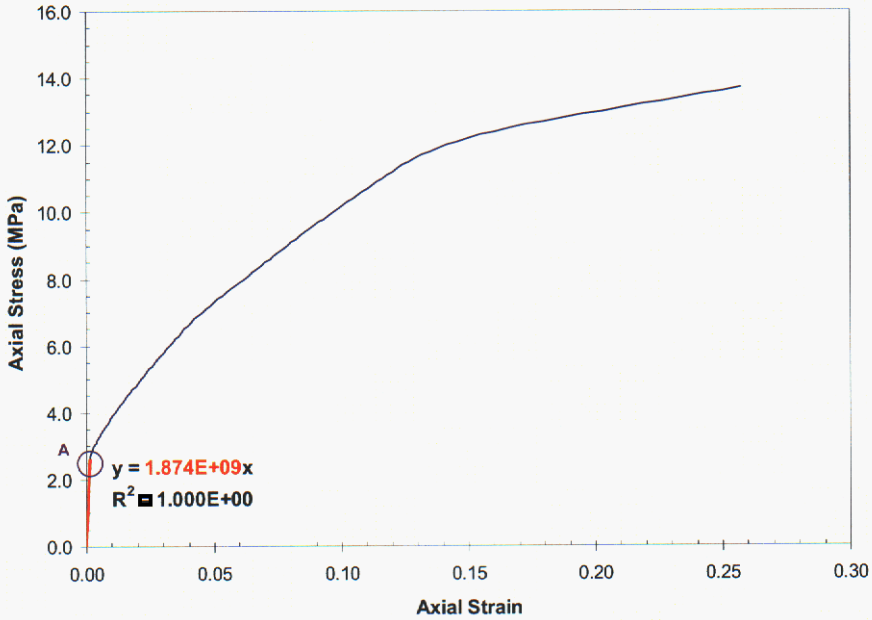

Figure 12. The axial stress-strain curve of 12-inch POP drum

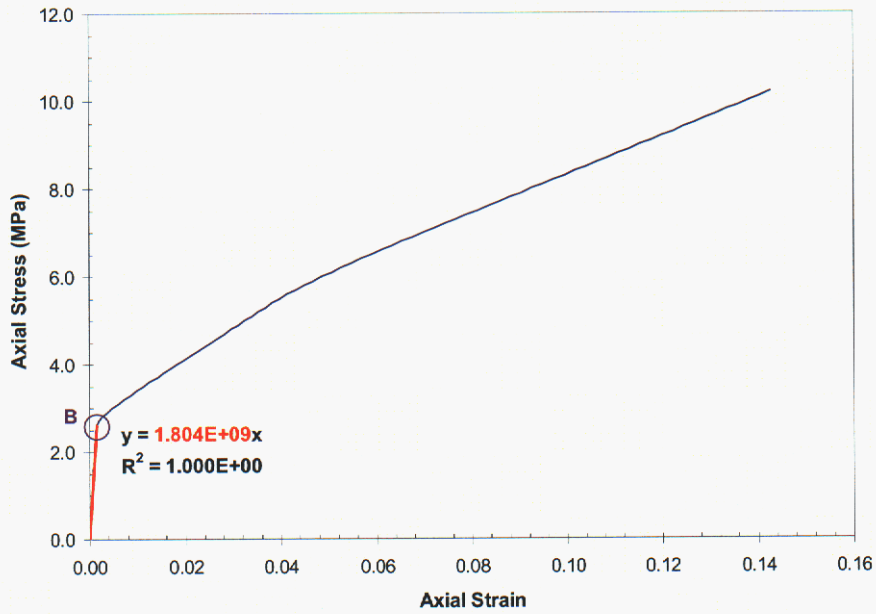

Figure 13. The axial stress-strain curve of 6-inch POP drum

4.3.3 Poisson's ratio (ν)

Poisson's ratio was determined over a larger region of strain than the elastic modulus because POP waste packages are composite materials. The radial strain-axial strain curve of 12-inch POP drum is plotted in Figure 14 and a similar plot for the 6-inch POP drum is plotted in Figure 15. The volume of the drum with the axial pressure is calculated first, because the radial strain along the drum wall is not uniform. The average cross sectional area of the drum is calculated from the changed volume divided by the changed height of the drum. The radial strain is derived from the changed cross section area. Poisson's ratio is obtained from the lateral strain divided by the axial strain of the drum. The regression line of the radial-axial strain curve is Poisson's ratio, which is 0.30 and 0.32 for the 12-inch POP and 6-inch POP, respectively.

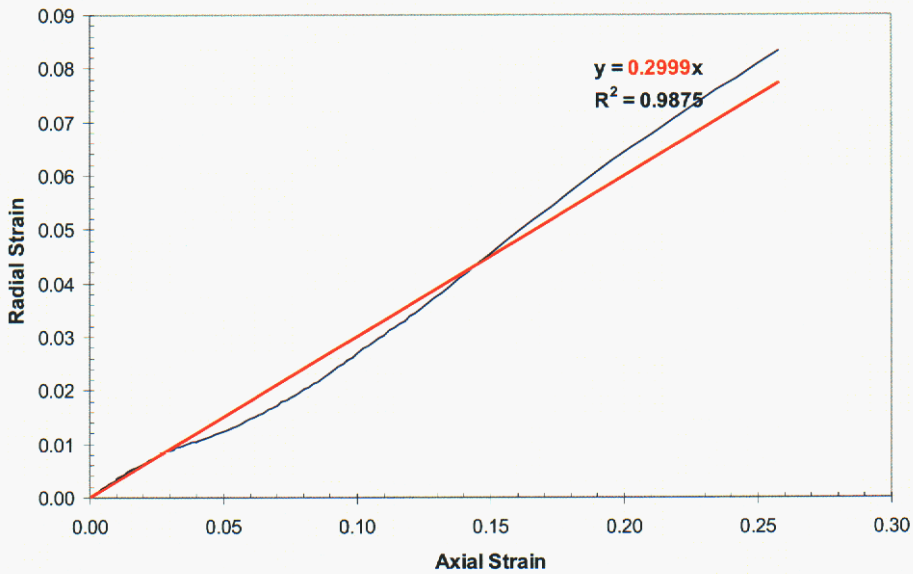

Figure 14: The radial-axial strain curve of 12-inch POP drum

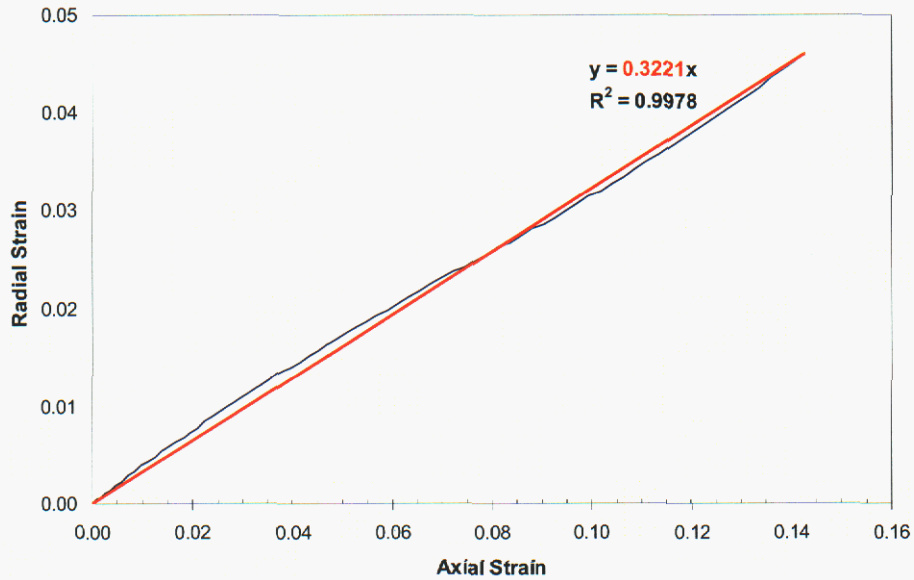

Figure 15: The radial-axial strain curve of 6-inch POP drum

4.3.4 Shear Modulus and Bulk Modulus

From the foregoing results, shear and bulk moduli are calculated as mentioned in Section 4.1. Substitution of the value E and ν into Equations (4) and (5) results in the shear modulus, G, and the bulk modulus, K, listed in Table 4. The calculation sheet to compute the above values is provided in Appendix A-1.

Table 4. The shear modulus and the bulk modulus of POP waste

	12-inch POP	6-inch POP
G (Two Mu) [Pa]	1.442×10^9	1.364×10^9
K [Pa]	1.561×10^9	1.690×10^9

5 TRIAXIAL TEST SIMULATION

5.1 Theoretical Background

In Butcher and Holmes (1995), the inelastic deviatoric response of the TRU waste is characterized by a constitutive equation of the form

$$J_2 = a_0 + a_1 p + a_2 p^2 \tag{8}$$

where J_2 is the second deviatoric stress invariant, p is the pressure (positive in compression), and a_0, a_1 and a_2 are material constants. Their material constants are defined for this particular form of deviatoric response. In SANTOS, the model for the waste is written in a different functional form

$$\bar{\sigma} = A_0 + A_1 p + A_2 p^2 \tag{9}$$

where $\bar{\sigma}$ is the von Mises equivalent stress and p is the pressure (positive in compression). The material constants A_0, A_1 and A_2 are different from a_0, a_1 and a_2.

The POP waste is considered isotropic and elastic until yield occurs. The yield function is assumed to be governed by the Drucker-Prager (D-P) criterion as follows:

$$\sqrt{J_2} = C - \alpha I_1 \tag{10}$$

where, I_1 = the first stress invariant

J_2 = the second deviatoric stress invariant

The constants α and C can be defined from conventional triaxial geotechnical tests. Later in this report, modeling results are presented using conventional Mohr-Coulomb (M-C) diagrams, so the relationship between D-P and M-C is highlighted here along with discussion of the yield function. Pressure sensitivity to failure is also commonly represented by the M-C criterion in two-dimensional stress space defined by two-constants cohesion, c, and friction angle, ϕ, in the following form

$$\tau = c + \sigma \tan\phi \tag{11}$$

The D-P criterion (10) is more commonly used in numerical analyses, whereas the M-C is convenient to illustrate the lack of pressure effects on the yield surface. This discussion is intended to set up the following discussion of the Mohr's circles for yield in Section 5.3.2. Figure 16 compares the D-P and M-C criteria and shows how the D-P inner circle coincides with the M-C polygon in extension and the D-P outer circle coincides with the M-C polygon in compression.

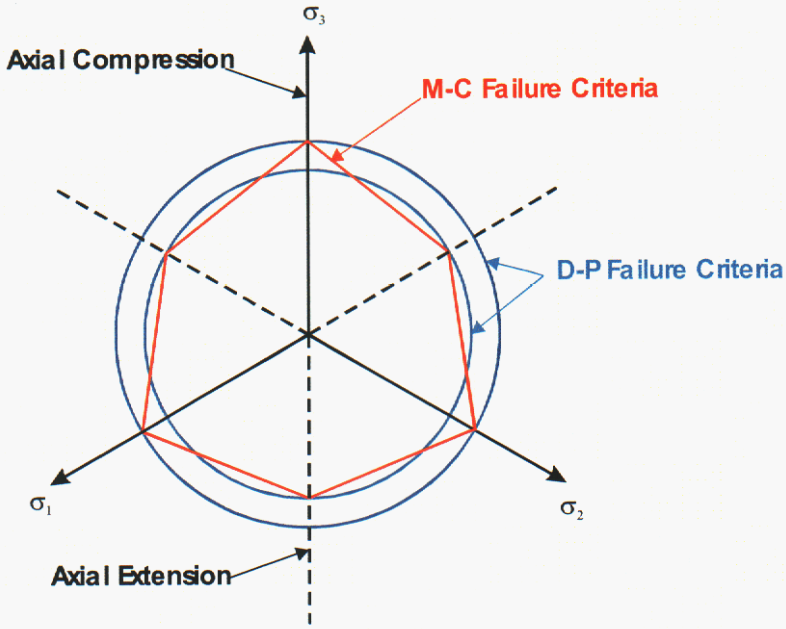

Figure 16. Deviatoric section of Mohr-Coulomb and Drucker-Prager criteria.

For the plane strain model, the relationships between D-P and M-C parameters derived by Zimmermann et al. (2001) are as follows:

$$\alpha = \sin\frac{\phi}{3}$$
$$C = c\cos\phi \tag{12}$$

The soil and foam model used in SANTOS was selected to represent the POP. Using Equation (12), D-P constants α and C are obtained from c and ϕ which are computed from the triaxial test simulation. SANTOS requires the input to the material model which describes the nonlinear response to be given in terms of effective stress, $\overline{\sigma} = \sqrt{3J_2}$, and pressure, $p = \frac{I_1}{3}$ (Butcher, 1997).

Rewriting Equation (9) in terms of $\overline{\sigma}$ and p, the following relationship is obtained:

$$\overline{\sigma} = \sqrt{3}C - 3\sqrt{3}\alpha p \tag{13}$$

Thus, the SANTOS input constant A_0, A_1 and A_2 are:

$$
\begin{aligned}
A_0 &= \sqrt{3}C \\
A_1 &= -3\sqrt{3}\alpha \\
A_2 &= 0
\end{aligned}
\tag{14}
$$

Note that the value of input parameter A_1 in SANTOS is required to be positive value (i.e., $3\sqrt{3}\alpha$ instead of $-3\sqrt{3}\alpha$).

5.2 Mesh Generation and Simulation

Figures 17 and 18 show the meshes and boundary conditions for the 12-inch and 6-inch POP triaxial test simulations, respectively. The uniform axial pressure is applied on the upper platen from 0.0 MPa to 16.0 MPa in 16,000 seconds at a rate identical to the uniaxial simulation. Four levels of confining pressure are applied on the drum wall boundary, as shown. The uniaxial test simulation is the case of zero confining pressure.

The FASTQ input file used to generate the meshes is the same as the one for uniaxial simulation. An example of the SANTOS input file for the triaxial test at 1.5 MPa confining pressure applied to a 12-inch POP is provided in Appendix C-2.

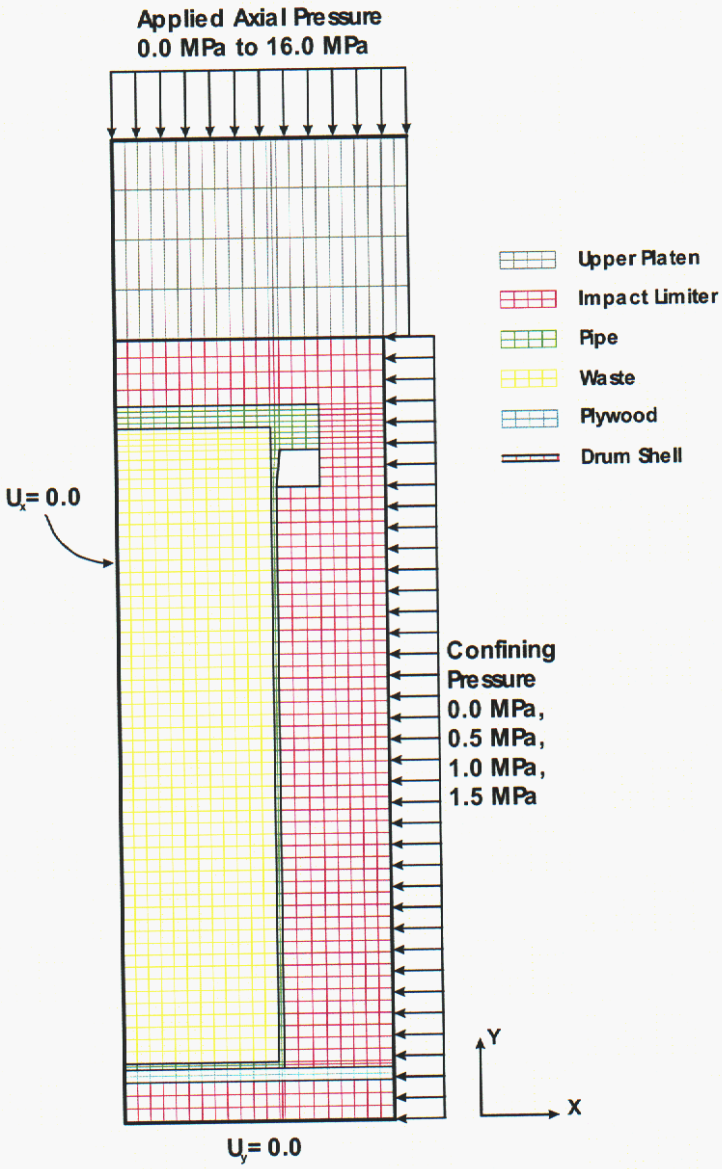

Figure 17. The finite element mesh and boundary conditions for the 12-inch POP triaxial test.

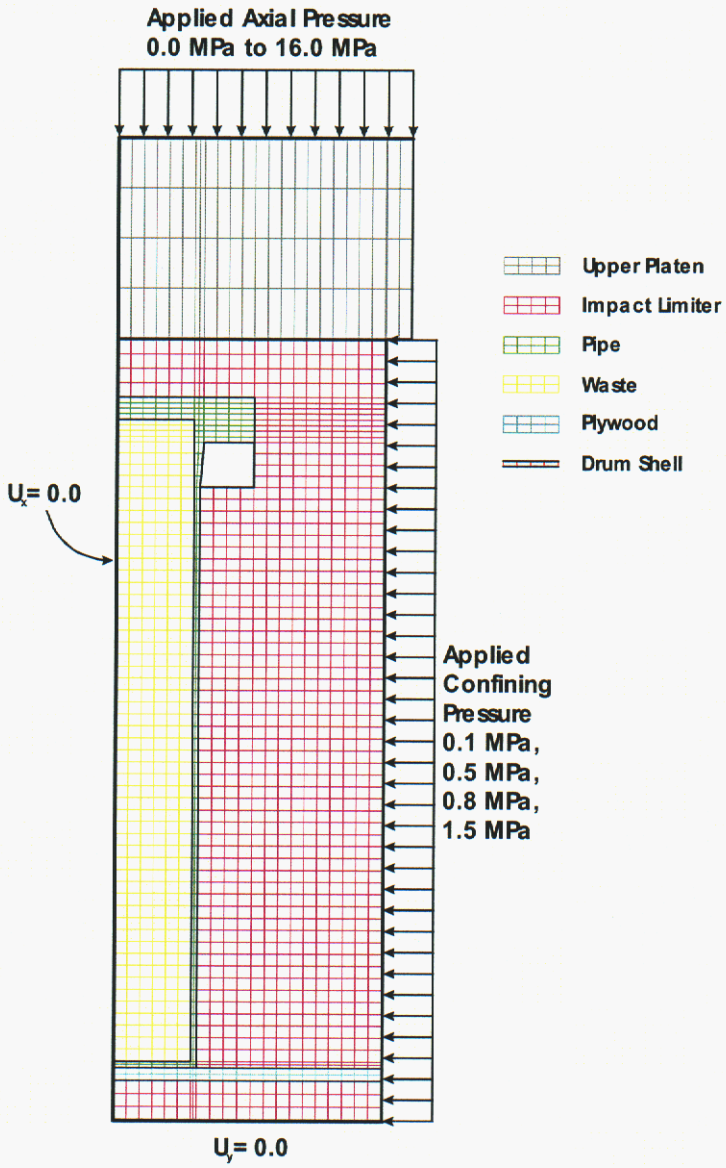

Figure 18. The finite element mesh and boundary conditions for the 6-inch POP triaxial test.

5.3 *Simulation Results*

5.3.1 Deformation pattern

Figure 19 is an example exhibiting deformation patterns of the 12-inch POP at various levels of axial pressures and a confining pressure of 1.5 MPa. Figure 20 illustrates the deformation pattern of the 6-inch POP for a similar range of axial pressures and a confining pressure of 1.5 MPa. In both cases, the axial strain in confined conditions is less than experienced when the POP is unconfined. The deformation of the 6-inch POP is slightly greater than the 12-inch POP. Because the 12-inch POP is slightly more rigid, its placement in the underground at WIPP will provide slightly more resistance to closure.

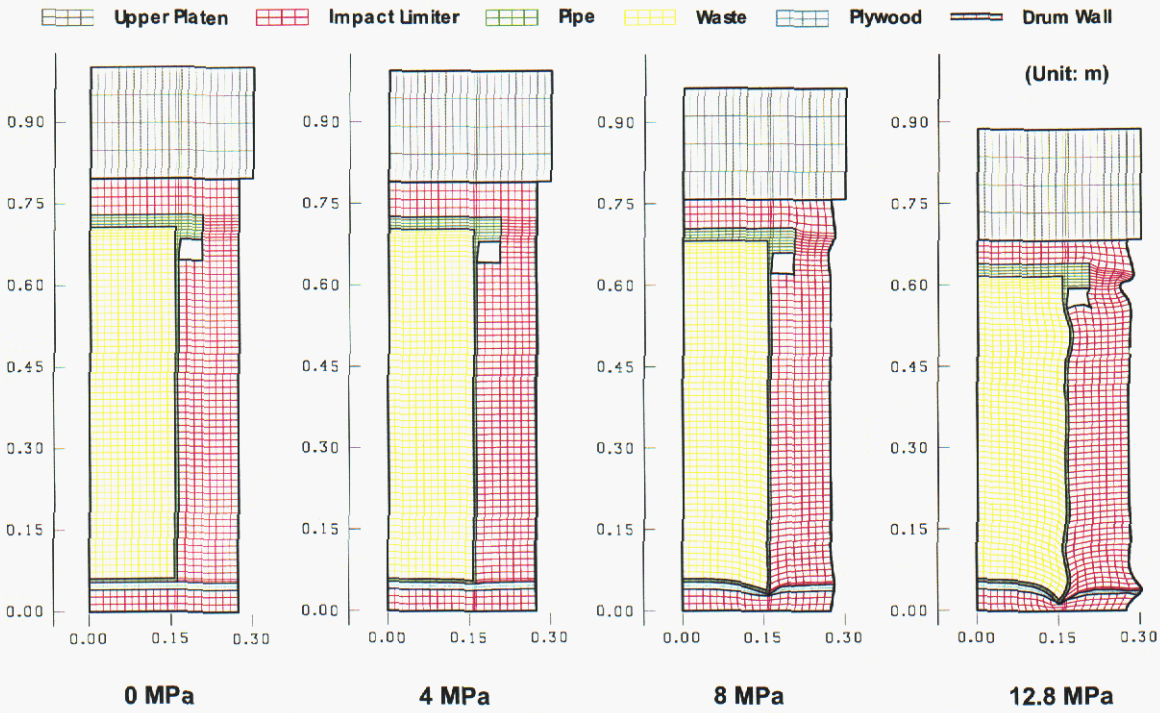

Figure 19. Deformation pattern of 12-inch POP triaxial simulation with 1.5 MPa confining pressure.

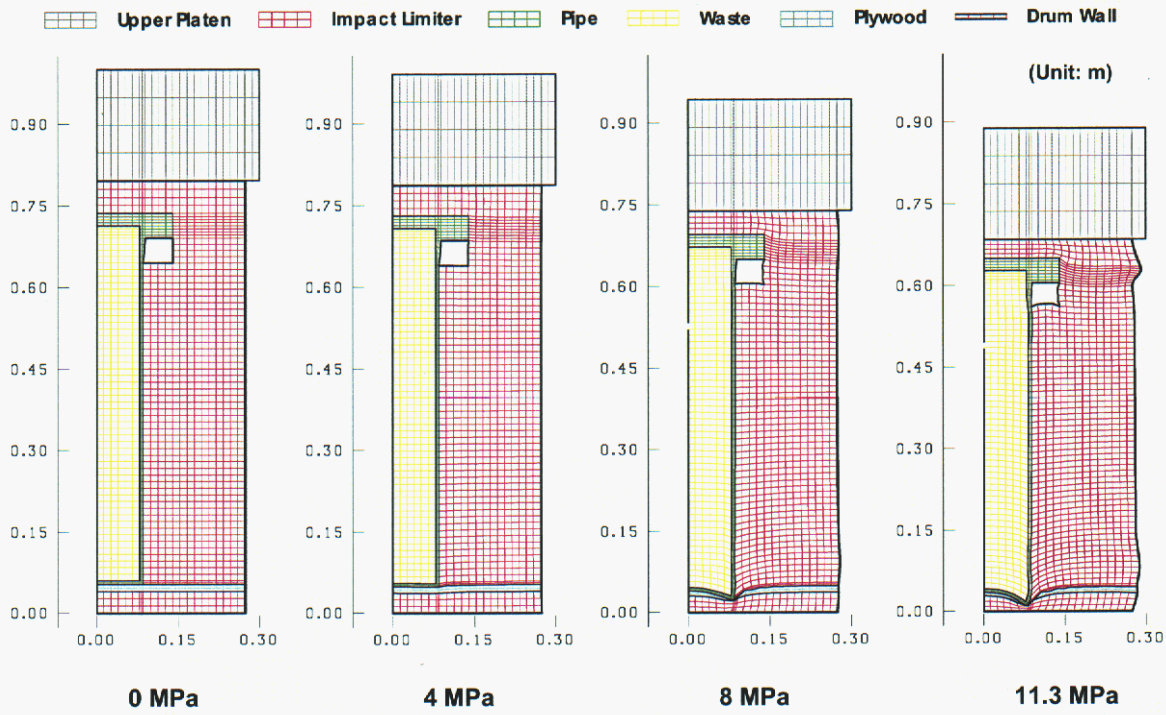

Figure 20. Deformation pattern of 6-inch POP triaxial simulation with 1.5 MPa confining pressure.

5.3.2 Yield surface constants

As discussed in Section 5.1, the SANTOS input constants A_0, A_1 and A_2 are derived from the Drucker-Prager parameters α and C. The parameters α and C are obtained from c and ϕ which are obtained from the triaxial test simulations. Determination of c and ϕ typically requires ascertainment of a "failure" condition. These simulations did not fail the composite material in the sense of loss of load bearing capacity. A subjective evaluation involving yield of the inner stainless steel pipe is used here to quantify the stress conditions at incipient buckling. This process involves engineering judgment and, as explained subsequently, allows determination of D-P parameters. The POP waste drum is a composite material, and the yield behavior of the inner drum is complex. The overriding purpose of these simulations is to describe mechanical response of the POP sufficiently to allow the assemblages to be represented reasonably well in models of the closure of disposal rooms at WIPP.

Figures 21 and 22 are used to illustrate how the yield or incipient buckling stress is determined. Figure 21 shows the von Mises stress contour at 11,200 seconds (11.2 MPa). The symbol ⊕ indicates the location of the minimum von Mises stress and the symbol ✳ indicates the location of the maximum von Mises stress. The location of the maximum value is the bottom corner of the pipe in Figure 21. Figure 22 shows these same reference symbols at the next load increment equaling 11.3 MPa. At this loading stage, the maximum von Mises stress appears along the pipe wall, approximately ¼ of the length downward from the top. We have assumed that when the maximal stress migrates from the

corner to the wall of the inner pipe, buckling is incipient and defines the yield stress condition. Thus, in this example, 11.3 MPa defines the yield stress in a conservative manner.

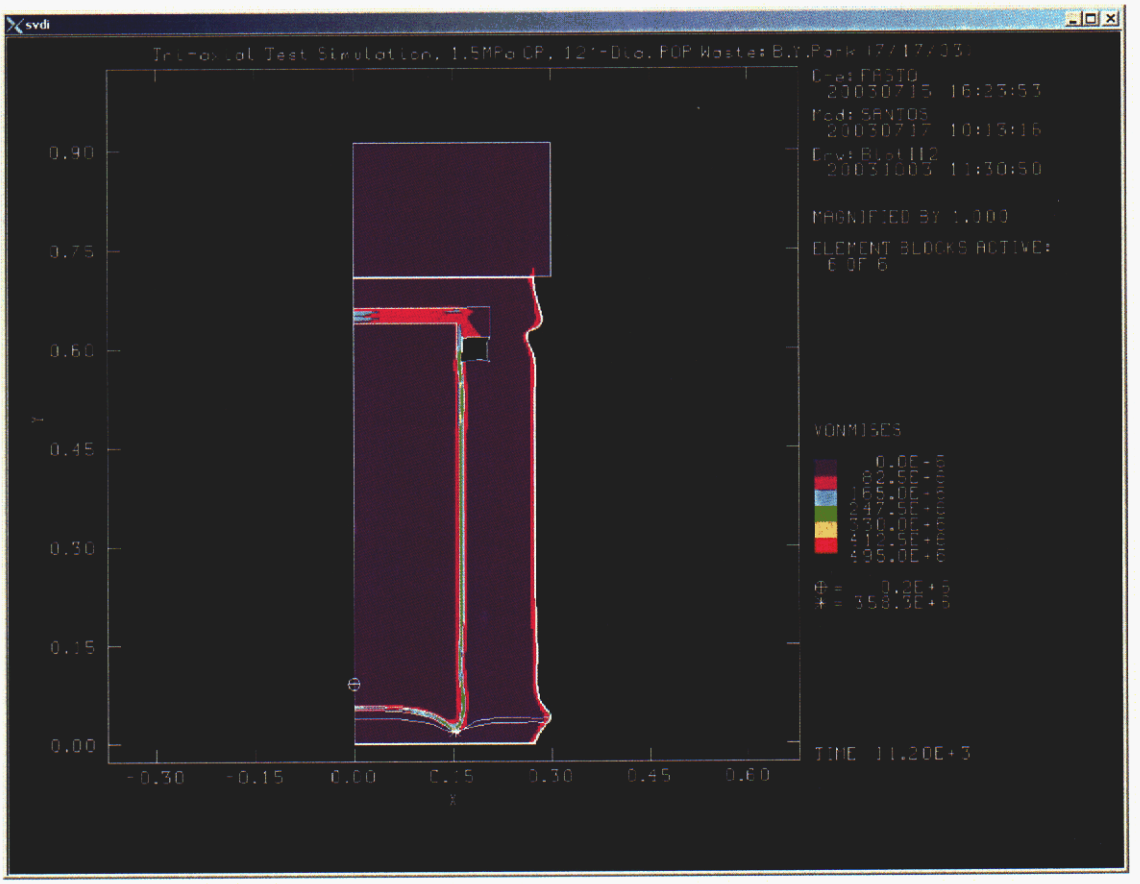

Figure 21. von Mises stress contour for 12-inch POP drum at 11.2 MPa axial pressure

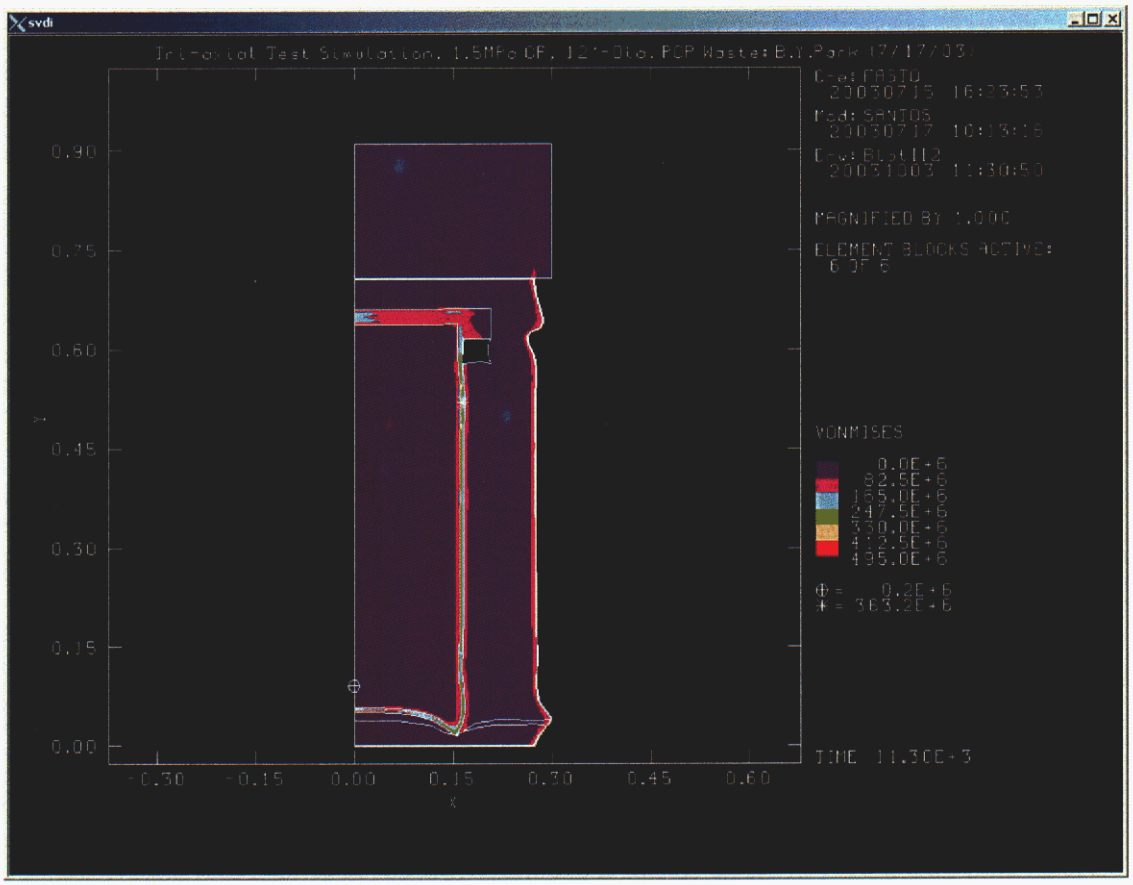

Figure 22. von Mises stress contour for 12-inch POP drum at 11.3 MPa axial pressure

Table 5 summarizes the axial pressure at incipient buckling as a function of confining pressure. These results show that the buckling phenomenon is essentially independent of confining pressure. The nominally zero values for friction angle are listed in Table 6.

Table 5. Axial pressure as a function of confining pressure to attain incipient buckling

(Units in MPa)

12-inch POP drum		6-inch POP drum	
Confining Pressure ($\sigma_2 = \sigma_3$)	Axial Pressure at Yield (σ_1)	Confining Pressure ($\sigma_2 = \sigma_3$)	Axial Pressure at Yield (σ_1)
0.0	9.6	0.1	7.9
0.5	10.2	0.5	8.3
1.0	10.8	0.8	8.6
1.5	11.3	1.5	9.2

The friction angle calculated from the numerical simulation of the 12-inch POP on the triaxial stress condition was 3.66 degrees. This small friction angle was deemed to be insignificant and probably falls within the range of numerical errors. Therefore, the friction angle of 12-inch POP is considered zero. The friction angle for 6-inch POP was calculated to be –1.592 degrees. This small negative friction angle was also deemed to be insignificant. Similarly to 12-inch POP, the friction angle of 6-inch POP is considered zero.

Then, the cohesions for 12-inch POP and 6-inch POP are calculated to be 4.89 MPa and 3.88 MPa respectively. The calculation sheet to compute these values is provided in Appendix A-2.

Table 6. Friction angle and cohesion of 12-inch and 6-inch POP drum

	12-inch POP	6-inch POP
ϕ (degrees)	0	0
c (MPa)	4.892	3.875

Substitution of the values in Table 6 into Equation (12) in Section 5.1 results in the Drucker-Prager constants, α and C. Then the SANTOS input constants A_0, A_1 and A_2 are determined by Equation (14) as shown in Table 7.

Table 7. Drucker-Prager constants and SANTOS input constants

	12-inch POP	6-inch POP
C (MPa)	4.892	3.875
α	0.0	0.0
A_0 (MPa)	8.473	6.712
A_1	0.0	0.0
A_2	0.0	0.0

6 HYDROSTATIC TEST SIMULATION

6.1 Theoretical Background

In this section, the pressure-volumetric strain curve corresponding to the function $g(\varepsilon_v)$ of Equation 3 in Section 2.3 will be derived from the hydrostatic test simulation. Volumetric strain for POP drum is:

$$\varepsilon_V = \frac{V_0 - V}{V_0} \tag{15}$$

where, V_0 = initial volume of the POP drum, and V = instantaneous volume of the POP drum as hydrostatic pressure is applied. The simulation allows determination of a stress-porosity function consistent with the procedure used in the CCA. Data have been converted into pressure-volumetric strain curves for use in mechanical simulations. The conversion from porosity to (natural log of) volume strain is follows (Butcher, 1997):

$$\varepsilon_V = \ln((1-e)\rho_s / \rho_0) \tag{16}$$

where, ε_V = Volumetric strain

e = Porosity of the waste

ρ_s = Solid density of the waste

ρ_0 = Initial density of the waste

The data points determined from the hydrostatic test simulation define the volumetric plasticity model as a piece-wise linear volumetric yield function.

6.2 Mesh Generation and Simulation

Figures 23 and 24 show the meshes and boundary conditions for the 12-inch and 6-inch POP hydrostatic test simulations, respectively. A uniform pressure is applied to the top, the bottom and the wall of the drum from 0.0 MPa to 16.0 MPa for 16,000 seconds (4.44 hours). The loading rate is 1,000 Pa/s.

The FASTQ input file to generate the mesh for 12-inch POP and 6-inch POP is provided in Appendix B-3 and B-4 respectively. Also, the SANTOS input file to simulate the hydrostatic test for 12-inch POP is provided in Appendix C-3.

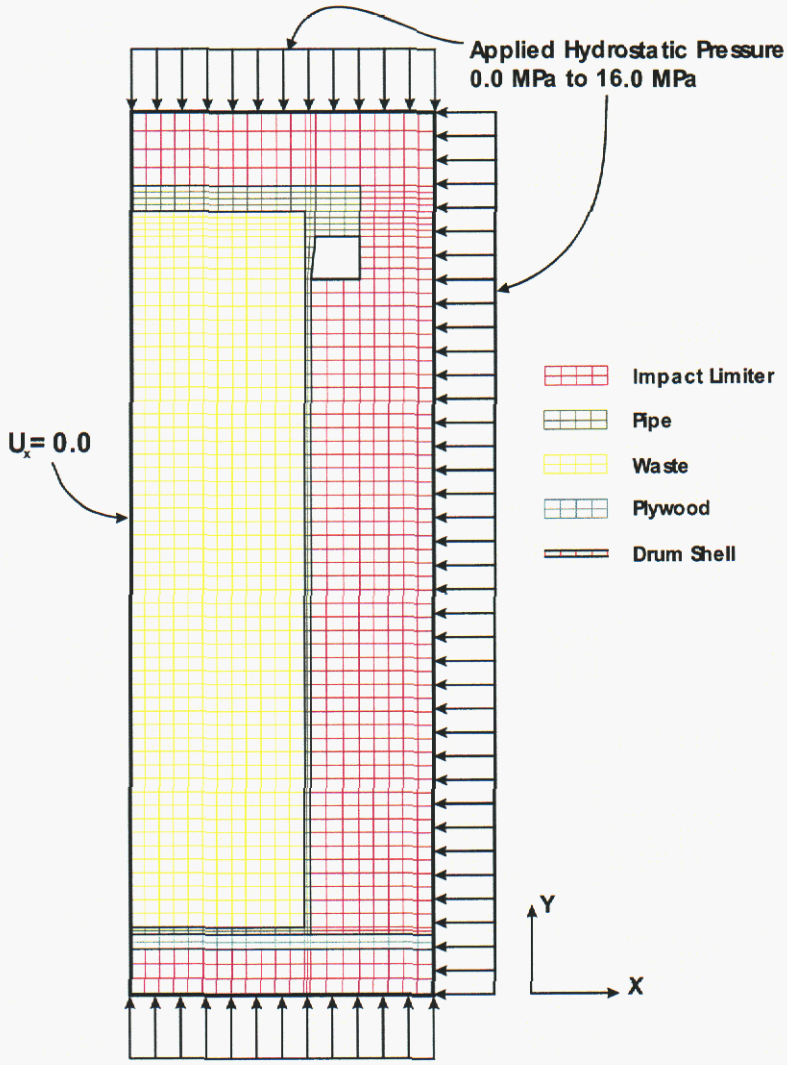

Figure 23. The finite element mesh and boundary conditions for the 12-inch POP hydrostatic test.

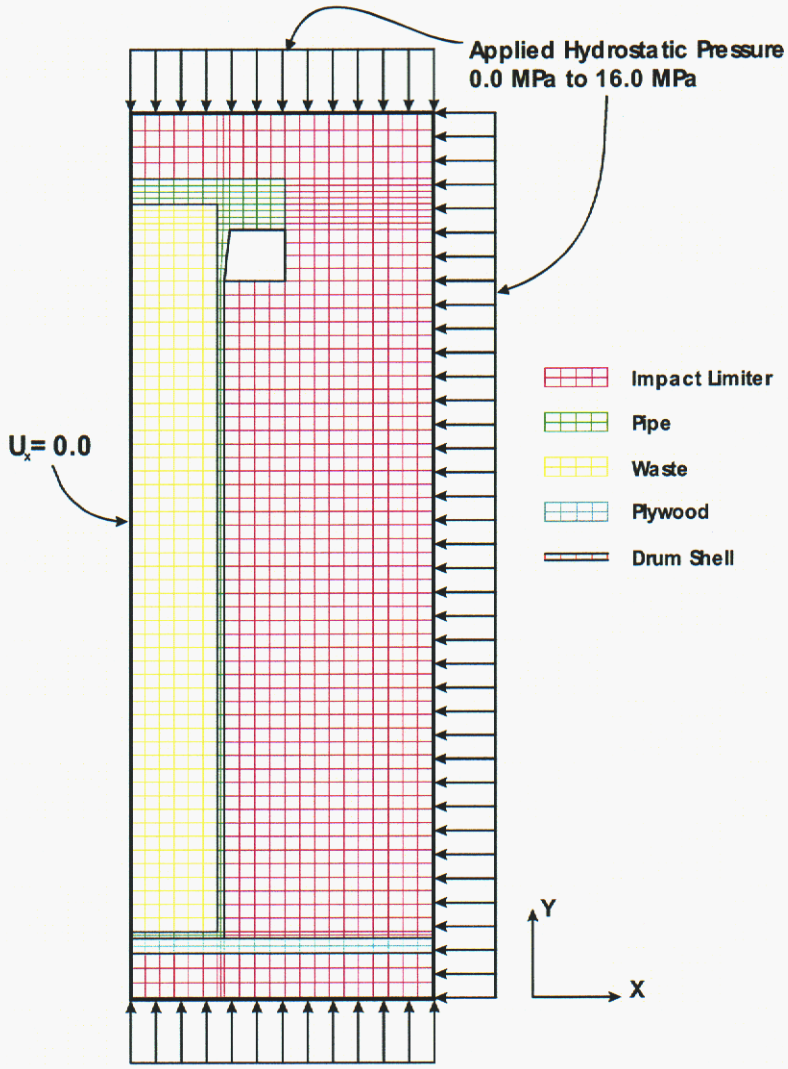

Figure 24. The finite element mesh and boundary conditions for the 6-inch POP hydrostatic test.

6.3 Simulation Results

6.3.1 Deformation pattern

Figure 25 shows the deformation patterns of the 12-inch POP at hydrostatic loading of 0 MPa, 4 MPa, 8 MPa and 13 MPa, and Figure 26 shows the deformation patterns of the 6-inch POP. The overall deformation of the 6-inch POP is slightly larger than the 12-inch POP's and the patterns are slightly different because of the size differences in the stainless steel pipes. The 6-inch POP is slightly more compressible than the 12-inch POP.

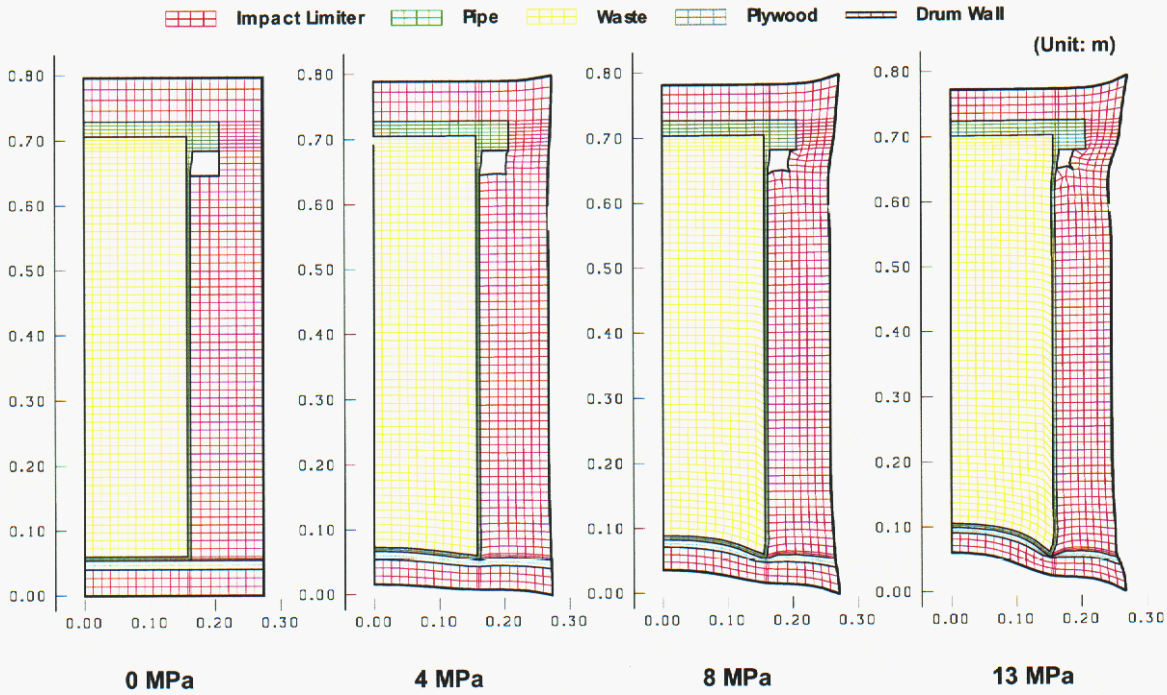

Figure 25. 12-inch POP hydrostatic test: Deformation with hydrostatic pressure

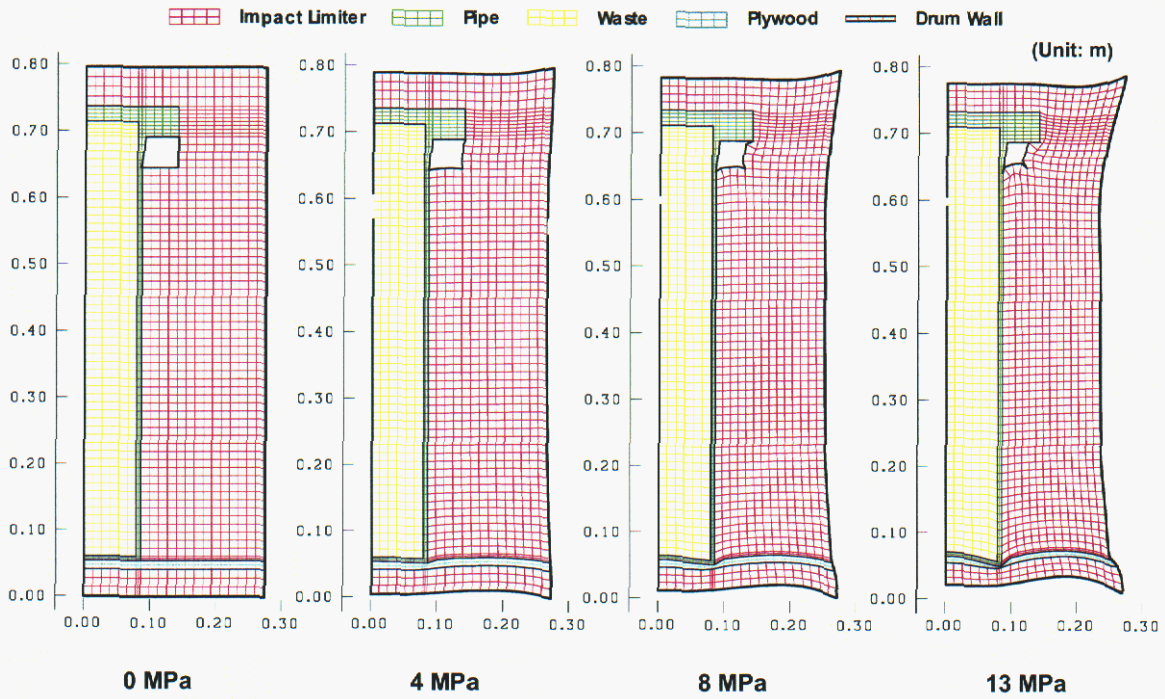

Figure 26. 6-inch POP hydrostatic test: Deformation with hydrostatic pressure

6.3.2 Pressure-volumetric strain function data

To obtain data points for the volumetric plasticity model, the volume change of the POP drum with hydrostatic pressure is calculated using Equation 15. The hydrostatic pressure-volumetric strain curve of the 12-inch POP drum is plotted in Figure 27 and similar data for the 6-inch POP drum are plotted in Figure 28. Coordinates are selected from these curves for pressure-volumetric strain data to facilitate comparison between POP and standard, 55-gallon drum deformation. This comparison and implementation as a waste constitutive model in SANTOS is the essential output of these analyses.

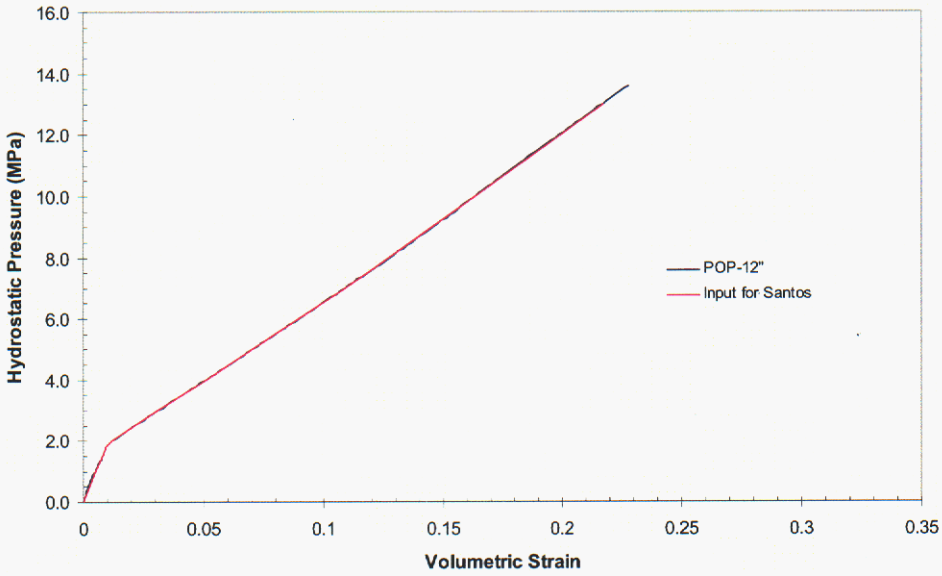

Figure 27. Pressure-volumetric strain curve for the 12-inch POP waste drum.

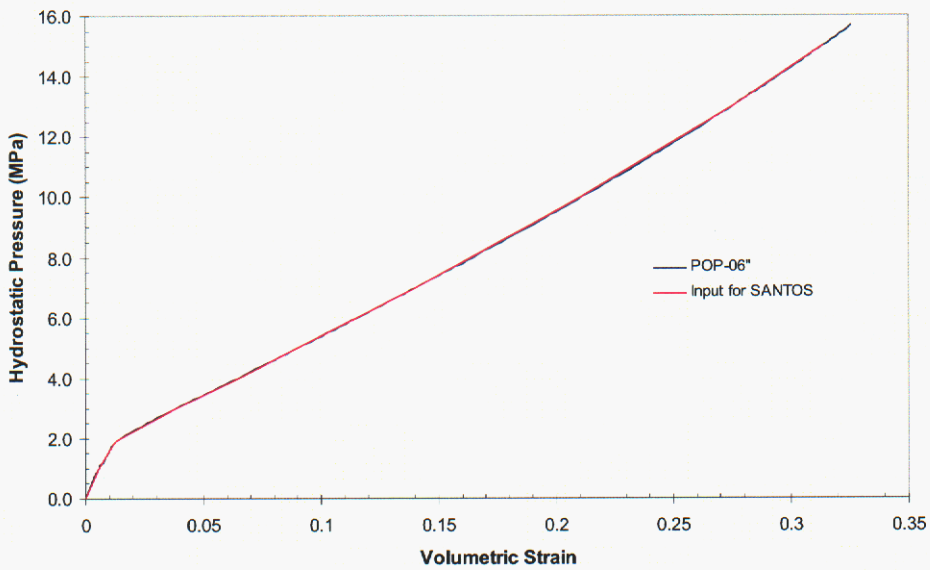

Figure 28. Pressure-volumetric strain curve for the 6-inch POP waste drum.

7 DISCUSSION AND CONCLUDING REMARKS

The calculations discussed in this report were executed to ascertain the mechanical properties of a WIPP waste package known as the pipe overpack or POP. The transuranic waste is packaged in a stainless steel pipe, which is placed inside a standard 55-gal drum. The interior pipe is further protected by a concentric, hollow cylinder of fiberboard. The composite package appears substantially more rigid and therefore, less compressible, then the standard waste residing in 55-gal drums. In addition, approximately half of the inventory placed in Panel 1 consists of POP waste packages. Rigid waste could affect room closure, which is a first-order input to performance assessment calculations in terms of a porosity surface. To determine porosity surfaces from room closure calculations, a material model for the constituents residing in the rooms is needed.

The material model for wastes implemented in the initial compliance certification calculations was based on laboratory testing of 55-gal drums containing surrogate wastes. Similar laboratory tests have not been conducted on the POP, but the composite material properties and geometries are known accurately, thus allowing deformational characteristics to be modeled readily using finite elements. This report presents the details of the several specific analyses used to develop model parameters for the POP.

The finite element code called SANTOS was used for these calculations. Documentation details are included in the main text and in the Appendices. SANTOS was used because it has been qualified and certified to requirements of the WIPP Quality Assurance Program. It should be noted that SANTOS results are corroborated in separate calculations for which a well-known code, JAS3D, was used. The JAS3D code allows three-dimensional calculations, whereas the SANTOS calculations utilize two-dimensional axisymmetry. The JAS3D code is not under WIPP QA configuration control and the calculations derived thereby are used only to corroborate the SANTOS results.

The SANTOS analyses allowed determination of shear modulus, bulk modulus, deviatoric yield surface constants, and a pressure-volumetric strain function. Simulations were run for 6-inch and 12-inch interior pipes and included uniaxial, triaxial, and hydrostatic stress applications.

Uniaxial Test Simulation The input to the soil and crushable foam model in the SANTOS code requires a shear modulus (2μ) and the bulk modulus, K. These values are derived from Young's modulus and Poisson's ratio of the POP drum simulations. Shear moduli are calculated as 1.44×10^9 Pa, 1.36×10^9 Pa for 12-inch POP and 6-inch POP respectively. Bulk moduli are calculated as 1.56×10^9 Pa, 1.69×10^9 Pa for 12-inch POP and 6-inch POP respectively.

Triaxial Test Simulation The POP waste package is considered isotropic and elastic until yield occurs. Yield is assumed to be governed by the Drucker-Prager criterion. SANTOS input constants for the deviatoric yield surface, A_0, A_1 and A_2, are listed in Table 8.

Hydrostatic Test Simulation To express the volumetric hardening of the POP, the data points defining the volumetric plasticity model are determined from calculating the volume change of POP drum with hydrostatic pressure. The pressure-volumetric strain curves show the 12-inch POP is slightly more rigid than the 6-inch POP.

These analyses examined the mechanical response of the pipe-overpack waste package under possible stresses in the WIPP disposal room. It is important to assess just how different the mechanical properties of the POP are from the mechanical properties used previously to describe the waste in the initial compliance certification calculations. **The pipe-overpack waste package is more rigid, much stronger, and far less collapsible than the 55-gal drums as characterized for the CCA.** These statements will be expounded upon in the tables and figures that follow. In Table 8, for example, the elastic parameters and the SANTOS input yield stress parameters are five to ten times greater for the POPs than for the 55-gal drums of the CCA.

From the simulations, the pressure-volumetric strain curve can be plotted and compared to the data used for standard waste in the CCA. Table 9 contains point-by-point comparisons between the overpack simulations and experimental data from Stone (1997a). Note that Table 9 is compiled in terms of stress-strain data from experiments on standard waste and from a series of stress levels, subjectively selected to describe the response adequately. Generally, the volumetric strain of the POP is an order-of-magnitude less than the standard waste. A plot of all the available volumetric strain versus pressure data is made in Figure 29.

Table 8. SANTOS input constants for waste constitutive model

	12-inch POP	6-inch POP	Standard (CCA)
G (Two Mu) [MPa]	1442.0	1364.0	333.3
K [MPa]	1561.0	1690.0	222.3
A_0 [MPa]	8.473	6.712	1.0
A_1	0.0	0.0	3.0
A_2	0.0	0.0	0.0

Table 9. Pressure-volumetric strain data used in the waste constitutive model

Pressure [MPa]	Volumetric Strain		
	12-in POP	6-in POP	Standard
0.00	0.000	0.000	
1.00	0.005	0.006	
1.53			0.510
1.60	0.008	0.010	
1.80	0.010	0.012	
1.90	0.011	0.013	
2.00	0.012	0.015	
2.03			0.631
2.53			0.719
3.00	0.031	0.038	
3.03			0.786
3.53			0.838
4.00	0.051	0.065	
4.03			0.881
4.93			0.942
5.00	0.070	0.090	
7.00	0.109	0.140	
10.00	0.164	0.211	
12.00			1.140
13.00	0.217	0.275	
15.00		0.314	

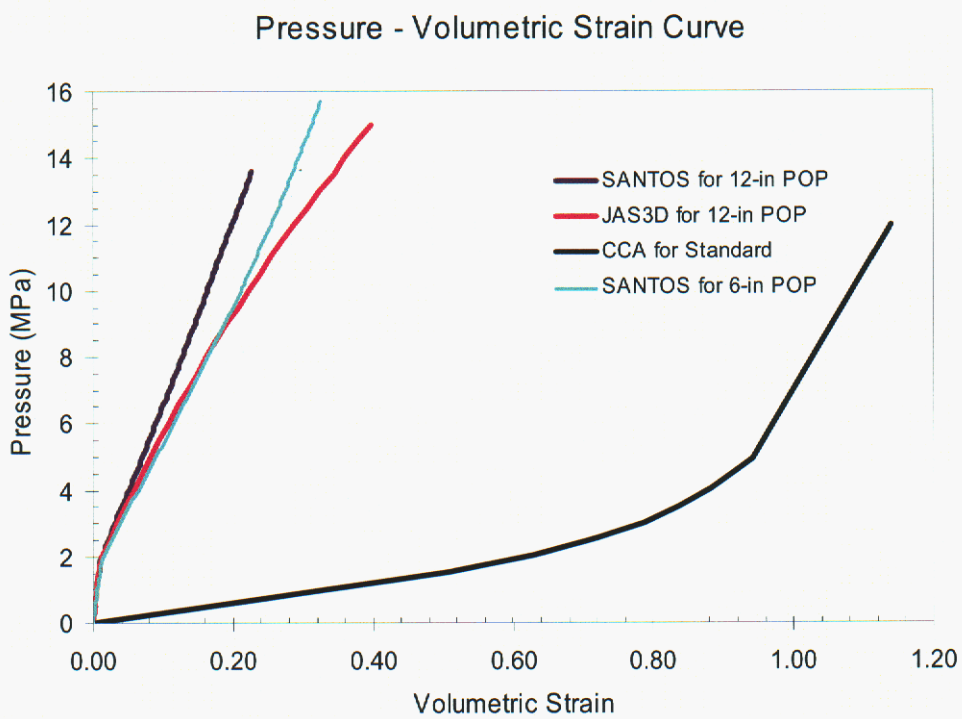

Figure 29. Simulated volumetric strain for POP compared to the standard 55-gal drum.

Figure 29 contains four relationships: the standard waste 55-gal drum, the 12-in and 6-in POPs from SANTOS runs and a corroborative calculation of the 12-in POP from JAS3D (Rath, 2003). The effect of the POP on closure might be appreciable because the volumetric collapse is very limited, especially when compared to the standard waste drums. The material characteristics and parameters determined in these studies will comprise the waste material models for the POP, which will be incorporated into structural room calculations in a companion report (Park and Hansen, 2003).

It is clear that the POP waste is much stiffer than the standard waste and the calculations presented here provide reasonable material parameters to facilitate room closure calculations. The purpose of these calculations is to characterize mechanical deformation of the POP sufficiently to bound closure of a WIPP waste room containing a large proportion of POP drums. The pipe overpacks could create stiff columns within the disposal rooms and influence room closure. It is possible that rigid waste columns would increase overall waste porosity by shielding adjacent standard waste from compaction. This effect would be reflected in the porosity surface look-up table accessed in PA. In order to evaluate the effect of these pillars on the repository performance, calculations will be made using SANTOS for bounding cases to determine the effect of these stiffer columns on the waste porosity.

8 REFERENCES

Blacker, T.D. 1988. *FASTQ Users Manual, Version 2.1*. SAND88-1326. Albuquerque, NM: Sandia National Laboratories.

Butcher, B.M. 1995. "Pre- and Post Processing of SANTOS code results." Memo from B.M. Butcher to J.J. Loukota, dated October 26, 1995. Carlsbad, NM: Sandia National Laboratories. (Copy on file in the Sandia WIPP Records Center [SWRC] as ERMS# 227538).

Butcher, B.M. 1997. *A Summary of the Sources of Input Parameter Values for the Waste Isolation Pilot Plant Final Porosity Surface Calculations*. SAND97-0796. Albuquerque, NM: Sandia National Laboratories.

Butcher, B.M., and J.T. Holmes. 1995. "Completion of Milestone DR015, Definition of Closure Analysis Input Parameters, Due March 31, 1995." Memo to Les Shephard and Martin Tierney, dated March 31, 1995. Albuquerque, NM: Sandia National Laboratories. (Copy on file in the SWRC as ERMS# 220876).

Butcher, B.M., and D.J. Morin. 1996. "Exceptions from Documentation Requirements for the SANTOS QA Package." Memo from B.M. Butcher and D.J. Morin to S.Y. Pickering, dated March 13, 1996. Carlsbad, NM: Sandia National Laboratories. (Copy on file in the SWRCs as ERMS# 237416).

Butcher, B.M., T.W. Thompson, R.G. VanBuskirk, and N.C. Patti. 1991. *Mechanical Compaction of Waste Isolation Pilot Plant Simulated Waste*. SAND90-1206. Albuquerque, NM: Sandia National Laboratories.

Chavez, M.J. 2003. "Software Requirements." NP 19-1, Revision 10. Carlsbad, NM: Sandia National Laboratories. (Copy on file in the SWRC as ERMS# 529692).

Fung, Y.C. 1965. *Foundations of Solid Mechanics*. Englewood Cliffs, NJ: Prentice-Hall, Inc.

Gilkey, A.P., and J.H. Glick. 1989. *BLOT - a Mesh and Curve Plot Program for the Output of a Finite Element Analysis*. SAND88-1432. Albuquerque, NM: Sandia National Laboratories.

Gross, M.B. 2002. *Assessment of Impacts on Long-Term Performance from Supercompacted Wastes Produced by the Advanced Mixed Waste Treatment Project*. Carlsbad, NM: U.S. Department of Energy, Carlsbad Field Office, Waste Isolation Pilot Plant. (Copy on file in the SWRC as ERMS# 533388).

Hansen, C.W., L.H. Brush, F.D. Hansen, and J.S. Stein. 2003. "Analysis Plan for Evaluating Assumptions of Waste Homogeneity in WIPP Performance Assessment." AP-107, Revision 1. Carlsbad, NM: Sandia National Laboratories. (Copy on file in the SWRC as ERMS# 531067).

Hoffman, E.L., and D.J. Ammerman. 1995. *Dynamic Pulse Buckling of Cylindrical Shells under Axial Impact: A Comparison of 2D and 3D Finite Element Calculations with Experimental Data.* SAND93-0350. Albuquerque, NM: Sandia National Laboratories.

Ludwigsen, J.S., D.J. Ammerman, and H.D. Radloff. 1998. *Analysis in Support of Storage of Residues in the Pipe Overpack Container.* SAND98-1003. Albuquerque, NM: Sandia National Laboratories.

NRC (National Research Council). 1996. *The Waste Isolation Pilot Plant: a Potential Solution for the Disposal of Transuranic Waste.* Washington, DC: National Academy Press.

Park, B.Y., and F.D. Hansen. 2003. "Analysis Report for Determination of the Porosity Surfaces of the Disposal Room Containing Various Waste Inventories for WIPP PA." Revision 0. Carlsbad, NM: Sandia National Laboratories. (Copy on file in the SWRC as ERMS# 533126).

Rath, J.S. 2003. "JAS3D Calculations in Support of FY2003 WIPP – AMWTP Waste Pipe Overpack Drum Analyses." Memo to F.D. Hansen and B.Y. Park, dated October 20, 2003. Albuquerque, NM: Sandia National Laboratories. (Copy on file in the SWRC as ERMS# 53317).

Sjaardema, G.D. 1989. *NUMBERS: a Collection of Utilities for Pre- and Post-processing Two- and Three-Dimensional EXODUS Finite Element Models.* SAND88-0737. Albuquerque, NM: Sandia National Laboratories.

Stone, C.M. 1997a. *Final Disposal Room Structural Response Calculations.* SAND97-0795. Albuquerque, NM: Sandia National Laboratories.

Stone, C.M., 1997b. *SANTOS - a Two-Dimensional Finite Element Program for the Quasistatic, Large Deformation, Inelastic Response of Solids.* SAND90-0543. Albuquerque, NM: Sandia National Laboratories.

Timoshenko, S.P., and J.N. Goodier. 1970. *Theory of Elasticity.* Third Edition, International Student Edition. New York, NY: McGraw-Hill, Inc.

WIPP PA (Performance Assessment). 2003. *Verification and Validation Plan, Validation Document for SANTOS, Version 2.1.7.* Document Version 1.20BOC. Carlsbad, NM: Sandia National Laboratories. (Copy on file in the SWRC as ERMS# 530421).

WTS (Westinghouse TRU Solutions). 2003. "TRUPACT-II Authorized Methods for Payload Control (TRAMPAC)." Revision 19c, April 2003. Carlsbad, NM: Westinghouse TRU Solutions, LLC. [Online version, 3/9/04, at http://www.wipp.ws/t2sar/Trampac/TRAMPAC.PDF]

Zimmermann, Th., A. Truty, A. Urbanski, S. Commend, and K. Podles. 2001. *ZSOIL.PC: a Unified Approach to Stability, Bearing Capacity, Consolidation, Creep and Flow for Two and Three-Dimensional Simulations in Geotechnical Practice.1*. Lausanne, Switzerland: Zace Services Ltd. [Online version, 3/9/04, at Zace homepage, http://www.zace.com/white_p/zswp30.htm]

Intentionally Blank

APPENDIX A: CALCULATION SHEET

A-1 Shear Modulus and Bulk Modulus

12"-POP

$E_{12} := 1.874\,10^{9} \cdot Pa$

$\nu_{12} := 0.2999$

$Two\mu_{12} := \frac{E_{12}}{(1 + \nu_{12})}$ $\qquad Two\mu_{12} = 1.442 \times 10^{9}\ Pa$

$K_{12} := \frac{E_{12}}{3 \cdot (1. - 2 \cdot \nu_{12})}$ $\qquad K_{12} = 1.561 \times 10^{9}\ Pa$

6"-POP

$E_{6} := 1.804\,10^{9} \cdot Pa$

$\nu_{6} := 0.3221$

$Two\mu_{6} := \frac{E_{6}}{(1 + \nu_{6})}$ $\qquad Two\mu_{6} = 1.364 \times 10^{9}\ Pa$

$K_{6} := \frac{E_{6}}{3 \cdot (1. - 2 \cdot \nu_{6})}$ $\qquad K_{6} = 1.69 \times 10^{9}\ Pa$

A-2 D-P, M-C, and SANTOS input constants

[12-inch POP drum]

$i := 1..4$ $\qquad \sigma3_i :=$ $\qquad \sigma1_i :=$ $\qquad MPa \equiv 10^6 \cdot Pa$

$\sigma3_i :=$	$\sigma1_i :=$
0.0·MPa	9.6·MPa
0.5·MPa	10.2·MPa
1.0·MPa	10.8·MPa
1.5·MPa	11.3·MPa

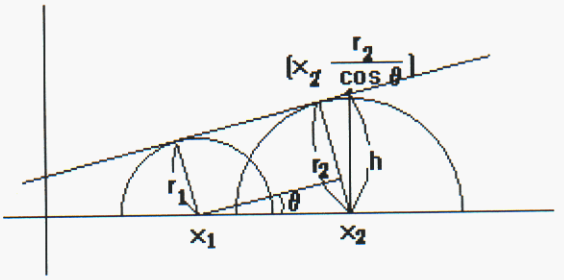

$$\sin(\theta) = \frac{r_2 - r_1}{x_2 - x_1} \qquad h = \frac{r_2}{\cos(\theta)}$$

Thus,

Slope of the line contacting with both circles: $\theta = \arcsin\left(\frac{r_2 - r_1}{x_2 - x_1}\right)$

Intercept of the line contacting with both circles: $c = \frac{r_2}{\cos(\theta)} - \tan(\theta)\cdot x_2$

To show the stress term:

$$x_i := \frac{\sigma1_i + \sigma3_i}{2} \qquad r_i := \frac{\sigma1_i - \sigma3_i}{2}$$

$\frac{x_i}{MPa} =$	$\frac{r_i}{MPa} =$
4.8	4.8
5.35	4.85
5.9	4.9
6.4	4.9

$k := 1..3$

For the line contacting with both the Mohr circle of Test(k) and the Mohr circle of Test(k+1):

Slope: $\phi_k := \operatorname{asin}\left(\frac{r_{k+1} - r_k}{x_{k+1} - x_k}\right)$ Intercept: $c_k := \frac{r_{k+1}}{\cos(\phi_k)} - \tan(\phi_k)\cdot x_{k+1}$

$\frac{\phi_k}{deg} =$

5.216
5.216
0

$\frac{c_k}{MPa} =$

4.382
4.382
4.9

For the line contacting with both the Mohr circle of Test(4) and the Mohr circle of Test(1):

Slope: $\phi_4 := \operatorname{asin}\left(\frac{r_4 - r_1}{x_4 - x_1}\right)$ Intercept: $c_4 := \frac{r_4}{\cos(\phi_4)} - \tan(\phi_4)\cdot x_4$

$\frac{\phi_4}{deg} = 3.583$ $c_4 = 4.509MPa$

For the line contacting with both the Mohr circle of Test(3) and the Mohr circle of Test(1):

Slope: $\phi_5 := \operatorname{asin}\left(\frac{r_3 - r_1}{x_3 - x_1}\right)$ Intercept: $c_5 := \frac{r_3}{\cos(\phi_5)} - \tan(\phi_5)\cdot x_3$

$\frac{\phi_5}{deg} = 5.216$ $c_5 = 4.382MPa$

For the line contacting with both the Mohr circle of Test(4) and the Mohr circle of Test(2):

Slope: $\phi_6 := \operatorname{asin}\left(\frac{r_4 - r_2}{x_4 - x_2}\right)$ Intercept: $c_6 := \frac{r_4}{\cos(\phi_6)} - \tan(\phi_6)\cdot x_4$

$\frac{\phi_6}{deg} = 2.729$ $c_6 = 4.6MPa$

$j := 1..6$

Thus,

Average Internal Friction Angle: $\phi_m := \frac{\sum_j \phi_j}{6}$ $\phi_m = 3.66deg$

==========

This small friction angle was deemed to be insignificant and problbly falls within the range of numerical errors. Therefore, the friction angle of 12-inch POP is considered zero.

$\phi_m := 0 \cdot deg$

$k := 1..3$

For the line contacting with both the Mohr circle of Test(k) and the Mohr circle of Test(k+1):

Slope: $\phi_k := 0$ Intercept: $c_k := \frac{r_{k+1}}{\cos(\phi_k)} - \tan(\phi_k) \cdot x_{k+1}$

$\frac{\phi_k}{deg} =$

0
0
0

$\frac{c_k}{MPa} =$

4.85
4.9
4.9

For the line contacting with both the Mohr circle of Test(4) and the Mohr circle of Test(1):

Slope: $\phi_4 := 0$ Intercept: $c_4 := \frac{r_4}{\cos(\phi_4)} - \tan(\phi_4) \cdot x_4$ $c_4 = 4.9MPa$

For the line contacting with both the Mohr circle of Test(3) and the Mohr circle of Test(1):

Slope: $\phi_5 := 0$ Intercept: $c_5 := \frac{r_3}{\cos(\phi_5)} - \tan(\phi_5) \cdot x_3$ $c_5 = 4.9MPa$

For the line contacting with both the Mohr circle of Test(4) and the Mohr circle of Test(2):

Slope: $\phi_6 := 0$ Intercept: $c_6 := \frac{r_4}{\cos(\phi_6)} - \tan(\phi_6) \cdot x_4$ $c_6 = 4.9MPa$

$j := 1..6$

Average Shear Strength Intercept:

$$c_m := \frac{\sum_j c_j}{6} \qquad c_m = 4.892MPa$$

==========

According to "Zimmermann, Th., A. Truty, A. Urbanski, S. Commend and K. Podles, 2001, *ZSOIL.PC: A Unified Approach to Stability, Bearing Capacity, Consolidation, Creep and Flow for Two and Three-Dimensional Simulations in Geotechnical Practice.1,* Zace Services Ltd."

$C := c_m \cdot \cos(\phi_m)$ $\qquad C = 4.892 \times 10^6\ \text{Pa}$

$\alpha := \dfrac{\sin(\phi_m)}{3}$ $\qquad \alpha = 0$

$A_0 := \sqrt{3} \cdot C$ $\qquad A_0 = 8.473 \times 10^6\ \text{Pa}$

$A_1 := 3 \cdot \sqrt{3} \cdot \alpha$ $\qquad A_1 = 0$

[6-inch POP drum]

$i := 1..4$ $\qquad \sigma3_i :=$ $\qquad \sigma1_i :=$ $\qquad MPa \equiv 10^6 \cdot Pa$

$\sigma3_i$
$0.1 \cdot MPa$
$0.5 \cdot MPa$
$0.8 \cdot MPa$
$1.5 \cdot MPa$

$\sigma1_i$
$7.9 \cdot MPa$
$8.3 \cdot MPa$
$8.6 \cdot MPa$
$9.2 \cdot MPa$

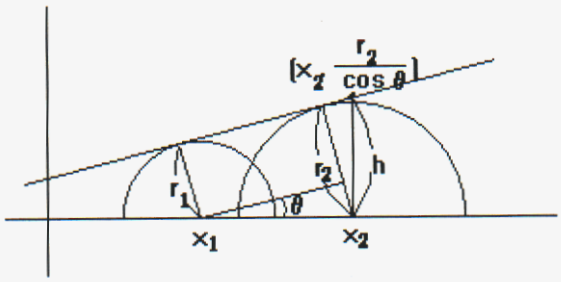

$$\sin(\theta) = \frac{r_2 - r_1}{x_2 - x_1} \qquad h = \frac{r_2}{\cos(\theta)}$$

Thus,

Slope of the line contacting with both circles: $\qquad \theta = \arcsin\left(\frac{r_2 - r_1}{x_2 - x_1}\right)$

Intercept of the line contacting with both circles: $\qquad c = \frac{r_2}{\cos(\theta)} - \tan(\theta) \cdot x_2$

To show the stress term:

$$x_i := \frac{\sigma1_i + \sigma3_i}{2} \qquad r_i := \frac{\sigma1_i - \sigma3_i}{2}$$

$\frac{x_i}{MPa} =$
4
4.4
4.7
5.35

$\frac{r_i}{MPa} =$
3.9
3.9
3.9
3.85

$k := 1..3$

For the line contacting with both the Mohr circle of Test(k) and the Mohr circle of Test(k+1):

Slope: $\phi_k := \operatorname{asin}\left(\frac{r_{k+1} - r_k}{x_{k+1} - x_k}\right)$ Intercept: $c_k := \frac{r_{k+1}}{\cos(\phi_k)} - \tan(\phi_k)\cdot x_{k+1}$

$\frac{\phi_k}{deg} =$

$6.67\cdot10^{-14}$
$-8.893\cdot10^{-14}$
-4.412

$\frac{c_k}{MPa} =$

3.9
3.9
4.274

For the line contacting with both the Mohr circle of Test(4) and the Mohr circle of Test(1):

Slope: $\phi_4 := \operatorname{asin}\left(\frac{r_4 - r_1}{x_4 - x_1}\right)$ Intercept: $c_4 := \frac{r_4}{\cos(\phi_4)} - \tan(\phi_4)\cdot x_4$

$\frac{\phi_4}{deg} = -2.123$ $c_4 = 4.051MPa$

For the line contacting with both the Mohr circle of Test(3) and the Mohr circle of Test(1):

Slope: $\phi_5 := \operatorname{asin}\left(\frac{r_3 - r_1}{x_3 - x_1}\right)$ Intercept: $c_5 := \frac{r_3}{\cos(\phi_5)} - \tan(\phi_5)\cdot x_3$

$\frac{\phi_5}{deg} = 0$ $c_5 = 3.9MPa$

For the line contacting with both the Mohr circle of Test(4) and the Mohr circle of Test(2):

Slope: $\phi_6 := \operatorname{asin}\left(\frac{r_4 - r_2}{x_4 - x_2}\right)$ Intercept: $c_6 := \frac{r_4}{\cos(\phi_6)} - \tan(\phi_6)\cdot x_4$

$\frac{\phi_6}{deg} = -3.017$ $c_6 = 4.137MPa$

$j := 1..6$

Thus,

Average Internal Friction Angle:

$$\phi_m := \frac{\sum_j \phi_j}{6} \qquad \phi_m = -1.592deg$$

==========

This small negative friction angle was deemed to be insignificant and problbly falls within the range of numerical errors. Therefore, the friction angle of 6-inch POP is considered zero.

$\phi_m := 0 \cdot deg$

$k := 1..3$

For the line contacting with both the Mohr circle of Test(k) and the Mohr circle of Test(k+1):

Slope: $\phi_k := 0$

Intercept: $c_k := \frac{r_{k+1}}{\cos(\phi_k)} - \tan(\phi_k) \cdot x_{k+1}$

$\frac{\phi_k}{deg} =$

0
0
0

$\frac{c_k}{MPa} =$

3.9
3.9
3.85

For the line contacting with both the Mohr circle of Test(4) and the Mohr circle of Test(1):

Slope: $\phi_4 := 0$

Intercept: $c_4 := \frac{r_4}{\cos(\phi_4)} - \tan(\phi_4) \cdot x_4$ $\quad c_4 = 3.85MPa$

For the line contacting with both the Mohr circle of Test(3) and the Mohr circle of Test(1):

Slope: $\phi_5 := 0$

Intercept: $c_5 := \frac{r_3}{\cos(\phi_5)} - \tan(\phi_5) \cdot x_3$ $\quad c_5 = 3.9MPa$

For the line contacting with both the Mohr circle of Test(4) and the Mohr circle of Test(2):

Slope: $\phi_6 := 0$

Intercept: $c_6 := \frac{r_4}{\cos(\phi_6)} - \tan(\phi_6) \cdot x_4$ $\quad c_6 = 3.85MPa$

$j := 1..6$

Average Shear Strength Intercept:

$$c_m := \frac{\sum_j c_j}{6} \qquad c_m = 3.875MPa$$

==========

According to "Zimmermann, Th., A. Truty, A. Urbanski, S. Commend and K. Podles, 2001, *ZSOIL.PC: A Unified Approach to Stability, Bearing Capacity, Consolidation, Creep and Flow for Two and Three-Dimensional Simulations in Geotechnical Practice.1,* Zace Services Ltd."

$C := c_m \cdot \cos(\phi_m)$ $\qquad C = 3.875 \times 10^6\ \mathrm{Pa}$

$\alpha := \dfrac{\sin(\phi_m)}{3}$ $\qquad \alpha = 0$

$A_0 := \sqrt{3} \cdot C$ $\qquad A_0 = 6.712 \times 10^6\ \mathrm{Pa}$

$A_1 := 3 \cdot \sqrt{3} \cdot \alpha$ $\qquad A_1 = 0$

APPENDIX B: FASTQ INPUT FILE

B-1 12-inch POP Waste Mesh for UTS and TTS

```
TITLE
 Assembled POP with platen - 12 INCH PIPE (07/10/03-B.Y.PARK)
$
$Define Point
$
$ Lower Impact Limiter
POINT  101     .0        -1.397E-3
POINT  102     .1569974 -1.397E-3
POINT  103     .16256   -1.397E-3
POINT  104     .20701   -1.397E-3
POINT  105     .27305   -1.397E-3
POINT  106     .274447  -1.397E-3
$
POINT    1     .0        .0
POINT    2     .1569974 .0
POINT    3     .16256   .0
POINT    4     .20701   .0
POINT    5     .27305   .0
POINT    6     .274447  .0
$
POINT   11     .0        .04
POINT   12     .1569974 .04
POINT   13     .16256   .04
POINT   14     .20701   .04
POINT   15     .27305   .04
POINT   16     .274447  .04
$
POINT   21     .0        .05334
POINT   22     .1569974 .05334
POINT   23     .16256   .05334
POINT   24     .20701   .05334
POINT   25     .27305   .05334
POINT   26     .274447  .05334
$
POINT   31     .0        .05969
POINT   32     .1569974 .05969
POINT   33     .16256   .05969
POINT   34     .20701   .05969
POINT   35     .27305   .05969
POINT   36     .274447  .05969
$
POINT   41     .0        .64516
POINT   42     .1569974 .64516
POINT   43     .16256   .64516
POINT   44     .20701   .64516
POINT   45     .27305   .64516
POINT   46     .274447  .64516
$
POINT   51     .0        .68326
POINT   52     .1569974 .68326
POINT   53     .1665224 .68326
POINT   54     .20701   .68326
POINT   55     .27305   .68326
POINT   56     .274447  .68326
$
POINT   61     .0        .70612
POINT   62     .1569974 .70612
POINT   63     .1665224 .70612
```

```
POINT   64      .20701   .70612
POINT   65      .27305   .70612
POINT   66      .274447  .70612
$
POINT   71      .0       .72898
POINT   72      .1569974 .72898
POINT   73      .1665224 .72898
POINT   74      .20701   .72898
POINT   75      .27305   .72898
POINT   76      .274447  .72898
$
POINT   81      .0       .79502
POINT   82      .1569974 .79502
POINT   83      .1665224 .79502
POINT   84      .20701   .79502
POINT   85      .27305   .79502
POINT   86      .274447  .79502
$
POINT   91      .0       .796417
POINT   92      .1569974 .796417
POINT   93      .1665224 .796417
POINT   94      .20701   .796417
POINT   95      .27305   .796417
POINT   96      .274447  .796417
$ Upper Platen
POINT   97      .3       .796417
POINT  191      .0       1.
POINT  192      .1569974 1.
POINT  193      .1665224 1.
POINT  194      .20701   1.
POINT  195      .27305   1.
POINT  196      .274447  1.
POINT  197      .3       1.
$
$Define line
$
LINE   101      STR  101  102    0    12   1.0
LINE   102      STR  102  103    0     2   1.0
LINE   103      STR  103  104    0     3   1.0
LINE   104      STR  104  105    0     5   1.0
LINE   105      STR  105  106    0     1   1.0
LINE   106      STR  101    1    0     1   1.0
LINE   107      STR  102    2    0     1   1.0
LINE   108      STR  103    3    0     1   1.0
LINE   109      STR  104    4    0     1   1.0
LINE   110      STR  105    5    0     1   1.0
LINE   111      STR  106    6    0     1   1.0
$
LINE     1      STR    1    2    0    12   1.0
LINE     2      STR    2    3    0     2   1.0
LINE     3      STR    3    4    0     3   1.0
LINE     4      STR    4    5    0     5   1.0
LINE   116      STR    5    6    0     1   1.0
LINE     5      STR    1   11    0     3   1.0
LINE     6      STR    2   12    0     3   1.0
LINE     7      STR    3   13    0     3   1.0
LINE     8      STR    4   14    0     3   1.0
LINE     9      STR    5   15    0     3   1.0
LINE    10      STR    6   16    0     3   1.0
$
LINE    11      STR   11   12    0    12   1.0
LINE    12      STR   12   13    0     2   1.0
LINE    13      STR   13   14    0     3   1.0
```

```
LINE    14      STR   14   15    0     5   1.0
LINE   115      STR   15   16    0     1   1.0
LINE    15      STR   11   21    0     2   1.0
LINE    16      STR   12   22    0     2   1.0
LINE    17      STR   13   23    0     2   1.0
LINE    18      STR   14   24    0     2   1.0
LINE    19      STR   15   25    0     2   1.0
LINE    20      STR   16   26    0     2   1.0
$
LINE    21      STR   21   22    0    12   1.0
LINE    22      STR   22   23    0     2   1.0
LINE    23      STR   23   24    0     3   1.0
LINE    24      STR   24   25    0     5   1.0
LINE   125      STR   25   26    0     1   1.0
LINE    25      STR   21   31    0     2   1.0
LINE    26      STR   22   32    0     2   1.0
LINE    27      STR   23   33    0     2   1.0
LINE    28      STR   24   34    0     2   1.0
LINE    29      STR   25   35    0     2   1.0
LINE    30      STR   26   36    0     2   1.0
$
LINE    31      STR   31   32    0    12   1.0
LINE    32      STR   32   33    0     2   1.0
LINE    33      STR   33   34    0     3   1.0
LINE    34      STR   34   35    0     5   1.0
LINE   135      STR   35   36    0     1   1.0
LINE    35      STR   31   41    0    48   1.0
LINE    36      STR   32   42    0    48   1.0
LINE    37      STR   33   43    0    48   1.0
LINE    38      STR   34   44    0    48   1.0
LINE    39      STR   35   45    0    48   1.0
LINE    40      STR   36   46    0    48   1.0
$
LINE    41      STR   41   42    0    12   1.0
LINE    42      STR   42   43    0     2   1.0
LINE    43      STR   43   44    0     3   1.0
LINE    44      STR   44   45    0     5   1.0
LINE   145      STR   45   46    0     1   1.0
LINE    45      STR   41   51    0     4   1.0
LINE    46      STR   42   52    0     4   1.0
LINE    47      STR   43   53    0     4   1.0
LINE    48      STR   44   54    0     4   1.0
LINE    49      STR   45   55    0     4   1.0
LINE    50      STR   46   56    0     4   1.0
$
LINE    51      STR   51   52    0    12   1.0
LINE    52      STR   52   53    0     2   1.0
LINE    53      STR   53   54    0     3   1.0
LINE    54      STR   54   55    0     5   1.0
LINE   155      STR   55   56    0     1   1.0
LINE    55      STR   51   61    0     4   1.0
LINE    56      STR   52   62    0     4   1.0
LINE    57      STR   53   63    0     4   1.0
LINE    58      STR   54   64    0     4   1.0
LINE    59      STR   55   65    0     4   1.0
LINE    60      STR   56   66    0     4   1.0
$
LINE    61      STR   61   62    0    12   1.0
LINE    62      STR   62   63    0     2   1.0
LINE    63      STR   63   64    0     3   1.0
LINE    64      STR   64   65    0     5   1.0
LINE   165      STR   65   66    0     1   1.0
LINE    65      STR   61   71    0     4   1.0
```

```
LINE     66      STR    62    72     0      4    1.0
LINE     67      STR    63    73     0      4    1.0
LINE     68      STR    64    74     0      4    1.0
LINE     69      STR    65    75     0      4    1.0
LINE     70      STR    66    76     0      4    1.0
$
LINE     71      STR    71    72     0     12    1.0
LINE     72      STR    72    73     0      2    1.0
LINE     73      STR    73    74     0      3    1.0
LINE     74      STR    74    75     0      5    1.0
LINE    175      STR    75    76     0      1    1.0
LINE     75      STR    71    81     0      4    1.0
LINE     76      STR    72    82     0      4    1.0
LINE     77      STR    73    83     0      4    1.0
LINE     78      STR    74    84     0      4    1.0
LINE     79      STR    75    85     0      4    1.0
LINE     80      STR    76    86     0      4    1.0
$
LINE     81      STR    81    82     0     12    1.0
LINE     82      STR    82    83     0      2    1.0
LINE     83      STR    83    84     0      3    1.0
LINE     84      STR    84    85     0      5    1.0
LINE    185      STR    85    86     0      1    1.0
LINE     85      STR    81    91     0      1    1.0
LINE     86      STR    82    92     0      1    1.0
LINE     87      STR    83    93     0      1    1.0
LINE     88      STR    84    94     0      1    1.0
LINE     89      STR    85    95     0      1    1.0
LINE     90      STR    86    96     0      1    1.0
$
LINE     91      STR    91    92     0     12    1.0
LINE     92      STR    92    93     0      2    1.0
LINE     93      STR    93    94     0      3    1.0
LINE     94      STR    94    95     0      5    1.0
LINE    195      STR    95    96     0      1    1.0
LINE    196      STR    96    97     0      2    1.0
LINE     95      STR    91   191     0      4    1.0
LINE     96      STR    92   192     0      4    1.0
LINE     97      STR    93   193     0      4    1.0
LINE     98      STR    94   194     0      4    1.0
LINE     99      STR    95   195     0      4    1.0
LINE    100      STR    96   196     0      4    1.0
LINE    197      STR    97   197     0      4    1.0
$
LINE    201      STR   191   192     0     12    1.0
LINE    202      STR   192   193     0      2    1.0
LINE    203      STR   193   194     0      3    1.0
LINE    204      STR   194   195     0      5    1.0
LINE    205      STR   195   196     0      1    1.0
LINE    206      STR   196   197     0      2    1.0
$
$ NODEBC CARDS
$
NODEBC   1    106   5  15  25  35  45  55  65  75 85 95 $ Axis of Model
NODEBC   2    101 102 103 104 105                 $ Bottom of Model
$
$ SIDEBC CARDS
$
SIDEBC 100  101 102 103 104 105      $ Bot of Drum
SIDEBC 200  106   5  15  25  35  45  55  65  75  85  95 $ Axis of Model
SIDEBC 300  111  10  20  30  40  50  60  70  80  90 $ R-Side of Drum
SIDEBC 400   91  92  93  94 195       $ Top of Drum
SIDEBC 401  201 202 203 204 205 206   $ Top of Platen
```

```
SIDEBC 500  101 102 103 104 105 111 10 20 30 40 50 60 70 80 90 91 92 93 94 195
SIDEBC 501  101 102 103 104 105 111 10 20 30 40 50 60 70 80 90 196 197 206 205
204 203 202 201
SIDEBC 643   43      $ Floor of Space
SIDEBC 648   48      $ Right wall of Space
SIDEBC 653   53      $ Roof of Space
SIDEBC 647   47      $ Left wall of Space
$
$ REGION CARDS
$
REGION   1    1   -1   -6  -11   -5
REGION   2    1   -2   -7  -12   -6
REGION   3    1   -3   -8  -13   -7
REGION   4    1   -4   -9  -14   -8
$
REGION  11    3  -11  -16  -21  -15
REGION  12    3  -12  -17  -22  -16
REGION  13    3  -13  -18  -23  -17
REGION  14    3  -14  -19  -24  -18
$
$
REGION  21    2  -21  -26  -31  -25
REGION  22    2  -22  -27  -32  -26
REGION  23    1  -23  -28  -33  -27
REGION  24    1  -24  -29  -34  -28
$
REGION  31    4  -31  -36  -41  -35
REGION  32    2  -32  -37  -42  -36
REGION  33    1  -33  -38  -43  -37
REGION  34    1  -34  -39  -44  -38
$
REGION  41    4  -41  -46  -51  -45
REGION  42    2  -42  -47  -52  -46
$REGION  43    2  -43  -48  -53  -47
REGION  44    1  -44  -49  -54  -48
$
REGION  51    4  -51  -56  -61  -55
REGION  52    2  -52  -57  -62  -56
REGION  53    2  -53  -58  -63  -57
REGION  54    1  -54  -59  -64  -58
$
REGION  61    2  -61  -66  -71  -65
REGION  62    2  -62  -67  -72  -66
REGION  63    2  -63  -68  -73  -67
REGION  64    1  -64  -69  -74  -68
$
REGION  71    1  -71  -76  -81  -75
REGION  72    1  -72  -77  -82  -76
REGION  73    1  -73  -78  -83  -77
REGION  74    1  -74  -79  -84  -78
$ Drum
REGION  81    5  -81  -86  -91  -85
REGION  82    5  -82  -87  -92  -86
REGION  83    5  -83  -88  -93  -87
REGION  84    5  -84  -89  -94  -88
$ Platen
REGION  91    6  -91  -96 -201  -95
REGION  92    6  -92  -97 -202  -96
REGION  93    6  -93  -98 -203  -97
REGION  94    6  -94  -99 -204  -98
REGION  95    6 -195 -100 -205  -99
REGION  96    6 -196 -197 -206 -100
$ Drum
```

```
REGION 101     5 -101 -107   -1 -106
REGION 102     5 -102 -108   -2 -107
REGION 103     5 -103 -109   -3 -108
REGION 104     5 -104 -110   -4 -109
REGION 105     5 -105 -111 -116 -110
$ Drum
REGION 106     5 -116  -10 -115   -9
REGION 115     5 -115  -20 -125  -19
REGION 125     5 -125  -30 -135  -29
REGION 135     5 -135  -40 -145  -39
REGION 145     5 -145  -50 -155  -49
REGION 155     5 -155  -60 -165  -59
REGION 165     5 -165  -70 -175  -69
REGION 175     5 -175  -80 -185  -79
REGION 185     5 -185  -90 -195  -89
$
SCHEME    0     M
EXIT
```

B-2 6-inch POP Waste Mesh for UTS and TTS

```
TITLE
Assembled POP pressed with platen - 6" Pipe (07/13/03-B.Y.PARK)
$
$Define Point
$
$ Lower Impact Limiter
POINT  101     .0       -1.397E-3
POINT  102     .07887   -1.397E-3
POINT  103     .08509   -1.397E-3
POINT  104     .13970   -1.397E-3
POINT  105     .27305   -1.397E-3
POINT  106     .274447  -1.397E-3
$
POINT    1     .0       .0
POINT    2     .07887   .0
POINT    3     .08509   .0
POINT    4     .13970   .0
POINT    5     .27305   .0
POINT    6     .274447  .0
$
POINT   11     .0       .04
POINT   12     .07887   .04
POINT   13     .08509   .04
POINT   14     .13970   .04
POINT   15     .27305   .04
POINT   16     .274447  .04
$
POINT   21     .0       .05334
POINT   22     .07887   .05334
POINT   23     .08509   .05334
POINT   24     .13970   .05334
POINT   25     .27305   .05334
POINT   26     .274447  .05334
$
POINT   31     .0       .05969
POINT   32     .07887   .05969
POINT   33     .08509   .05969
POINT   34     .13970   .05969
POINT   35     .27305   .05969
POINT   36     .274447  .05969
$
POINT   41     .0       .64516
POINT   42     .07887   .64516
POINT   43     .08509   .64516
POINT   44     .13970   .64516
POINT   45     .27305   .64516
POINT   46     .274447  .64516
$
POINT   51     .0       .69088
POINT   52     .07887   .69088
POINT   53     .08905   .69088
POINT   54     .13970   .69088
POINT   55     .27305   .69088
POINT   56     .274447  .69088
$
POINT   61     .0       .71374
POINT   62     .07887   .71374
POINT   63     .08905   .71374
POINT   64     .13970   .71374
POINT   65     .27305   .71374
POINT   66     .274447  .71374
```

```
$
POINT   71      .0        .73660
POINT   72      .07887    .73660
POINT   73      .08905    .73660
POINT   74      .13970    .73660
POINT   75      .27305    .73660
POINT   76      .274447   .73660
$
POINT   81      .0        .79502
POINT   82      .07887    .79502
POINT   83      .08905    .79502
POINT   84      .13970    .79502
POINT   85      .27305    .79502
POINT   86      .274447   .79502
$
POINT   91      .0        .796417
POINT   92      .07887    .796417
POINT   93      .08905    .796417
POINT   94      .13970    .796417
POINT   95      .27305    .796417
POINT   96      .274447   .796417
$ Upper Platen
POINT   97      .3        .796417
POINT  191      .0        1.
POINT  192      .07887    1.
POINT  193      .08905    1.
POINT  194      .13970    1.
POINT  195      .27305    1.
POINT  196      .274447   1.
POINT  197      .3        1.
$
$Define line
$
LINE   101      STR  101  102    0     6   1.0
LINE   102      STR  102  103    0     2   1.0
LINE   103      STR  103  104    0     4   1.0
LINE   104      STR  104  105    0    10   1.0
LINE   105      STR  105  106    0     1   1.0
LINE   106      STR  101    1    0     1   1.0
LINE   107      STR  102    2    0     1   1.0
LINE   108      STR  103    3    0     1   1.0
LINE   109      STR  104    4    0     1   1.0
LINE   110      STR  105    5    0     1   1.0
LINE   111      STR  106    6    0     1   1.0
$
LINE     1      STR    1    2    0     6   1.0
LINE     2      STR    2    3    0     2   1.0
LINE     3      STR    3    4    0     4   1.0
LINE     4      STR    4    5    0    10   1.0
LINE   116      STR    5    6    0     1   1.0
LINE     5      STR    1   11    0     3   1.0
LINE     6      STR    2   12    0     3   1.0
LINE     7      STR    3   13    0     3   1.0
LINE     8      STR    4   14    0     3   1.0
LINE     9      STR    5   15    0     3   1.0
LINE    10      STR    6   16    0     3   1.0
$
LINE    11      STR   11   12    0     6   1.0
LINE    12      STR   12   13    0     2   1.0
LINE    13      STR   13   14    0     4   1.0
LINE    14      STR   14   15    0    10   1.0
LINE   115      STR   15   16    0     1   1.0
LINE    15      STR   11   21    0     2   1.0
```

```
LINE    16      STR   12   22    0     2   1.0
LINE    17      STR   13   23    0     2   1.0
LINE    18      STR   14   24    0     2   1.0
LINE    19      STR   15   25    0     2   1.0
LINE    20      STR   16   26    0     2   1.0
$
LINE    21      STR   21   22    0     6   1.0
LINE    22      STR   22   23    0     2   1.0
LINE    23      STR   23   24    0     4   1.0
LINE    24      STR   24   25    0    10   1.0
LINE   125      STR   25   26    0     1   1.0
LINE    25      STR   21   31    0     2   1.0
LINE    26      STR   22   32    0     2   1.0
LINE    27      STR   23   33    0     2   1.0
LINE    28      STR   24   34    0     2   1.0
LINE    29      STR   25   35    0     2   1.0
LINE    30      STR   26   36    0     2   1.0
$
LINE    31      STR   31   32    0     6   1.0
LINE    32      STR   32   33    0     2   1.0
LINE    33      STR   33   34    0     4   1.0
LINE    34      STR   34   35    0    10   1.0
LINE   135      STR   35   36    0     1   1.0
LINE    35      STR   31   41    0    48   1.0
LINE    36      STR   32   42    0    48   1.0
LINE    37      STR   33   43    0    48   1.0
LINE    38      STR   34   44    0    48   1.0
LINE    39      STR   35   45    0    48   1.0
LINE    40      STR   36   46    0    48   1.0
$
LINE    41      STR   41   42    0     6   1.0
LINE    42      STR   42   43    0     2   1.0
LINE    43      STR   43   44    0     4   1.0
LINE    44      STR   44   45    0    10   1.0
LINE   145      STR   45   46    0     1   1.0
LINE    45      STR   41   51    0     4   1.0
LINE    46      STR   42   52    0     4   1.0
LINE    47      STR   43   53    0     4   1.0
LINE    48      STR   44   54    0     4   1.0
LINE    49      STR   45   55    0     4   1.0
LINE    50      STR   46   56    0     4   1.0
$
LINE    51      STR   51   52    0     6   1.0
LINE    52      STR   52   53    0     2   1.0
LINE    53      STR   53   54    0     4   1.0
LINE    54      STR   54   55    0    10   1.0
LINE   155      STR   55   56    0     1   1.0
LINE    55      STR   51   61    0     4   1.0
LINE    56      STR   52   62    0     4   1.0
LINE    57      STR   53   63    0     4   1.0
LINE    58      STR   54   64    0     4   1.0
LINE    59      STR   55   65    0     4   1.0
LINE    60      STR   56   66    0     4   1.0
$
LINE    61      STR   61   62    0     6   1.0
LINE    62      STR   62   63    0     2   1.0
LINE    63      STR   63   64    0     4   1.0
LINE    64      STR   64   65    0    10   1.0
LINE   165      STR   65   66    0     1   1.0
LINE    65      STR   61   71    0     4   1.0
LINE    66      STR   62   72    0     4   1.0
LINE    67      STR   63   73    0     4   1.0
LINE    68      STR   64   74    0     4   1.0
```

```
LINE    69     STR   65   75    0     4   1.0
LINE    70     STR   66   76    0     4   1.0
$
LINE    71     STR   71   72    0     6   1.0
LINE    72     STR   72   73    0     2   1.0
LINE    73     STR   73   74    0     4   1.0
LINE    74     STR   74   75    0    10   1.0
LINE   175     STR   75   76    0     1   1.0
LINE    75     STR   71   81    0     4   1.0
LINE    76     STR   72   82    0     4   1.0
LINE    77     STR   73   83    0     4   1.0
LINE    78     STR   74   84    0     4   1.0
LINE    79     STR   75   85    0     4   1.0
LINE    80     STR   76   86    0     4   1.0
$
LINE    81     STR   81   82    0     6   1.0
LINE    82     STR   82   83    0     2   1.0
LINE    83     STR   83   84    0     4   1.0
LINE    84     STR   84   85    0    10   1.0
LINE   185     STR   85   86    0     1   1.0
LINE    85     STR   81   91    0     1   1.0
LINE    86     STR   82   92    0     1   1.0
LINE    87     STR   83   93    0     1   1.0
LINE    88     STR   84   94    0     1   1.0
LINE    89     STR   85   95    0     1   1.0
LINE    90     STR   86   96    0     1   1.0
$
LINE    91     STR   91   92    0     6   1.0
LINE    92     STR   92   93    0     2   1.0
LINE    93     STR   93   94    0     4   1.0
LINE    94     STR   94   95    0    10   1.0
LINE   195     STR   95   96    0     1   1.0
LINE   196     STR   96   97    0     2   1.0
LINE    95     STR   91  191    0     4   1.0
LINE    96     STR   92  192    0     4   1.0
LINE    97     STR   93  193    0     4   1.0
LINE    98     STR   94  194    0     4   1.0
LINE    99     STR   95  195    0     4   1.0
LINE   100     STR   96  196    0     4   1.0
LINE   197     STR   97  197    0     4   1.0
$
LINE   201     STR  191  192    0     6   1.0
LINE   202     STR  192  193    0     2   1.0
LINE   203     STR  193  194    0     4   1.0
LINE   204     STR  194  195    0    10   1.0
LINE   205     STR  195  196    0     1   1.0
LINE   206     STR  196  197    0     2   1.0
$
$ NODEBC CARDS
$
NODEBC   1    106   5  15  25  35  45  55  65  75 85 95 $ Axis of Model
NODEBC   2    101 102 103 104 105                 $ Bottom of Model
$
$ SIDEBC CARDS
$
SIDEBC 100  101 102 103 104 105      $ Bot of Drum
SIDEBC 200  106   5  15  25  35  45  55  65  75  85  95 $ Axis of Model
SIDEBC 300  111  10  20  30  40  50  60  70  80  90 $ R-Side of Drum
SIDEBC 400   91  92  93  94 195       $ Top of Drum
SIDEBC 401  201 202 203 204 205 206   $ Top of Platen
SIDEBC 500  101 102 103 104 105 111 10 20 30 40 50 60 70 80 90 195 94 93 92 91
SIDEBC 501  101 102 103 104 105 111 10 20 30 40 50 60 70 80 90 196 197 206 205
204 203 202 201
```

```
SIDEBC 643   43      $ Floor of Space
SIDEBC 648   48      $ Right wall of Space
SIDEBC 653   53      $ Roof of Space
SIDEBC 647   47      $ Left wall of Space
$
$ REGION CARDS
$
REGION   1    1   -1   -6  -11   -5
REGION   2    1   -2   -7  -12   -6
REGION   3    1   -3   -8  -13   -7
REGION   4    1   -4   -9  -14   -8
$
REGION  11    3  -11  -16  -21  -15
REGION  12    3  -12  -17  -22  -16
REGION  13    3  -13  -18  -23  -17
REGION  14    3  -14  -19  -24  -18
$
$
REGION  21    2  -21  -26  -31  -25
REGION  22    2  -22  -27  -32  -26
REGION  23    1  -23  -28  -33  -27
REGION  24    1  -24  -29  -34  -28
$
REGION  31    4  -31  -36  -41  -35
REGION  32    2  -32  -37  -42  -36
REGION  33    1  -33  -38  -43  -37
REGION  34    1  -34  -39  -44  -38
$
REGION  41    4  -41  -46  -51  -45
REGION  42    2  -42  -47  -52  -46
$REGION  43    2  -43  -48  -53  -47
REGION  44    1  -44  -49  -54  -48
$
REGION  51    4  -51  -56  -61  -55
REGION  52    2  -52  -57  -62  -56
REGION  53    2  -53  -58  -63  -57
REGION  54    1  -54  -59  -64  -58
$
REGION  61    2  -61  -66  -71  -65
REGION  62    2  -62  -67  -72  -66
REGION  63    2  -63  -68  -73  -67
REGION  64    1  -64  -69  -74  -68
$
REGION  71    1  -71  -76  -81  -75
REGION  72    1  -72  -77  -82  -76
REGION  73    1  -73  -78  -83  -77
REGION  74    1  -74  -79  -84  -78
$ Drum
REGION  81    5  -81  -86  -91  -85
REGION  82    5  -82  -87  -92  -86
REGION  83    5  -83  -88  -93  -87
REGION  84    5  -84  -89  -94  -88
$ Platen
REGION  91    6  -91  -96 -201  -95
REGION  92    6  -92  -97 -202  -96
REGION  93    6  -93  -98 -203  -97
REGION  94    6  -94  -99 -204  -98
REGION  95    6 -195 -100 -205  -99
REGION  96    6 -196 -197 -206 -100
$ Drum
REGION 101    5 -101 -107   -1 -106
REGION 102    5 -102 -108   -2 -107
REGION 103    5 -103 -109   -3 -108
```

```
REGION 104     5 -104 -110   -4 -109
REGION 105     5 -105 -111 -116 -110
$ Drum
REGION 106     5 -116  -10 -115   -9
REGION 115     5 -115  -20 -125  -19
REGION 125     5 -125  -30 -135  -29
REGION 135     5 -135  -40 -145  -39
REGION 145     5 -145  -50 -155  -49
REGION 155     5 -155  -60 -165  -59
REGION 165     5 -165  -70 -175  -69
REGION 175     5 -175  -80 -185  -79
REGION 185     5 -185  -90 -195  -89
$
SCHEME   0     M
EXIT
```

B-3 12-inch POP Waste Mesh for HTS

```
TITLE
 Assembled POP - 12 INCH PIPE (07/10/03-B.Y.PARK)
$
$Define Point
$
$ Lower Impact Limiter
POINT  101     .0        -1.397E-3
POINT  102     .1569974 -1.397E-3
POINT  103     .16256   -1.397E-3
POINT  104     .20701   -1.397E-3
POINT  105     .27305   -1.397E-3
POINT  106     .274447  -1.397E-3
$
POINT    1     .0        .0
POINT    2     .1569974 .0
POINT    3     .16256   .0
POINT    4     .20701   .0
POINT    5     .27305   .0
POINT    6     .274447  .0
$
POINT   11     .0        .04
POINT   12     .1569974 .04
POINT   13     .16256   .04
POINT   14     .20701   .04
POINT   15     .27305   .04
POINT   16     .274447  .04
$
POINT   21     .0        .05334
POINT   22     .1569974 .05334
POINT   23     .16256   .05334
POINT   24     .20701   .05334
POINT   25     .27305   .05334
POINT   26     .274447  .05334
$
POINT   31     .0        .05969
POINT   32     .1569974 .05969
POINT   33     .16256   .05969
POINT   34     .20701   .05969
POINT   35     .27305   .05969
POINT   36     .274447  .05969
$
POINT   41     .0        .64516
POINT   42     .1569974 .64516
POINT   43     .16256   .64516
POINT   44     .20701   .64516
POINT   45     .27305   .64516
POINT   46     .274447  .64516
$
POINT   51     .0        .68326
POINT   52     .1569974 .68326
POINT   53     .1665224 .68326
POINT   54     .20701   .68326
POINT   55     .27305   .68326
POINT   56     .274447  .68326
$
POINT   61     .0        .70612
POINT   62     .1569974 .70612
POINT   63     .1665224 .70612
POINT   64     .20701   .70612
POINT   65     .27305   .70612
POINT   66     .274447  .70612
```

```
$
POINT   71      .0        .72898
POINT   72      .1569974 .72898
POINT   73      .1665224 .72898
POINT   74      .20701   .72898
POINT   75      .27305   .72898
POINT   76      .274447  .72898
$
POINT   81      .0        .79502
POINT   82      .1569974 .79502
POINT   83      .1665224 .79502
POINT   84      .20701   .79502
POINT   85      .27305   .79502
POINT   86      .274447  .79502
$
POINT   91      .0        .796417
POINT   92      .1569974 .796417
POINT   93      .1665224 .796417
POINT   94      .20701   .796417
POINT   95      .27305   .796417
POINT   96      .274447  .796417
$
$Define line
$
LINE   101      STR  101  102    0    12   1.0
LINE   102      STR  102  103    0     2   1.0
LINE   103      STR  103  104    0     3   1.0
LINE   104      STR  104  105    0     5   1.0
LINE   105      STR  105  106    0     1   1.0
LINE   106      STR  101    1    0     1   1.0
LINE   107      STR  102    2    0     1   1.0
LINE   108      STR  103    3    0     1   1.0
LINE   109      STR  104    4    0     1   1.0
LINE   110      STR  105    5    0     1   1.0
LINE   111      STR  106    6    0     1   1.0
$
LINE     1      STR    1    2    0    12   1.0
LINE     2      STR    2    3    0     2   1.0
LINE     3      STR    3    4    0     3   1.0
LINE     4      STR    4    5    0     5   1.0
LINE   116      STR    5    6    0     1   1.0
LINE     5      STR    1   11    0     3   1.0
LINE     6      STR    2   12    0     3   1.0
LINE     7      STR    3   13    0     3   1.0
LINE     8      STR    4   14    0     3   1.0
LINE     9      STR    5   15    0     3   1.0
LINE    10      STR    6   16    0     3   1.0
$
LINE    11      STR   11   12    0    12   1.0
LINE    12      STR   12   13    0     2   1.0
LINE    13      STR   13   14    0     3   1.0
LINE    14      STR   14   15    0     5   1.0
LINE   115      STR   15   16    0     1   1.0
LINE    15      STR   11   21    0     2   1.0
LINE    16      STR   12   22    0     2   1.0
LINE    17      STR   13   23    0     2   1.0
LINE    18      STR   14   24    0     2   1.0
LINE    19      STR   15   25    0     2   1.0
LINE    20      STR   16   26    0     2   1.0
$
LINE    21      STR   21   22    0    12   1.0
LINE    22      STR   22   23    0     2   1.0
LINE    23      STR   23   24    0     3   1.0
```

```
LINE    24      STR   24   25    0     5   1.0
LINE   125      STR   25   26    0     1   1.0
LINE    25      STR   21   31    0     2   1.0
LINE    26      STR   22   32    0     2   1.0
LINE    27      STR   23   33    0     2   1.0
LINE    28      STR   24   34    0     2   1.0
LINE    29      STR   25   35    0     2   1.0
LINE    30      STR   26   36    0     2   1.0
$
LINE    31      STR   31   32    0    12   1.0
LINE    32      STR   32   33    0     2   1.0
LINE    33      STR   33   34    0     3   1.0
LINE    34      STR   34   35    0     5   1.0
LINE   135      STR   35   36    0     1   1.0
LINE    35      STR   31   41    0    48   1.0
LINE    36      STR   32   42    0    48   1.0
LINE    37      STR   33   43    0    48   1.0
LINE    38      STR   34   44    0    48   1.0
LINE    39      STR   35   45    0    48   1.0
LINE    40      STR   36   46    0    48   1.0
$
LINE    41      STR   41   42    0    12   1.0
LINE    42      STR   42   43    0     2   1.0
LINE    43      STR   43   44    0     3   1.0
LINE    44      STR   44   45    0     5   1.0
LINE   145      STR   45   46    0     1   1.0
LINE    45      STR   41   51    0     4   1.0
LINE    46      STR   42   52    0     4   1.0
LINE    47      STR   43   53    0     4   1.0
LINE    48      STR   44   54    0     4   1.0
LINE    49      STR   45   55    0     4   1.0
LINE    50      STR   46   56    0     4   1.0
$
LINE    51      STR   51   52    0    12   1.0
LINE    52      STR   52   53    0     2   1.0
LINE    53      STR   53   54    0     3   1.0
LINE    54      STR   54   55    0     5   1.0
LINE   155      STR   55   56    0     1   1.0
LINE    55      STR   51   61    0     4   1.0
LINE    56      STR   52   62    0     4   1.0
LINE    57      STR   53   63    0     4   1.0
LINE    58      STR   54   64    0     4   1.0
LINE    59      STR   55   65    0     4   1.0
LINE    60      STR   56   66    0     4   1.0
$
LINE    61      STR   61   62    0    12   1.0
LINE    62      STR   62   63    0     2   1.0
LINE    63      STR   63   64    0     3   1.0
LINE    64      STR   64   65    0     5   1.0
LINE   165      STR   65   66    0     1   1.0
LINE    65      STR   61   71    0     4   1.0
LINE    66      STR   62   72    0     4   1.0
LINE    67      STR   63   73    0     4   1.0
LINE    68      STR   64   74    0     4   1.0
LINE    69      STR   65   75    0     4   1.0
LINE    70      STR   66   76    0     4   1.0
$
LINE    71      STR   71   72    0    12   1.0
LINE    72      STR   72   73    0     2   1.0
LINE    73      STR   73   74    0     3   1.0
LINE    74      STR   74   75    0     5   1.0
LINE   175      STR   75   76    0     1   1.0
LINE    75      STR   71   81    0     4   1.0
```

```
LINE    76     STR   72   82    0     4   1.0
LINE    77     STR   73   83    0     4   1.0
LINE    78     STR   74   84    0     4   1.0
LINE    79     STR   75   85    0     4   1.0
LINE    80     STR   76   86    0     4   1.0
$
LINE    81     STR   81   82    0    12   1.0
LINE    82     STR   82   83    0     2   1.0
LINE    83     STR   83   84    0     3   1.0
LINE    84     STR   84   85    0     5   1.0
LINE   185     STR   85   86    0     1   1.0
LINE    85     STR   81   91    0     1   1.0
LINE    86     STR   82   92    0     1   1.0
LINE    87     STR   83   93    0     1   1.0
LINE    88     STR   84   94    0     1   1.0
LINE    89     STR   85   95    0     1   1.0
LINE    90     STR   86   96    0     1   1.0
$
LINE    91     STR   91   92    0    12   1.0
LINE    92     STR   92   93    0     2   1.0
LINE    93     STR   93   94    0     3   1.0
LINE    94     STR   94   95    0     5   1.0
LINE   195     STR   95   96    0     1   1.0
$
$ NODEBC CARDS
$
NODEBC   1    106    5   15   25   35   45   55   65   75  85 $ Axis of Model
NODEBC   2    101  102  103  104  105                 $ Bottom of Model
$
$ SIDEBC CARDS
$
SIDEBC 100  101  102  103  104  105      $ Bot of Drum
SIDEBC 200  106    5   15   25   35   45   55   65   75   85 $ Axis of Model
SIDEBC 300  111   10   20   30   40   50   60   70   80   90 $ R-Side of Drum
SIDEBC 400   91   92   93   94  195                           $ Top of Top Im-
pact Limiter
SIDEBC 500  101 102 103 104 105 111 10 20 30 40 50 60 70 80 90 91 92 93 94 195
$ Vol of Drum
SIDEBC 643   43      $ Floor of Space
SIDEBC 648   48      $ Right wall of Space
SIDEBC 653   53      $ Roof of Space
SIDEBC 647   47      $ Left wall of Space
$
$ REGION CARDS
$
REGION   1    1   -1   -6  -11   -5
REGION   2    1   -2   -7  -12   -6
REGION   3    1   -3   -8  -13   -7
REGION   4    1   -4   -9  -14   -8
$
REGION  11    3  -11  -16  -21  -15
REGION  12    3  -12  -17  -22  -16
REGION  13    3  -13  -18  -23  -17
REGION  14    3  -14  -19  -24  -18
$
$
REGION  21    2  -21  -26  -31  -25
REGION  22    2  -22  -27  -32  -26
REGION  23    1  -23  -28  -33  -27
REGION  24    1  -24  -29  -34  -28
$
REGION  31    4  -31  -36  -41  -35
REGION  32    2  -32  -37  -42  -36
```

```
REGION  33    1  -33  -38  -43  -37
REGION  34    1  -34  -39  -44  -38
$
REGION  41    4  -41  -46  -51  -45
REGION  42    2  -42  -47  -52  -46
$REGION  43    2  -43  -48  -53  -47
REGION  44    1  -44  -49  -54  -48
$
REGION  51    4  -51  -56  -61  -55
REGION  52    2  -52  -57  -62  -56
REGION  53    2  -53  -58  -63  -57
REGION  54    1  -54  -59  -64  -58
$
REGION  61    2  -61  -66  -71  -65
REGION  62    2  -62  -67  -72  -66
REGION  63    2  -63  -68  -73  -67
REGION  64    1  -64  -69  -74  -68
$
REGION  71    1  -71  -76  -81  -75
REGION  72    1  -72  -77  -82  -76
REGION  73    1  -73  -78  -83  -77
REGION  74    1  -74  -79  -84  -78
$
REGION  81    5  -81  -86  -91  -85
REGION  82    5  -82  -87  -92  -86
REGION  83    5  -83  -88  -93  -87
REGION  84    5  -84  -89  -94  -88
$
$
REGION 101    5 -101 -107   -1 -106
REGION 102    5 -102 -108   -2 -107
REGION 103    5 -103 -109   -3 -108
REGION 104    5 -104 -110   -4 -109
REGION 105    5 -105 -111 -116 -110
$
REGION 106    5 -116  -10 -115   -9
REGION 115    5 -115  -20 -125  -19
REGION 125    5 -125  -30 -135  -29
REGION 135    5 -135  -40 -145  -39
REGION 145    5 -145  -50 -155  -49
REGION 155    5 -155  -60 -165  -59
REGION 165    5 -165  -70 -175  -69
REGION 175    5 -175  -80 -185  -79
REGION 185    5 -185  -90 -195  -89
$
SCHEME   0    M
EXIT
```

B-4 6-inch POP Waste Mesh for HTS

```
TITLE
POP Waste for Hydrostatic Test Simulation - 6" Pipe (07/13/03-B.Y.PARK)
$
$Define Point
$
$ Lower Impact Limiter
POINT  101     .0        -1.397E-3
POINT  102     .07887    -1.397E-3
POINT  103     .08509    -1.397E-3
POINT  104     .13970    -1.397E-3
POINT  105     .27305    -1.397E-3
POINT  106     .274447   -1.397E-3
$
POINT    1     .0        .0
POINT    2     .07887    .0
POINT    3     .08509    .0
POINT    4     .13970    .0
POINT    5     .27305    .0
POINT    6     .274447   .0
$
POINT   11     .0        .04
POINT   12     .07887    .04
POINT   13     .08509    .04
POINT   14     .13970    .04
POINT   15     .27305    .04
POINT   16     .274447   .04
$
POINT   21     .0        .05334
POINT   22     .07887    .05334
POINT   23     .08509    .05334
POINT   24     .13970    .05334
POINT   25     .27305    .05334
POINT   26     .274447   .05334
$
POINT   31     .0        .05969
POINT   32     .07887    .05969
POINT   33     .08509    .05969
POINT   34     .13970    .05969
POINT   35     .27305    .05969
POINT   36     .274447   .05969
$
POINT   41     .0        .64516
POINT   42     .07887    .64516
POINT   43     .08509    .64516
POINT   44     .13970    .64516
POINT   45     .27305    .64516
POINT   46     .274447   .64516
$
POINT   51     .0        .69088
POINT   52     .07887    .69088
POINT   53     .089905   .69088
POINT   54     .13970    .69088
POINT   55     .27305    .69088
POINT   56     .274447   .69088
$
POINT   61     .0        .71374
POINT   62     .07887    .71374
POINT   63     .089905   .71374
POINT   64     .13970    .71374
POINT   65     .27305    .71374
POINT   66     .274447   .71374
```

```
$
POINT   71      .0        .73660
POINT   72      .07887    .73660
POINT   73      .089905   .73660
POINT   74      .13970    .73660
POINT   75      .27305    .73660
POINT   76      .274447   .73660
$
POINT   81      .0        .79502
POINT   82      .07887    .79502
POINT   83      .089905   .79502
POINT   84      .13970    .79502
POINT   85      .27305    .79502
POINT   86      .274447   .79502
$
POINT   91      .0        .796417
POINT   92      .07887    .796417
POINT   93      .089905   .796417
POINT   94      .13970    .796417
POINT   95      .27305    .796417
POINT   96      .274447   .796417
$
$Define line
$
LINE   101      STR  101  102    0     6   1.0
LINE   102      STR  102  103    0     2   1.0
LINE   103      STR  103  104    0     4   1.0
LINE   104      STR  104  105    0    10   1.0
LINE   105      STR  105  106    0     1   1.0
LINE   106      STR  101    1    0     1   1.0
LINE   107      STR  102    2    0     1   1.0
LINE   108      STR  103    3    0     1   1.0
LINE   109      STR  104    4    0     1   1.0
LINE   110      STR  105    5    0     1   1.0
LINE   111      STR  106    6    0     1   1.0
$
LINE     1      STR    1    2    0     6   1.0
LINE     2      STR    2    3    0     2   1.0
LINE     3      STR    3    4    0     4   1.0
LINE     4      STR    4    5    0    10   1.0
LINE   116      STR    5    6    0     1   1.0
LINE     5      STR    1   11    0     3   1.0
LINE     6      STR    2   12    0     3   1.0
LINE     7      STR    3   13    0     3   1.0
LINE     8      STR    4   14    0     3   1.0
LINE     9      STR    5   15    0     3   1.0
LINE    10      STR    6   16    0     3   1.0
$
LINE    11      STR   11   12    0     6   1.0
LINE    12      STR   12   13    0     2   1.0
LINE    13      STR   13   14    0     4   1.0
LINE    14      STR   14   15    0    10   1.0
LINE   115      STR   15   16    0     1   1.0
LINE    15      STR   11   21    0     2   1.0
LINE    16      STR   12   22    0     2   1.0
LINE    17      STR   13   23    0     2   1.0
LINE    18      STR   14   24    0     2   1.0
LINE    19      STR   15   25    0     2   1.0
LINE    20      STR   16   26    0     2   1.0
$
LINE    21      STR   21   22    0     6   1.0
LINE    22      STR   22   23    0     2   1.0
LINE    23      STR   23   24    0     4   1.0
```

```
LINE    24      STR   24    25     0     10    1.0
LINE   125      STR   25    26     0      1    1.0
LINE    25      STR   21    31     0      2    1.0
LINE    26      STR   22    32     0      2    1.0
LINE    27      STR   23    33     0      2    1.0
LINE    28      STR   24    34     0      2    1.0
LINE    29      STR   25    35     0      2    1.0
LINE    30      STR   26    36     0      2    1.0
$
LINE    31      STR   31    32     0      6    1.0
LINE    32      STR   32    33     0      2    1.0
LINE    33      STR   33    34     0      4    1.0
LINE    34      STR   34    35     0     10    1.0
LINE   135      STR   35    36     0      1    1.0
LINE    35      STR   31    41     0     48    1.0
LINE    36      STR   32    42     0     48    1.0
LINE    37      STR   33    43     0     48    1.0
LINE    38      STR   34    44     0     48    1.0
LINE    39      STR   35    45     0     48    1.0
LINE    40      STR   36    46     0     48    1.0
$
LINE    41      STR   41    42     0      6    1.0
LINE    42      STR   42    43     0      2    1.0
LINE    43      STR   43    44     0      4    1.0
LINE    44      STR   44    45     0     10    1.0
LINE   145      STR   45    46     0      1    1.0
LINE    45      STR   41    51     0      4    1.0
LINE    46      STR   42    52     0      4    1.0
LINE    47      STR   43    53     0      4    1.0
LINE    48      STR   44    54     0      4    1.0
LINE    49      STR   45    55     0      4    1.0
LINE    50      STR   46    56     0      4    1.0
$
LINE    51      STR   51    52     0      6    1.0
LINE    52      STR   52    53     0      2    1.0
LINE    53      STR   53    54     0      4    1.0
LINE    54      STR   54    55     0     10    1.0
LINE   155      STR   55    56     0      1    1.0
LINE    55      STR   51    61     0      4    1.0
LINE    56      STR   52    62     0      4    1.0
LINE    57      STR   53    63     0      4    1.0
LINE    58      STR   54    64     0      4    1.0
LINE    59      STR   55    65     0      4    1.0
LINE    60      STR   56    66     0      4    1.0
$
LINE    61      STR   61    62     0      6    1.0
LINE    62      STR   62    63     0      2    1.0
LINE    63      STR   63    64     0      4    1.0
LINE    64      STR   64    65     0     10    1.0
LINE   165      STR   65    66     0      1    1.0
LINE    65      STR   61    71     0      4    1.0
LINE    66      STR   62    72     0      4    1.0
LINE    67      STR   63    73     0      4    1.0
LINE    68      STR   64    74     0      4    1.0
LINE    69      STR   65    75     0      4    1.0
LINE    70      STR   66    76     0      4    1.0
$
LINE    71      STR   71    72     0      6    1.0
LINE    72      STR   72    73     0      2    1.0
LINE    73      STR   73    74     0      4    1.0
LINE    74      STR   74    75     0     10    1.0
LINE   175      STR   75    76     0      1    1.0
LINE    75      STR   71    81     0      4    1.0
```

```
LINE     76      STR    72    82     0      4    1.0
LINE     77      STR    73    83     0      4    1.0
LINE     78      STR    74    84     0      4    1.0
LINE     79      STR    75    85     0      4    1.0
LINE     80      STR    76    86     0      4    1.0
$
LINE     81      STR    81    82     0      6    1.0
LINE     82      STR    82    83     0      2    1.0
LINE     83      STR    83    84     0      4    1.0
LINE     84      STR    84    85     0     10    1.0
LINE    185      STR    85    86     0      1    1.0
LINE     85      STR    81    91     0      1    1.0
LINE     86      STR    82    92     0      1    1.0
LINE     87      STR    83    93     0      1    1.0
LINE     88      STR    84    94     0      1    1.0
LINE     89      STR    85    95     0      1    1.0
LINE     90      STR    86    96     0      1    1.0
$
LINE     91      STR    91    92     0      6    1.0
LINE     92      STR    92    93     0      2    1.0
LINE     93      STR    93    94     0      4    1.0
LINE     94      STR    94    95     0     10    1.0
LINE    195      STR    95    96     0      1    1.0
$
$ NODEBC CARDS
$
NODEBC   1    106    5   15   25   35   45   55   65   75  85 $ Axis of Model
NODEBC   2    101  102  103  104  105                  $ Bottom of Model
$
$ SIDEBC CARDS
$
SIDEBC 100  101  102  103  104  105      $ Bot of Drum
SIDEBC 200  106    5   15   25   35   45   55   65   75   85 $ Axis of Model
SIDEBC 300  111   10   20   30   40   50   60   70   80   90 $ R-Side of Drum
SIDEBC 400   91   92   93   94  195                          $ Top of Top Impact
Limiter
SIDEBC 500  101 102 103 104 105 111 10 20 30 40 50 60 70 80 90 91 92 93 94 195
$ Vol of Drum
SIDEBC 643   43      $ Floor of Space
SIDEBC 648   48      $ Right wall of Space
SIDEBC 653   53      $ Roof of Space
SIDEBC 647   47      $ Left wall of Space
$
$ REGION CARDS
$
REGION   1    1   -1   -6  -11   -5
REGION   2    1   -2   -7  -12   -6
REGION   3    1   -3   -8  -13   -7
REGION   4    1   -4   -9  -14   -8
$
REGION  11    3  -11  -16  -21  -15
REGION  12    3  -12  -17  -22  -16
REGION  13    3  -13  -18  -23  -17
REGION  14    3  -14  -19  -24  -18
$
$
REGION  21    2  -21  -26  -31  -25
REGION  22    2  -22  -27  -32  -26
REGION  23    1  -23  -28  -33  -27
REGION  24    1  -24  -29  -34  -28
$
REGION  31    4  -31  -36  -41  -35
REGION  32    2  -32  -37  -42  -36
```

```
REGION  33    1  -33  -38  -43  -37
REGION  34    1  -34  -39  -44  -38
$
REGION  41    4  -41  -46  -51  -45
REGION  42    2  -42  -47  -52  -46
$REGION  43    2  -43  -48  -53  -47
REGION  44    1  -44  -49  -54  -48
$
REGION  51    4  -51  -56  -61  -55
REGION  52    2  -52  -57  -62  -56
REGION  53    2  -53  -58  -63  -57
REGION  54    1  -54  -59  -64  -58
$
REGION  61    2  -61  -66  -71  -65
REGION  62    2  -62  -67  -72  -66
REGION  63    2  -63  -68  -73  -67
REGION  64    1  -64  -69  -74  -68
$
REGION  71    1  -71  -76  -81  -75
REGION  72    1  -72  -77  -82  -76
REGION  73    1  -73  -78  -83  -77
REGION  74    1  -74  -79  -84  -78
$
REGION  81    5  -81  -86  -91  -85
REGION  82    5  -82  -87  -92  -86
REGION  83    5  -83  -88  -93  -87
REGION  84    5  -84  -89  -94  -88
$
$
REGION 101    5 -101 -107   -1 -106
REGION 102    5 -102 -108   -2 -107
REGION 103    5 -103 -109   -3 -108
REGION 104    5 -104 -110   -4 -109
REGION 105    5 -105 -111 -116 -110
$
REGION 106    5 -116  -10 -115   -9
REGION 115    5 -115  -20 -125  -19
REGION 125    5 -125  -30 -135  -29
REGION 135    5 -135  -40 -145  -39
REGION 145    5 -145  -50 -155  -49
REGION 155    5 -155  -60 -165  -59
REGION 165    5 -165  -70 -175  -69
REGION 175    5 -175  -80 -185  -79
REGION 185    5 -185  -90 -195  -89
$
SCHEME   0    M
EXIT
```

APPENDIX C: SAMPLE SANTOS INPUT FILES FOR TEST SIMULATION

C-1 For UTS

```
TITLE $ Card 1
Uni-axial Test Simulation, 12"-Dia. POP Waste: B.Y.Park (7/14/03)
$ Card 3
AXISYMMETRIC $ Drum shape
$ Card 12 $ Default = 0.5 (%)
RESIDUAL TOLERANCE = 1.0
$ Card 13 (Default=2*num of nodes)
MAXIMUM ITERATIONS = 10000000
$
STEP CONTROL
10000,  1.E-3
  100,  1.
  100,  1.E3
  150, 16.E3
END
PLOT TIME
1000,    1.E-3
  10,    1.
  10,    1.E3
   1,   16.E3
END
OUTPUT TIME
1000,    1.E-3
  10,    1.
  10,    1.E3
   1,   16.E3
END
$ Card 8
PLOT NODAL, DISPLACEMENT, RESIDUAL
$ Card 9
PLOT ELEMENT, STRESS, STRAIN, VONMISES, PRESSURE
$ Card 10
PLOT STATE, EQCS, EV
$ Card 32
FUNCTION,1  $ Axial Pressure: 0 to 16 MPa
  0.        0.
  1.E-3     1.
  1.        1.E3
  1.E3      1.E6
 16.E3     16.E6
END
$ Card 33
NO DISPLACEMENT X  1 $ Axis of Model
NO DISPLACEMENT Y  2 $ Bottom of Model
$ Card 37
PRESSURE 401 1 1.0 $ Applying the pressure on the top of Upper Rigid Platen
$ Card 39: Coarser mesh should be designated as the master surface.
$             master,slave,   mu,   dis, tenrel
CONTACT SURFACE, 643, 647,   0.0, 1.E-4, 1.E4 $ btwn floor and LW of space
CONTACT SURFACE, 653, 648,   0.0, 1.E-4, 1.E4 $ btwn roof and RW of space
CONTACT SURFACE, 643, 648,   0.0, 1.E-4, 1.E4 $ btwn floor and RW of space
$ Card 41
$Impact Limiter based on SAND98-1003 Table 2
MATERIAL, 1, ELASTIC PLASTIC, 256.485
YOUNGS MODULUS     6.895E7
POISSONS RATIO     0.05
YIELD STRESS       3.447E5
HARDENING MODULUS  2.413E7
```

```
BETA                0.5
END
$ Stainless Steel Grade 304 based on SAND98-1003 Table 1
MATERIAL, 2, EP POWER HARD, 7908.
YOUNGS MODULUS      1.931E11
POISSONS RATIO      0.27
YIELD STRESS        1.931E8
HARDENING CONSTANT 1.329E9
HARDENING EXPONENT 0.748190
LUDERS STRAIN       0.0
END
$Plywood based on SAND98-1003 Table 2
MATERIAL, 3, ELASTIC PLASTIC, 427.476
YOUNGS MODULUS      3.103E7
POISSONS RATIO      0.2
YIELD STRESS        3.477E6
HARDENING MODULUS   6.895E4
BETA                0.5
END
$ Contents based on SAND98-1003 (Table 2)
MATERIAL, 4, ELASTIC PLASTIC, 256.485
YOUNGS MODULUS      6.895E7
POISSONS RATIO      0.2
YIELD STRESS        1.724E5
HARDENING MODULUS   0.0
BETA                0.0
END
$ Drum wall based on SAND98-1003 (Table 2)
MATERIAL, 5, ELASTIC PLASTIC, 7908.
YOUNGS MODULUS      1.931E11
POISSONS RATIO      0.27
YIELD STRESS        2.785E8
HARDENING MODULUS   6.895E7
BETA                0.0
END
$ Rigid Platen based on SANTOS V&Q Problem 8
$ MATERIAL, 6, ELASTIC, 1.
MATERIAL, 6, EP POWER HARD, 1.
YOUNGS MODULUS     30.E11
POISSONS RATIO      0.3
YIELD STRESS        1.931E9
HARDENING CONSTANT 1.329E9
HARDENING EXPONENT 0.748190
LUDERS STRAIN       0.0
END
$ Card 31
EXIT
```

C-2 For TTS

```
TITLE $ Card 1
Tri-axial Test Simulation, 1.5MPa CP, 12"-Dia. POP Waste: B.Y.Park (7/17/03)
$ Card 3
AXISYMMETRIC $ Drum shape
$ Card 12 $ Default = 0.5 (%)
RESIDUAL TOLERANCE = 1.0
$ Card 13 (Default=2*num of nodes)
MAXIMUM ITERATIONS = 10000000
$
STEP CONTROL
10000,  1.E-3
  100,  1.5
  100,  1.5E3
  145,  16.E3
END
PLOT TIME
1000,    1.E-3
  10,   1.5
  10,   1.5E3
   1,   16.E3
END
OUTPUT TIME
1000,    1.E-3
  10,   1.5
  10,   1.5E3
   1,   16.E3
END
$ Card 8
PLOT NODAL, DISPLACEMENT, RESIDUAL
$ Card 9
PLOT ELEMENT, STRESS, STRAIN, VONMISES, PRESSURE
$ Card 10
PLOT STATE, EQCS, EV
$ Card 32
FUNCTION,1  $ Axial Pressure: 0 to 16 MPa
  0.       0.
  1.E-3    1.
 1.5       1.5E3
 1.5E3     1.5E6
 16.E3     16.E6
END
FUNCTION,2   $ Confining Pressure: 1.5 MPa
  0.       0.0
  1.E-3    1.0
 1.5       1.5E3
 1.5E3     1.5E6
 16.E3     1.5E6
END
$ Card 33
NO DISPLACEMENT X  1 $ Axis of Model
NO DISPLACEMENT Y  2 $ Bottom of Model
$ Card 37
PRESSURE 300 2 1.0 $ Applying the confining pressure on the drum wall
PRESSURE 401 1 1.0 $ Applying the pressure on the top of Upper Rigid Platen
$ Card 39: Coarser mesh should be designated as the master surface.
$              master,slave,   mu,   dis, tenrel
CONTACT SURFACE, 643, 647,   0.0, 1.E-4, 1.E4 $ btwn floor and LW of space
CONTACT SURFACE, 653, 648,   0.0, 1.E-4, 1.E4 $ btwn roof and RW of space
CONTACT SURFACE, 643, 648,   0.0, 1.E-4, 1.E4 $ btwn floor and RW of space
$ Card 41
$Impact Limiter based on SAND98-1003 Table 2
```

```
MATERIAL, 1, ELASTIC PLASTIC, 256.485
YOUNGS MODULUS      6.895E7
POISSONS RATIO      0.05
YIELD STRESS        3.447E5
HARDENING MODULUS   2.413E7
BETA                0.5
END
$ Stainless Steel Grade 304 based on SAND98-1003 Table 1
MATERIAL, 2, EP POWER HARD, 7908.
YOUNGS MODULUS      1.931E11
POISSONS RATIO      0.27
YIELD STRESS        1.931E8
HARDENING CONSTANT 1.329E9
HARDENING EXPONENT 0.748190
LUDERS STRAIN       0.0
END
$Plywood based on SAND98-1003 Table 2
MATERIAL, 3, ELASTIC PLASTIC, 427.476
YOUNGS MODULUS      3.103E7
POISSONS RATIO      0.2
YIELD STRESS        3.477E6
HARDENING MODULUS   6.895E4
BETA                0.5
END
$ Contents based on SAND98-1003 (Table 2)
MATERIAL, 4, ELASTIC PLASTIC, 256.485
YOUNGS MODULUS      6.895E7
POISSONS RATIO      0.2
YIELD STRESS        1.724E5
HARDENING MODULUS   0.0
BETA                0.0
END
$ Drum wall based on SAND98-1003 (Table 2)
MATERIAL, 5, ELASTIC PLASTIC, 7908.
YOUNGS MODULUS      1.931E11
POISSONS RATIO      0.27
YIELD STRESS        2.785E8
HARDENING MODULUS   6.895E7
BETA                0.0
END
$ Rigid Platen based on SANTOS V&Q Problem 8
$ MATERIAL, 6, ELASTIC, 1.
MATERIAL, 6, EP POWER HARD, 1.
YOUNGS MODULUS     30.E11
POISSONS RATIO      0.3
YIELD STRESS        1.931E9
HARDENING CONSTANT 1.329E9
HARDENING EXPONENT 0.748190
LUDERS STRAIN       0.0
END
$ Card 31
EXIT
```

C-3 For HTS

```
TITLE $ Card 1
Hydrostatic Test Simulation, 12"-Dia. POP Waste : B.Y.Park (7/14/03)
$ Card 3
AXISYMMETRIC $ Drum shape
$ Card 12 $ Default = 0.5 (%)
RESIDUAL TOLERANCE = 0.5
$ Card 13 (Default=2*num of nodes)
MAXIMUM ITERATIONS = 10000000
$
STEP CONTROL
10000,  1.0E-3
  100,  1.0
  100,  1.0E3
  150,  16.E3
END
PLOT TIME
1000,   1.0E-3
  10,   1.0
  10,   1.0E3
   1,   16.E3
END
OUTPUT TIME
1000,   1.0E-3
  10,   1.0
  10,   1.0E3
   1,   16.E3
END
$ Card 8
PLOT NODAL, DISPLACEMENT, RESIDUAL
$ Card 9
PLOT ELEMENT, STRESS, STRAIN, VONMISES, PRESSURE
$ Card 10
PLOT STATE, EQCS, EV
$ Card 32
FUNCTION,1 $ Hydraulic Pressure
 0.        0.
 1.0E-3    1.
 1.0       1.0E3
 1.0E3     1.0E6
 16.E3     16.E6
END
$ Card 33
NO DISPLACEMENT X  1 $ Axis of Model
$ Card 37
PRESSURE 100 1 1.0 $ Applying the pressure on the bottom of drum
PRESSURE 300 1 1.0 $ Applying the pressure on the drum wall
PRESSURE 400 1 1.0 $ Applying the pressure on the top of drum lid
$ Card 39: Coarser mesh should be designated as the master surface.
$             master,slave,   mu,   dis, tenrel
CONTACT SURFACE, 643, 647,   0.0, 1.E-4, 1.E4 $ btwn floor and LW of space
CONTACT SURFACE, 653, 648,   0.0, 1.E-4, 1.E4 $ btwn roof and RW of space
CONTACT SURFACE, 643, 648,   0.0, 1.E-4, 1.E4 $ btwn floor and RW of space
$Impact Limiter based on SAND98-1003 Table 2
MATERIAL, 1, ELASTIC PLASTIC, 256.485
YOUNGS MODULUS      6.895E7
POISSONS RATIO      0.05
YIELD STRESS        3.447E5
HARDENING MODULUS   2.413E7
BETA                0.5
END
$ Stainless Steel Grade 304 based on SAND98-1003 Table 1
```

```
MATERIAL, 2, EP POWER HARD, 7908.
YOUNGS MODULUS      1.931E11
POISSONS RATIO      0.27
YIELD STRESS        1.931E8
HARDENING CONSTANT 1.329E9
HARDENING EXPONENT 0.748190
LUDERS STRAIN       0.0
END
$Plywood based on SAND98-1003 Table 2
MATERIAL, 3, ELASTIC PLASTIC, 427.476
YOUNGS MODULUS      3.103E7
POISSONS RATIO      0.2
YIELD STRESS        3.477E6
HARDENING MODULUS   6.895E4
BETA                0.5
END
$ Contents based on SAND98-1003 (Table 2)
MATERIAL, 4, ELASTIC PLASTIC, 256.485
YOUNGS MODULUS      6.895E7
POISSONS RATIO      0.2
YIELD STRESS        1.724E5
HARDENING MODULUS   0.0
BETA                0.0
END
$ Drum wall based on SAND98-1003 (Table 2)
MATERIAL, 5, ELASTIC PLASTIC, 7908.
YOUNGS MODULUS      1.931E11
POISSONS RATIO      0.27
YIELD STRESS        2.785E8
HARDENING MODULUS   6.895E7
BETA                0.0
END
$ Card 31
EXIT
```

Intentionally Blank

DISTRIBUTION:

Federal Agencies

1 US Department of Energy
Office of Civilian Radioactive Waste Mgmt.
Attn: Deputy Director, RW-2
Forrestal Building
Washington, DC 20585

8 US Department of Energy
Carlsbad Field Office
Attn: P. Detwiler
C. Wu
G. Basabilvazo
S. Casey
D. Mercer
R. Nelson
R. Patterson
Mailroom
P.O. Box 3090
Carlsbad, NM 88221-3090

1 US Department of Energy
Office of Environmental Restoration and Waste Management
Attn: P. Bubar, EM-20
Forrestal Building
Washington, DC 20585-0002

1 US Department of Energy
Office of Environmental Restoration and Waste Management
Attn: Mary Bisesi/Lynne Smith, EM-23
Washington, DC 20585-0002

1 US Environmental Protection Agency
Radiation Protection Programs
Attn: B. Forinash
ANR-460
Washington, DC 20460

Boards

1 Defense Nuclear Facilities Safety Board
Attn: D. Winters
625 Indiana Ave. NW, Suite 700
Washington, DC 20004

State Agencies

1 Attorney General of New Mexico
P.O. Drawer 1508
Santa Fe, NM 87504-1508

2 Environmental Evaluation Group
Attn: Library
7007 Wyoming NE
Suite F-2
Albuquerque, NM 87109

1 NMED Hazardous Waste Bureau
WIPP Project Leader
2905 Rodeo Park Dr E., Bldg 1
Santa Fe, NM 87505-6303

1 NM Bureau of Geology & Mineral Resources
801 Leroy Place
Socorro, NM 87801

Laboratories/Corporations

1 Battelle Pacific Northwest Laboratories
Battelle Blvd.
Richland, WA 99352

1 Los Alamos National Laboratory
Attn: B. Erdal, INC-12
P.O. Box 1663
Los Alamos, NM 87544

3 Washington TRU Solutions
Attn: Library, GSA-214
P.O. Box 2078
Carlsbad, NM 88221

National Academy of Sciences WIPP Panel

1 National Academies
Attn: Barbara Pastina
Committee on WIPP
Board on Radioactive Waste Management
500 Fifth Ave NW; Keck 634
Washington, DC 20001

Universities

1 University of New Mexico
Geology Department
Attn: Library
141 Northrop Hall
Albuquerque, NM 87131

1 North Carolina State University
Department of Nuclear Engineering
Attn: Man-Sung Yim
Box 7909
Raleigh, NC 27695-7909

Libraries

1 Government Information Department
Zimmerman Library
University of New Mexico
MSCO5 3020
Albuquerque, NM 87131-0001

1 New Mexico Junior College
Pannell Library
Attn: Earl Dye
5317 Lovington Highway
Hobbs, NM 88240

1 New Mexico State Library
Attn: L. Canepa
1209 Camino Carlos Rey
Santa Fe, NM 87507

1 New Mexico Tech
Joseph R. Skeen Library
801 Leroy Place
Socorro, NM 87801

Foreign Addresses

2 OECD Nuclear Energy Agency
Attn: OECD NEA Library
Le Seine Saint-Germain
12, boulevard des Îles
F-92130 Issy-les-Moulineaux
FRANCE

2 Francois Chenevier
ANDRA
Parc de la Croix Blanche
1-7 rue Jean Monnet
92298 Chatenay-Malabry Cedex
FRANCE

1 Commissariat a L'Energie Atomique
Attn: D. Alexandre
Centre d'Etudes de Cadarache
13108 Saint Paul Lez Durance Cedex
FRANCE

1 Bundesanstalt fur Geowissenschaften und Rohstoffe
Attn: M. Wallner
Postfach 510 153
D-30631 Hannover
GERMANY

1 Bundesministerium fur Forschung und Technologie
Postfach 200 706
5300 Bonn 2
GERMANY

1 Gesellschaft fur Anlagen und Reaktorsicherheit (GRS)
Attn: B. Baltes
Schwertnergasse 1
D-50667 Cologne
GERMANY

1 Dr.-Ing. Klaus Kuhn
TU Clausthal Institut fur Bergbau
Erzstr. 20
D-38678 Clausthal-Zellerfeld
GERMANY

1 Dr. Chung-Won Cho
Ministry of Science & Technology
Government Complex-Gwacheon Gwacheon City,
Gyeonggi-Do 427-715,
Republic of KOREA

1 Dr. Myung-Jae Song
Nuclear Environment Technology Institute
Korea Hydro & Nuclear Power Co., Ltd (KHNP)
150 Duckjin-dong, Yusong-ku, Taejon, 305-600,
Republic of KOREA

10 Korea Atomic Energy Research Institute
Attn: Overseas Attachment Section
Library (6)
Dr. In-Soon Chang
Dr. Hyun-Soo Park
Dr. Pil-Soo Hahn
150 Duckjin-dong, Yusong-ku, Taejon, 305-600,
Republic of KOREA

1 Prof. Chang Sun Kang
Seoul National University
Department of Nuclear Engineering
Shillim-dong, Kwanak-gu, Seoul, 151-742
Republic of KOREA

1 Prof. Chung In Lee
Seoul National University
School of Civil, Urban and Geosystem Engineering
Shillim-dong, Kwanak-gu, Seoul, 151-742
Republic of KOREA

2 Japan Nuclear Cycle Development Institute
Attn: Dr. Massao Shiotsuki
Takashi Toshikawa
4-49, Muramatsu, Tokai-Mura
Naka-Gun, Ibaraki, 319-1184
JAPAN

1 Dr. Susumu Muraoka
Nuclear Material Control Center
Tokai-Mura, Ibaraki-Ken, 319-11
JAPAN

2 Nationale Genossenschaft fur die Lagerung Radioaktiver Abfalle
Attn: NAGRA Library
Hardstrasse 73
CH-5430 Wettingen
SWITZERLAND

2 AEA Technology
Attn: J. H. Rees
Lee J. Hartley
424-4 Harwell
Didcot, Oxfordshire OX11 OQJ
UNITED KINGDOM

Internal

	MS	Org.	
1	0701	6100	P. B. Davies
2	0731	6800	823 Library
1	0751	6117	L. S. Costin
1	0751	6117	M. Lee
1	0751	6117	T. W. Pfeifle
1	0771	6800	D. Berry
10	0771	6820	F. D. Hansen
1	0776	6852	M. K. Knowles
1	0776	6852	J. S. Stein
1	0847	9127	J. Jung
1	0847	9127	J. F. Holland
1	1395	6820	P. E. Shoemaker
1	1395	6821	D. Kessel
1	1395	6821	C. W. Hansen
1	1395	6820	M. J. Chavez
10	1395	6821	B. Y. Park
8	1395	6820	WIPP Library
1	9018	8940-2	Central Technical Files
2	0899	9616	Technical Library